



# QEX

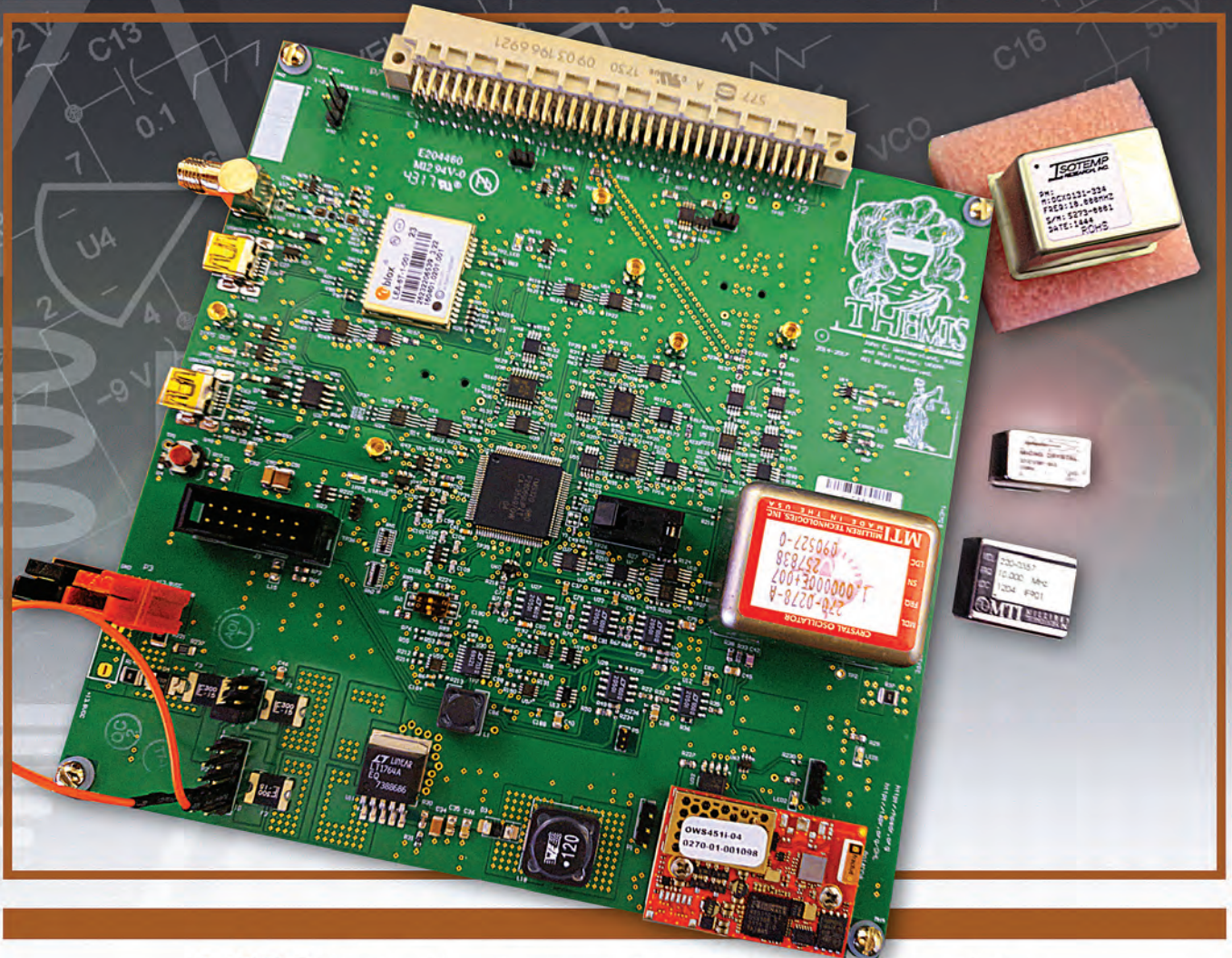
\$7

July/August 2019

[www.arrl.org](http://www.arrl.org)

## A Forum for Communications Experimenters

Issue No. 315



**AJ6BC** describes Themis, an experimental GPS-disciplined oscillator.

# KENWOOD

3rd IMDR 110 dB\*

RMDR 122 dB\*

BDR 150 dB\*

## Performance Exceeding Expectations.

The most happy and sublime encounters happen in the worst circumstances and under the harshest conditions.

There are enthusiasts who know this all too well because of their love of HF radio.

Results born of certainty and not circumstance. Delivered through impeccable performance. This is our offering to you.



"The Kenwood TS-890S has the highest RMDR of any radio I have ever measured."

- Rob Sherwood - NCOB - December 2018

HF/50MHz TRANSCEIVER

# TS-890S

NEW

### Top-class receiving performance

3 kinds of dynamic range make for top-class performance.

- ▶ Third order intermodulation Dynamic Range (3rd IMDR) 110dB\*
- ▶ Reciprocal Mixing Dynamic Range (RMDR) 122dB\*
- ▶ Blocking Dynamic Range (BDR) 150dB\*

\*Values are measured examples. (2kHz spacing:14.1 MHz, CW, BW 500 Hz, Pre Amp OFF)

- ▶ Full Down Conversion RX
- ▶ High Carrier to Noise Ratio 1st LO
- ▶ H-mode mixer

### 4 kinds of built-in roofing filters

500Hz / 2.7kHz / 6kHz / 15kHz (270Hz Option)

### 7 inch Color TFT Display

- ▶ Roofing frequency sampling band scope
- ▶ Band scope auto-scroll mode
- ▶ Multi-information display including filter scope

### Clean and tough 100W output

Built-in high-speed automatic antenna tuner

32-bit floating-point DSP for RX / TX and Bandscope

Customer Support: (310) 639-4200

[www.kenwood.com/usa](http://www.kenwood.com/usa)



ISO9001 Registered  
UKAS Quality Management System  
13000  
13001

ADS#02119

QEX (ISSN: 0886-8093) is published bimonthly in January, March, May, July, September, and November by the American Radio Relay League, 225 Main St., Newington, CT 06111-1494. Periodicals postage paid at Hartford, CT and at additional mailing offices.

POSTMASTER: Send address changes to: QEX, 225 Main St., Newington, CT 06111-1494 Issue No 315

*Publisher*  
American Radio Relay League

Kazimierz "Kai" Siwiak, KE4PT  
*Editor*

Lori Weinberg, KB1EIB  
*Assistant Editor*

Zack Lau, W1VT  
Ray Mack, W5IFS  
*Contributing Editors*

#### Production Department

Steve Ford, WB8IMY  
*Publications Manager*

Michelle Bloom, WB1ENT  
*Production Supervisor*

Sue Fagan, KB1OKW  
*Graphic Design Supervisor*

David Pingree, N1NAS  
*Senior Technical Illustrator*

Brian Washing  
*Technical Illustrator*

#### Advertising Information Contact:

Janet L. Rocco, W1JLR  
*Business Services*  
860-594-0203 – Direct  
800-243-7768 – ARRL  
860-594-4285 – Fax

#### Circulation Department

Cathy Stepina, QEX Circulation

#### Offices

225 Main St., Newington, CT 06111-1494 USA  
Telephone: 860-594-0200  
Fax: 860-594-0259 (24 hour direct line)  
e-mail: [qex@arrl.org](mailto:qex@arrl.org)

#### Subscription rate for 6 issues:

In the US: \$29;

US by First Class Mail: \$40;

International and Canada by Airmail: \$35

Members are asked to include their membership control number or a label from their QST when applying.

In order to ensure prompt delivery, we ask that you periodically check the address information on your mailing label. If you find any inaccuracies, please contact the Circulation Department immediately. Thank you for your assistance.



Copyright © 2019 by the American Radio Relay League Inc. For permission to quote or reprint material from QEX or any ARRL publication, send a written request including the issue date (or book title), article, page numbers and a description of where you intend to use the reprinted material. Send the request to the office of the Publications Manager ([permission@arrl.org](mailto:permission@arrl.org)).

### About the Cover

John Westmoreland, AJ6BC, discusses the origins of the Themis project and its design goals. Themis is an experimental Global Positioning System Disciplined Oscillator (GPSDO) for the Open High Performance Software Defined Radio, that can also be used as a stand-alone source for supplying a 10 MHz reference clock output. It includes an output to the Atlas bus, and provides several additional outputs intended for various levels of experimentation. AJ6BC describes the GPSDO control algorithms and some techniques for disciplining and synchronizing an Oven Controlled Crystal Oscillator (OCXO) with the GPS satellite system one-pulse-per-second (1PPS) signaling.



### In This Issue

## Features

**2 Perspectives**  
Kazimierz "Kai" Siwiak, KE4PT

**3 Themis**  
John C. Westmoreland, AJ6BC

**14 A Different Look at the Phase Locked Loop**  
Andrzej (Andy) Przedpelski, KØABP

**16 Get Started with 3D Printing**  
Joseph Pingree, WB2TVB

**20 Pi Networks With or Without Inductor Loss — Part 1**  
Tuck Choy, MØTCC

**29 Errata**

**30 Receiver Step Attenuator**  
Scott Roleson, KC7CJ

**36 Upcoming Conferences**

### Index of Advertisers

DX Engineering: .....Cover III  
Harris Corporation: ..... 19  
Kenwood Communications: .....Cover II

Stepplr Communication Systems.....Cover IV  
Tucson Amateur Packet Radio: .....29

## The American Radio Relay League



The American Radio Relay League, Inc. is a noncommercial association of radio amateurs, organized for the promotion of interest in Amateur Radio communication and experimentation, for the establishment of networks to provide communications in the event of disasters or other emergencies, for the advancement of the radio art and of the public welfare, for the representation of the radio amateur in legislative matters, and for the maintenance of fraternalism and a high standard of conduct.

ARRL is an incorporated association without capital stock chartered under the laws of the state of Connecticut, and is an exempt organization under Section 501(c)(3) of the Internal Revenue Code of 1986. Its affairs are governed by a Board of Directors, whose voting members are elected every three years by the general membership. The officers are elected or appointed by the Directors. The League is noncommercial, and no one who could gain financially from the shaping of its affairs is eligible for membership on its Board.

"Of, by, and for the radio amateur," ARRL numbers within its ranks the vast majority of active amateurs in the nation and has a proud history of achievement as the standard-bearer in amateur affairs.

A *bona fide* interest in Amateur Radio is the only essential qualification of membership; an Amateur Radio license is not a prerequisite, although full voting membership is granted only to licensed amateurs in the US.

Membership inquiries and general correspondence should be addressed to the administrative headquarters:

ARRL  
225 Main St.  
Newington, CT 06111 USA  
Telephone: 860-594-0200  
FAX: 860-594-0259 (24-hour direct line)

### Officers

**President:** Rick Roderick, K5UR  
P.O. Box 1463, Little Rock, AR 72203

**Chief Executive Officer:** Howard Michel, WB2ITX

The purpose of *QEX* is to:

- 1) provide a medium for the exchange of ideas and information among Amateur Radio experimenters,
- 2) document advanced technical work in the Amateur Radio field, and
- 3) support efforts to advance the state of the Amateur Radio art.

All correspondence concerning *QEX* should be addressed to The American Radio Relay League, 225 Main St., Newington, CT 06111 USA. Envelopes containing manuscripts and letters for publication in *QEX* should be marked Editor, *QEX*.

Both theoretical and practical technical articles are welcomed. Manuscripts should be submitted in word-processor format, if possible. We can redraw any figures as long as their content is clear.

Photos should be glossy, color or black-and-white prints of at least the size they are to appear in *QEX* or high-resolution digital images (300 dots per inch or higher at the printed size). Further information for authors can be found on the Web at [www.arrl.org/qex/](http://www.arrl.org/qex/) or by e-mail to [qex@arrl.org](mailto:qex@arrl.org).

Any opinions expressed in *QEX* are those of the authors, not necessarily those of the Editor or the League. While we strive to ensure all material is technically correct, authors are expected to defend their own assertions. Products mentioned are included for your information only; no endorsement is implied. Readers are cautioned to verify the availability of products before sending money to vendors.

Kazimierz "Kai" Siwiak, KE4PT

## Perspectives

### Another Mode for the Basic SDR System

The basic Software Defined Radio (SDR) System has been identified in *Wikipedia* and in this column as comprising some form of RF front end (a stable transceiver), followed by conversion between the analog and digital realms (such as by an audio sound card), along with a general purpose personal computer (PC). We emphasize that the *software defined* part of this basic radio system is the Amateur Radio communications software that operates on the PC, producing a wide range of communications protocols, or "waveforms" that are not native to the transceiver used as the RF front end. While modern SDR platform architectures do provide a transceiver function that continues to migrate the boundary between the analog and digital realms ever closer to the antenna — those SDR platforms still require, and benefit from, the PC-based waveforms and modes.

New modes or digital protocols continue to proliferate — now with the addition of FT4 (in beta testing as of this writing) to the *WSJT-X* suite. Your basic SDR System (or SDR platform plus PC) benefits once again, without the need of any additional piece of hardware. All of the magic happens in the software running on the PC. Our Amateur Radio communications capabilities have again grown without the need to change the basic hardware.

According to *WSJT-X* developers Joe Taylor, K1JT; Steve Franke, K9AN; and Bill Somerville, G4WJS; "FT4 is an experimental digital mode designed specifically for radio contesting... FT4 can work with signals 10 dB weaker than needed for RTTY, while using much less bandwidth." Watch these pages for additional modulation waveforms, and for further SDR System evolution.

### In This Issue

We feature a range of topics in this issue of *QEX*.

John Westmoreland, AJ6BC, describes THEMIS, a GPS-disciplined oscillator.

Andy Przedpelski, KØABP, takes a different look at the phase locked loop.

Joseph Pingree, WB2TVB, shows how to design and print 3D components.

Tuck Choy, MØTCC, considers pi networks with and without inductor loss in this first of a two-part series.

Scott Roleson, KC7CJ, constructs a receiver step attenuator.

### Writing for *QEX*

Keep the full-length *QEX* articles flowing in, or share a **Technical Note** of several hundred words in length plus a figure or two. Let us know that your submission is intended as a **Note**. *QEX* is edited by Kazimierz "Kai" Siwiak, KE4PT, ([ksiwiak@arrl.org](mailto:ksiwiak@arrl.org)) and is published bimonthly. *QEX* is a forum for the free exchange of ideas among communications experimenters. The content is driven by you, the reader and prospective author. The subscription rate (6 issues per year) in the United States is \$29. First Class delivery in the US is available at an annual rate of \$40. For international subscribers, including those in Canada and Mexico, *QEX* can be delivered by airmail for \$35 annually. Subscribe today at [www.arrl.org/qex](http://www.arrl.org/qex).

Would you like to write for *QEX*? We pay \$50 per published page for articles and Technical Notes. Get more information and an Author Guide at [www.arrl.org/qex-author-guide](http://www.arrl.org/qex-author-guide). If you prefer postal mail, send a business-size self-addressed, stamped (US postage) envelope to: *QEX* Author Guide, c/o Maty Weinberg, ARRL, 225 Main St, Newington, CT 06111.

Very best regards,

Kazimierz "Kai" Siwiak, KE4PT

### Dr. Ulrich Rohde, N1UL, Wins 2019 IEEE CAS Industrial Pioneer Award

The Industrial Pioneer Award honors the individual(s) with exceptional and pioneering contributions in translating academic and industrial research results into improved industrial applications and/or commercial products. The award is given by IEEE Circuits and Systems Society and president Yong Lian extended his congratulations and looks forward to honoring Dr. Rohde at their flagship conference, ISCAS 2019.

The purpose of the annual IEEE Circuits & Systems Society Awards is to illuminate the accomplishments of CAS Society members and celebrate their dedication and contributions both within the field and to the CAS Society. Award recipients are nominated by their CASS peers in order to honor the service and contributions that further strengthen the CAS Society.

# Themis

*An experimental GPS-disciplined oscillator for Open High Performance Software Defined Radio, that can also be used as a stand-alone source.*

The Themis project has been discussed for some time. The first public discussion was part of a 2014 Pacificon presentation.<sup>1</sup> Prior to that, Themis was discussed at length with the members of the Open High Performance Software Defined Radio (OpenHPSDR) initiative. The first public posting of the Themis schematic was in January 2014.<sup>2</sup>

Themis is an experimenter's platform for developing Global Positioning System Disciplined Oscillator (GPSDO) control algorithms for synchronizing an Oven Controlled Crystal Oscillator (OCXO) with the GPS satellite system one-pulse-per-second (1PPS) signaling. Themis also supplies a 10 MHz reference clock output to the Atlas bus<sup>3</sup> and through various on-board micro-miniature coaxial (MMCX) connectors. Several MMCX connector outputs are provided for various levels of experimentation.

This article discusses the origins of the Themis project, the design goals, the heart of the GPSDO engine, some techniques for disciplining the OCXO, and some ideas for the future.

---

## Project Background

All radio systems need a reference clock. Modern radio systems need a reference clock that is synchronized to a global standard like GPS. In OpenHPSDR for instance, the reference clock is used for frequency calibration.

The OpenHPSDR project was in need of a GPSDO based design. The predecessor of Themis was Khronos, also presented at Pacificon 2014.

Several other project ideas had been proposed before Khronos and Themis, but OpenHPSDR relies on volunteer hours of Amateur Radio enthusiasts, so many attempts

at a GPSDO either were not completed or took on another life of their own.

While doing the schematic and completing the layout for Khronos, I became more and more curious of how a GPSDO really works. The more I dug into this, the more I hit dead ends. It was like the proverbial Gordian Knot — the more I wanted to know, the more difficult it became to get details. Of course, there have been many attempts using similar ideas. Some OCXO designs require periodic calibration with a Rubidium standard<sup>4</sup> as one of the classic examples. Anyone who has done that at least once will appreciate a way to keep their OCXO not only in calibration, but synchronized to a standard as well, without needing a Rubidium or other non-automatic external standard.

I talked to many hams and people not close to the ham community, as well as some who are very involved in the timing industry. I received much advice and many comments, but my curiosity continued to grow. I decided to research and study how GPS began and what people and companies were involved with the first GPSDO designs.

While searching, I discovered Austron, Inc. I consider Austron to be a kind of 'Bell-Labs' in the early days of the satellite signal based timing business, especially regarding GPSDOs.<sup>5</sup> My searches also turned up National Institute of Standards and Technology (NIST).<sup>6</sup> [As a point of interest the Department of the Navy [www.usno.navy.mil/](http://www.usno.navy.mil/) serves as the official timekeeper of the US, with the Master Clock facility at the U.S. Naval Observatory, Washington, DC — *Ed.*].

I studied as much as I could about prior GPSDO designs and their history, to possibly develop a design that would be suitable not only for the OpenHPSDR architecture but could also be useful in a stand-alone mode of operation.

---

## Project Design Goals

My major project design goals for Themis are as follows.

- Make the GPS interface as generic as possible with a path to upgrading with more than one current GPS option.
- Allow for more than one type (brand) of OCXO within practical limits.
- Develop a platform where experimentation on disciplined OCXOs would be possible.
- Develop a platform that works either in or out of the OpenHPSDR Atlas bus, but can provide both a reference clock and GPS data to the Atlas bus or to another system via MMCX connectors.
- Provide an option to broadcast the GPS signaling via Bluetooth or Wi-Fi.
- Have at least one USB port available to the experimenter's discretion.

---

## The GPS Engine

After considering many options I decided upon the LEA-6T family from u-Blox.<sup>7</sup> The LEA-6T-001 is the current GPS engine that is installed on the Themis board. The footprint of this device and subsequent devices are either exactly the same and if not, require just some different resistor stuffing options in most cases. Those pads are on the Themis board. Upgrade pin and package compatible paths are available for the LEA-6T family from u-Blox.

The LEA-6T family is specifically for timing and has a special timing mode that is designed for base station designs. The LEA-6T module has two timing outputs, both of which are programmable. Typically, at least one output is set to 1PPS, but that is not a hard requirement.

## USB Interfaces

Themis has two USB 2.0 interfaces, one provided via the LEA-6T and one provided via the TI DSP/MCU. The USB for the LEA-6T provides the path in which to do the set-up configuration of the GPS Engine using a tool like the u-Blox u-center<sup>8</sup> Windows<sup>®</sup> interface. The USB interface for the DSP/MCU can be used for debug data, system monitoring, or can be tasked based on the experimenter's needs.

## OCXOs

The Themis board currently has land patterns on the PCB for four popular OCXO package sizes making the choices for OCXO a little easier. To date, two major brands of OCXOs have been used and tested in the OpenHSPDR Atlas bus.

## Disciplining Engine

Based on my discussions and research, I decided on an approach that I call a DLL, meaning digitally locked-loop akin to a phase-locked-loop but using a technique that is made possible by the High-Resolution Capture (HRCAP)<sup>9</sup> registers provided by Digital Signal Processors (DSPs) such as the TI C2000<sup>™</sup> MCU, TMS320F28069.<sup>10</sup> The TI DSP/MCU has on-board USB 2.0 as well, making it a good fit for this application.

## Themis Features

Figure 1 shows some of the major features of the Themis design.

(1) — LEA-6T-001 GPS Engine with active/

passive antenna interface and USB interface. MMCX with 1PPS output and additional MMCX on second timing output.

- (2) — Atlas bus interface. Main ECL driven 10 MHz clock is driven onto the Atlas bus.
- (3) — 1PPS, GPS Packet, I2C, and MMCX common with 10 MHz Atlas reference clock.
- (4) — 10 MHz output from OCXO, programmable output controlled by DSP/MCU High Resolution Pulse Width Modulation (HRPWM)<sup>11</sup> register. This allows the experimenter full control of an output clock.
- (5) — Joint Test Action Group (JTAG) programming interface for DSP/MCU, USB interface for DSP/MCU, 1PPS output MMCX option from DSP/MCU.
- (6) — TI TMS320F28069 DSP/MCU with MEMs<sup>12</sup> (technology based on micro-electro-mechanical architecture) socket (there is also a MEMs socket on the solder side of the PCBA) ECL AND forming the input to the HRCAP interface.
- (7) — OCXO with optional land patterns. The OCXO is mounted on standoffs for development.
- (8) — Wi-Fi/Bluetooth wireless option, provides streaming data and two-way communication.
- (9) — Power supply input with optional Anderson Powerpole connectors and onboard regulators. Themis can also take power from the Atlas bus.
- (10) — Circuitry for EFC voltage

conditioning.

- (11) — The solder-side (back) of Themis has a coin-cell battery holder for battery backup of data for the GPS Engine that assists in fast warm-boots as well.

## Design Details

The LEA-6T has two timing output options. Either one can be used to provide the signal in which the OCXO is disciplined. See the schematic diagram “QEX-1905-Westmoreland-Timing-Outputs=QEXfiles.jpg” on the [www.arrl.org/QEXfiles](http://www.arrl.org/QEXfiles) web page. In that schematic snippet, TIMEPULSE and TIMEPULSE2 are the two timing outputs.

The LEA-6T has a programmable multiplier, and its value is the experimenter's choice. The current implementation uses a multiplier that is the same frequency as the OCXO, in this case 10 MHz. The basis of the disciplining engine is 1PPS.

Themis uses Emitter Coupled Logic (ECL) for all timing-critical paths. The board is laid out using 50 Ω and ECL differential design rule guidelines. All OCXO timing critical paths are done on layer 1 of the PCB, which is the component side of the board.

The output of the OCXO goes into a divide-by-8 ECL circuit and the output from the GPS disciplining engine also goes into a divide-by-8 circuit. Note that this can be changed as well. Those go into a 2-input ECL AND gate and then that goes into one of the TI DSP/MCU HRCAP input registers. The HRCAP interface has its own library from TI — the HRCAP Library<sup>13</sup> that not only lets the user get IQ data<sup>14</sup> to represent the values captured in the HRCAP register but also allows for run-time calibration of the HRCAP registers to make sure they remain in calibration during runtime and compensate for temperature variation as well.

The HRCAP interface is essentially the heart of the digitally locked loop. Themis uses MEMS clock options. For the HRCAP clock, a 30 MHz programmable MEMS device is used that is internally multiplied by 3 to give a 90 MHz system clock and multiplied by 4 to get a 120 MHz HRCAP clock. This means each HRCAP count has a resolution of 8.333 ns. The inputs to the ECL AND gate run at 1.25 MHz (10 MHz/8), which yields 800 ns. Taking 800 ns and dividing by 8.333 ns yields 96. Taking into account the duty cycle of most OCXOs this results in an ideal count of 48 that comes out of the ECL AND gate. This design concept is the basis of the disciplining engine. A count of 48 represents ‘digital lock’ of the system and is provided by the TI HRCAP library interface in IQ format. An OCXO with a different duty cycle will have to be adjusted accordingly.

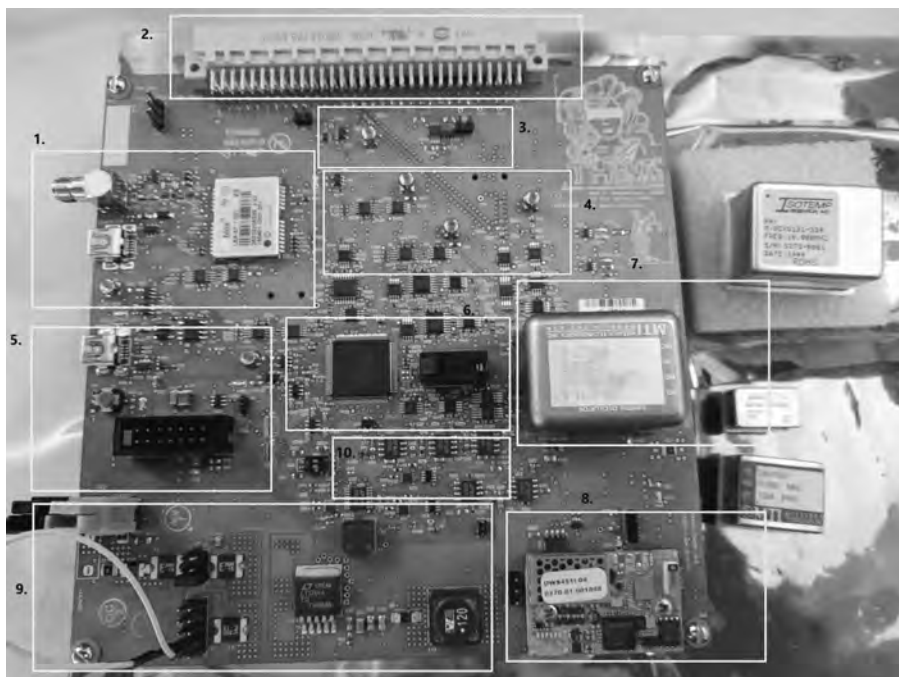


Figure 1 — Themis PCBA with major blocks outlined.

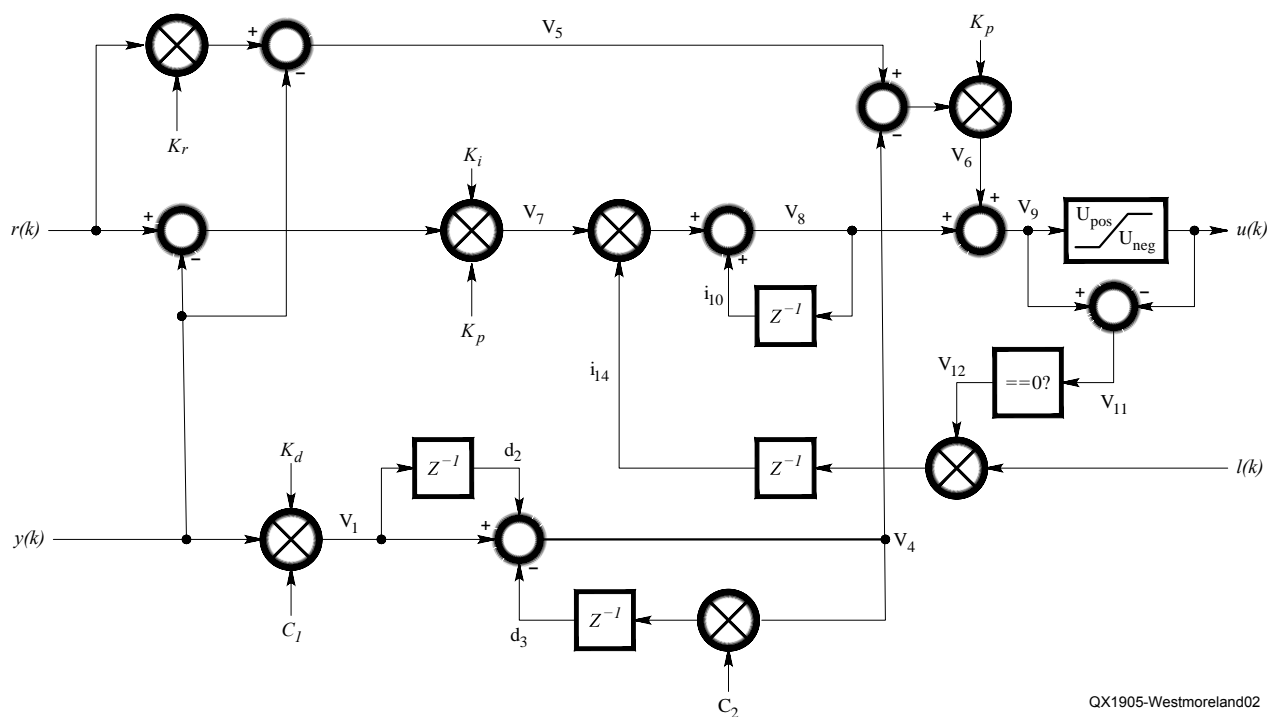


Figure 2 — A representation of a linear control PID (Courtesy of TI).

Summarizing:  
 HRCAP CLK is 120 MHz (8.333 ns)  
 10 MHz/8 = 1.25 MHz (800 ns)  
 HRCAP clock count = (800 ns) / (8.333 ns) =  
 96 HRCAP counts  
 96 HRCAP clock counts per normal capture  
 cycle  
 50% duty cycle (example) yields 48 positive  
 counts and 48 negative counts.

This works out nicely with some popular  
 control algorithms.

The ECL AND gate circuit was originally  
 meant to provide only a synchronization  
 (SYNC) pulse to the rest of the TI DSP/  
 MCU for all of the HRCAP measurements.  
 However, as development progressed, in  
 addition to the SYNC pulse requirement, I  
 felt it was necessary to also feed the SYNC  
 pulse width into one of the HRCAP registers  
 so that could be measured as well, using that  
 as another disciplining metric. The 1PPS  
 signal inputs also serve as triggers in which  
 the PID takes measurements and applies  
 correction, making sure the OCXO is in  
 synchronization with the GPS 1PPS signal.

### EFC System Control

Themis is designed to control OCXOs  
 that have an Electronic Frequency Tuning  
 Control (EFC)<sup>15</sup> input pin in which the output  
 frequency can be adjusted. Each OCXO  
 from different manufacturers is a bit different  
 so it's necessary to tune the EFC circuit to  
 the particular OCXO that has been installed,

creating tuning profiles for the respective  
 OCXO models.

Themis has three primary ways to control  
 the EFC voltage. 1) pulse-width modulation  
 digital to analog converter (PWM DAC)  
 that uses a 6-pole Sallen-Key filter with  
 Butterworth response. 2) Two 16-bit DACs –  
 one is used as high meaning higher count or  
 weight, and the other is used as low or lower  
 weight for fine tuning. 3) A programmable  
 gain amplifier (PGA) as an option for the  
 voltage reference for the DACs.

Page 3 in “QEX-1905-Westmoreland-  
 Schematics=QEXfiles.PDF” on the [www.  
 arri.org/QEXfiles](http://www.arri.org/QEXfiles) web page shows the  
 Themis EFC circuitry schematic.

Themis can also use the voltage reference  
 from the OCXO, if it's available. There's  
 an onboard precision reference that can be  
 used as an option. Themis has several ways  
 in which the EFC voltage can be controlled,  
 tuned and conditioned.

### Firmware Details

Themis is based on firmware running  
 on the TI TMS320F28069 and also on user  
 setup of the LEA-6T (current stuff option).  
 The current firmware build is almost entirely  
 written in C code<sup>16</sup> with exception of some  
 routines for the operating system and some of  
 the optimized Digital Control Library (DCL)<sup>17</sup>  
 routines. The firmware for Themis was  
 developed in the TI Code Composer Studio.<sup>18</sup>

Themis is running a port of the Free Real-

Time Operating System (FreeRTOS)<sup>19</sup> using  
 the TI USB Library Interface, and is also using  
 the HRCAP Library. At the time of this writing  
 the firmware is still in beta testing, but soon  
 version 1.0 should be ready for release.

Themis is running the TI DCL, which  
 incorporates linear and non-linear proportional,  
 integral, differential (PID) control algorithms  
 to set and tune the EFC voltage. The HRCAP  
 count acts as the process variable (PV), and  
 the set point (SP) is the HRCAP count of 48.  
 The current Themis firmware also includes a  
 grass-roots<sup>20</sup> PID as well to use as a baseline  
 for the PID results.

This article cannot go into all details of  
 the vast subject of control theory and PIDs.  
 It is at the experimenter's discretion on what  
 PID to apply and how to tune a PID. PID  
 tuning, by itself, is a vast subject. One should  
 not be afraid to do PID tuning. However  
 there is a phrase used that I like to call 'PID  
 Safeties' for a reason.

Figure 2 shows a depiction of a PID that  
 uses SP weighting. This is just an example  
 of the PID architectures that are available via  
 the DCL library. In Figure 2,  $r(k)$  is the SP,  
 $y(k)$  is the PV,  $u(k)$  is the plant output  
 variable that will control PWM, and  $l(k)$  is  
 used to control PID saturation state conditions.  
 $K_r$  sets the weight for the SP.

The most important voltages on Themis  
 are brought into the onboard ADC, so an  
 alternative way to run the PID is to use the  
 voltage reading as well. An inner and outer  
 PID control method can be done using both

the ADC readings and the HRCAP counts.

Figure 3 shows an example of the output from the grass-roots PID. As an experiment to measure the efficacy of the PID algorithm, the SP was set to one-half of normal.

- CH — represents high HRCAP counts as converted from the HRCAP Lib in IQ format. CH is typically used as the PV in the Themis code.
- CL — represents the low HRCAP counts. Keep in mind that unless a non-linearity is encountered,  $CH + CL = 96$ .
- D — represents the positive duty counts as in the full-scale counts of the HRPWM register setting.
- PWM\_X — represents the non-filtered or unconditioned output from the PID function.
- PV — represents the Process Variable — what's being measured/observed.
- SP — represents the Set Point — the desired value the PID should settle upon.
- PDC — represents the Positive Duty Cycle as related to the total HRPWM count as the basis.
- Err — represents the difference between the Process Variable and Set Point.
- PID Delta — represents the difference between the new PWM\_X and the (n-1) PWM\_X.
- DC — represents a data set counter — IQ data is stored in buffers and circularly rotated.

Having a debug display of this nature is invaluable to the experimenter while PID algorithms are being developed.

## Bluetooth/Wi-Fi Wireless Interface

Themis has an optional connector for a Bluetooth or Wi-Fi (or perhaps another radio interface that meets the connector specification)<sup>21</sup> in which to send out GPS data or other data the experimenter would like sent. Two-way communication has been tested on this interface. Figure 4 depicts the GPS data being received from an adjacent PC over Bluetooth.

## Results

Themis has been used with a 3.3V as well as a 5.0 V OCXO, and has been plugged into the Atlas bus. The OpenHPSDR platform uses the 10 MHz reference clock and can frequency-calibrate using the Themis 10 MHz clock signal on the Atlas bus.

Figure 5 shows a candid image of the Themis board plugged into the Atlas bus, inside the Pandora chassis.

The following images from the u-center application show the LEA-6T-1 GPS module in timing mode and showing satellite data. Figure 6 shows the u-center with LEA-6T in timing mode. Figure 7 shows the u-center screen output from LEA-6T

```

COM10 - PuTTY
Session Special Command Window Logging Files Transfer Hangup ?
CH:24,CL:73,D:895.68,PWM_X:0.00,PV:24.00,SP:24.00,PDC:37.80,Err:0.00,PD:0.00,DC:4
CH:22,CL:73,D:1010.88,PWM_X:40.40,PV:22.00,SP:24.00,PDC:29.80,Err:-2.00,PD:10.60,DC:5
CH:22,CL:72,D:1009.44,PWM_X:40.20,PV:22.00,SP:24.00,PDC:29.90,Err:-2.00,PD:-0.20,DC:1
CH:25,CL:70,D:896.40,PWM_X:24.50,PV:25.00,SP:24.00,PDC:37.75,Err:1.00,PD:-15.70,DC:2
CH:25,CL:69,D:900.00,PWM_X:25.00,PV:25.00,SP:24.00,PDC:37.50,Err:1.00,PD:0.50,DC:3
CH:25,CL:70,D:899.28,PWM_X:24.90,PV:25.00,SP:24.00,PDC:37.55,Err:1.00,PD:-0.10,DC:4
CH:22,CL:72,D:1013.04,PWM_X:40.70,PV:22.00,SP:24.00,PDC:29.65,Err:-2.00,PD:15.80,DC:5
CH:24,CL:71,D:1013.04,PWM_X:0.00,PV:24.00,SP:24.00,PDC:29.65,Err:0.00,PD:-10.60,DC:1
CH:26,CL:68,D:860.40,PWM_X:19.50,PV:26.00,SP:24.00,PDC:40.25,Err:2.00,PD:-10.60,DC:2
CH:26,CL:71,D:861.84,PWM_X:19.70,PV:26.00,SP:24.00,PDC:40.15,Err:2.00,PD:0.20,DC:3
CH:24,CL:70,D:861.84,PWM_X:0.00,PV:24.00,SP:24.00,PDC:40.15,Err:0.00,PD:10.00,DC:4
CH:21,CL:74,D:1048.32,PWM_X:45.60,PV:21.00,SP:24.00,PDC:27.20,Err:-3.00,PD:15.90,DC:5
CH:24,CL:73,D:1048.32,PWM_X:0.00,PV:24.00,SP:24.00,PDC:27.20,Err:0.00,PD:-15.60,DC:1
CH:25,CL:69,D:897.64,PWM_X:24.70,PV:25.00,SP:24.00,PDC:37.65,Err:1.00,PD:-5.30,DC:2
CH:25,CL:70,D:898.56,PWM_X:24.80,PV:25.00,SP:24.00,PDC:37.60,Err:1.00,PD:0.10,DC:3
CH:25,CL:69,D:897.64,PWM_X:24.70,PV:25.00,SP:24.00,PDC:37.65,Err:1.00,PD:-0.10,DC:4
CH:25,CL:73,D:897.12,PWM_X:24.60,PV:25.00,SP:24.00,PDC:37.70,Err:1.00,PD:-0.10,DC:5
CH:24,CL:73,D:897.12,PWM_X:0.00,PV:24.00,SP:24.00,PDC:37.70,Err:0.00,PD:5.00,DC:1
CH:22,CL:73,D:1009.44,PWM_X:40.20,PV:22.00,SP:24.00,PDC:29.90,Err:-2.00,PD:10.60,DC:2
CH:23,CL:72,D:969.64,PWM_X:34.70,PV:23.00,SP:24.00,PDC:32.65,Err:-1.00,PD:-5.50,DC:3
CH:23,CL:71,D:972.00,PWM_X:35.00,PV:23.00,SP:24.00,PDC:32.50,Err:-1.00,PD:0.30,DC:4
CH:25,CL:70,D:896.40,PWM_X:24.50,PV:25.00,SP:24.00,PDC:37.75,Err:1.00,PD:-10.50,DC:5
CH:26,CL:69,D:860.40,PWM_X:19.50,PV:26.00,SP:24.00,PDC:40.25,Err:2.00,PD:-5.20,DC:1
CH:25,CL:69,D:898.56,PWM_X:24.80,PV:25.00,SP:24.00,PDC:37.60,Err:1.00,PD:-5.30,DC:2
CH:25,CL:72,D:896.40,PWM_X:24.50,PV:25.00,SP:24.00,PDC:37.75,Err:1.00,PD:-0.30,DC:3
CH:24,CL:73,D:896.40,PWM_X:0.00,PV:24.00,SP:24.00,PDC:37.75,Err:0.00,PD:5.00,DC:4
CH:22,CL:73,D:1009.72,PWM_X:40.10,PV:22.00,SP:24.00,PDC:29.95,Err:-2.00,PD:10.60,DC:5
CH:23,CL:72,D:969.12,PWM_X:34.60,PV:23.00,SP:24.00,PDC:32.70,Err:-1.00,PD:-5.50,DC:1
CH:23,CL:71,D:971.28,PWM_X:34.90,PV:23.00,SP:24.00,PDC:32.55,Err:-1.00,PD:0.30,DC:2
00:00:47 Connected SERIAL/19200 8 N 1
  
```

Figure 3 — An example of the output from the grass-roots PID output.

```

COM20 - PuTTY
Session Special Command Window Logging Files Transfer Hangup ?
GPGSV,4,4,15,32,71,036,46,46,192,46,51,44,156,47*40
GPGGLL,3718.52448,N,12147.72028,W,022227.00,A,D*75
GGPZDA,022227.00,20,08,2018,00,00*60
GPRMTC,022228.00,A,3718.52447,N,12147.72030,W,0.005,,200818,,D*63
GPEVTG,,T,M,0.005,N,0.010,K,D*22
GPGGA,022228.00,3718.52447,N,12147.72030,W,2,11,0.94,70.8,M,-29.9,M,0.000*52
GPGSA,A,3,10,14,18,51,20,31,32,11,08,22,01,,1.78,0.94,1.51*05
GPGSV,4,1,16,01,23,316,34,04,,28,08,28,250,47,10,45,071,42*40
GPGSV,4,2,16,11,32,303,30,14,81,236,48,18,48,307,37,20,21,092,44*72
GPGSV,4,3,16,21,03,143,35,22,18,289,17,24,01,032,,27,19,215,*78
GPGSV,4,4,16,31,29,157,48,32,71,036,46,46,46,192,47,51,44,156,47*74
GPGGLL,3718.52447,N,12147.72030,W,022228.00,A,D*7C
GGPZDA,022228.00,20,08,2018,00,00*6F
GPRMTC,022229.00,A,3718.52445,N,12147.72032,W,0.007,,200818,,D*60
GPEVTG,,T,M,0.007,N,0.013,K,D*23
GPGGA,022229.00,3718.52445,N,12147.72032,W,2,12,0.94,70.8,M,-29.9,M,0.000*50
GPGSA,A,3,10,14,18,51,20,27,31,32,11,08,22,01,,1.78,0.94,1.51*00
GPGSV,4,1,16,01,23,316,34,04,,27,08,28,250,47,10,45,071,42*4F
GPGSV,4,2,16,11,32,303,29,14,81,236,48,18,48,307,38,20,21,092,44*75
GPGSV,4,3,16,21,03,143,35,22,18,289,19,24,01,032,,27,19,215,27*73
GPGSV,4,4,16,31,29,157,48,32,71,036,46,46,46,192,47,51,44,156,47*74
GPGGLL,3718.52445,N,12147.72032,W,022229.00,A,D*7D
GGPZDA,022229.00,20,08,2018,00,00*6E
GPRMTC,022230.00,A,3718.52443,N,12147.72034,W,0.008,,200818,,D*67
GPEVTG,,T,M,0.008,N,0.016,K,D*29
GPGGA,022230.00,3718.52443,N,12147.72034,W,2,11,0.94,70.8,M,-29.9,M,0.000*5B
GPGSA,A,3,10,14,18,51,20,31,32,11,08,22,01,,1.78,0.94,1.51*05
GPGSV,4,2,16,11,32,303,29,14,81,236,48,18,48,307,38,20,21,092,44*75
GPGSV,4,3,16,21,03,143,35,22,18,289,19,24,01,032,,27,19,215,*76
GPGSV,4,4,16,31,29,157,48,32,71,036,46,46,46,192,46,51,44,156,47*75
GPGGLL,3718.52443,N,12147.72034,W,022230.00,A,D*75
GGPZDA,022230.00,20,08,2018,00,00*66
00:00:15 Connected SERIAL/115200 8 N 1
  
```

Figure 4 — GPS data from the Bluetooth option on Themis.



Figure 5 — An image of the Themis board plugged into the Atlas bus inside the Pandora chassis.



Figure 6 — The u-center with LEA-6T in timing mode.

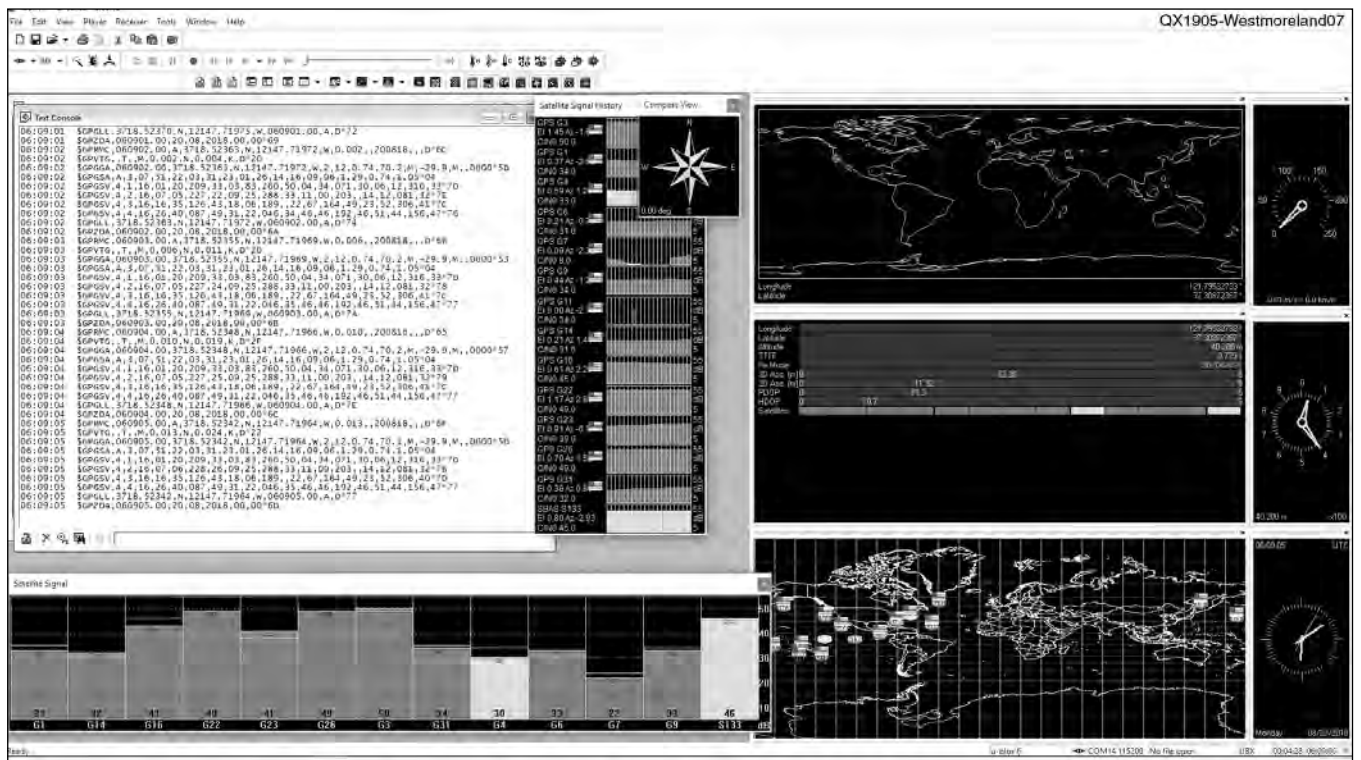
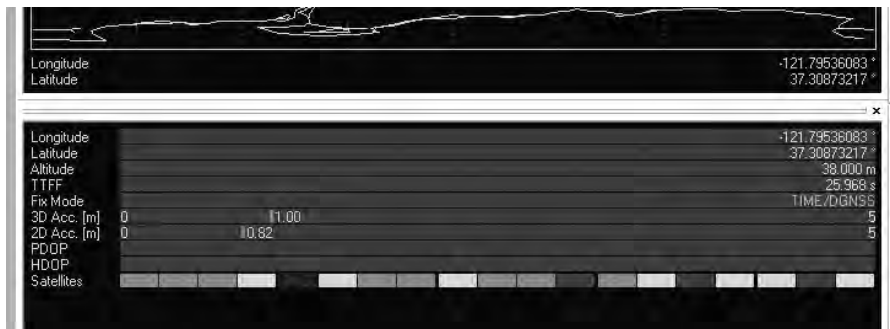


Figure 7 — The u-center screen output from LEA-6T module.

module. Figure 8 shows the PowerSDR display that currently has a frequency reference slightly off frequency. You can see by the spectral image that the current reference is off frequency.

Figure 9 shows the Atlas bus selected as the Themis 10 MHz clock reference in

PowerSDR. Figure 10 shows the frequency calibration returned (notice correction factor) before switching to Themis. Finally, Figure 11 shows the results after using the Themis GPSDO as the 10 MHz clock input. You can now see from the spectral image waterfall plus the correction factor that the frequency

is corrected to 10 MHz using the GPSDO provided by Themis.

The PC running PowerSDR can use the output from the LEA-6T USB interface to synchronize the PC clock to GPS time. This is especially useful when running digital modes with OpenHPSDR. Figure 12 shows

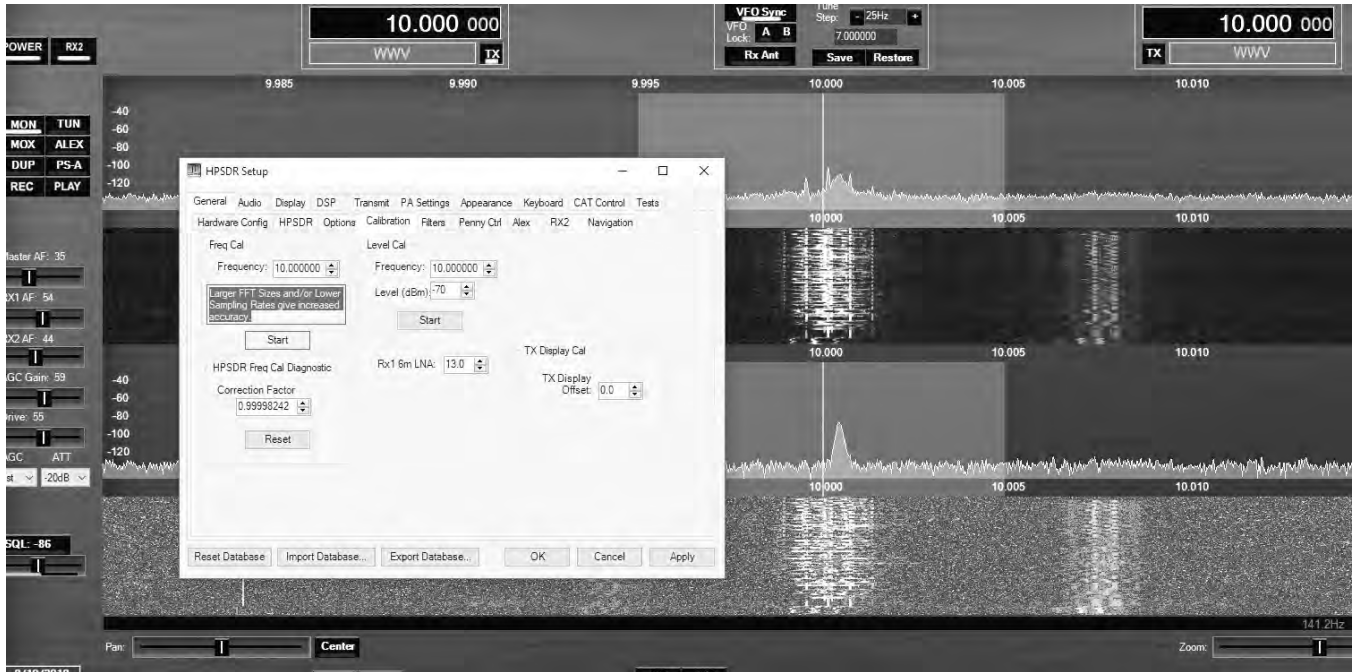


Figure 8 — PowerSDR showing a frequency reference that is off frequency.

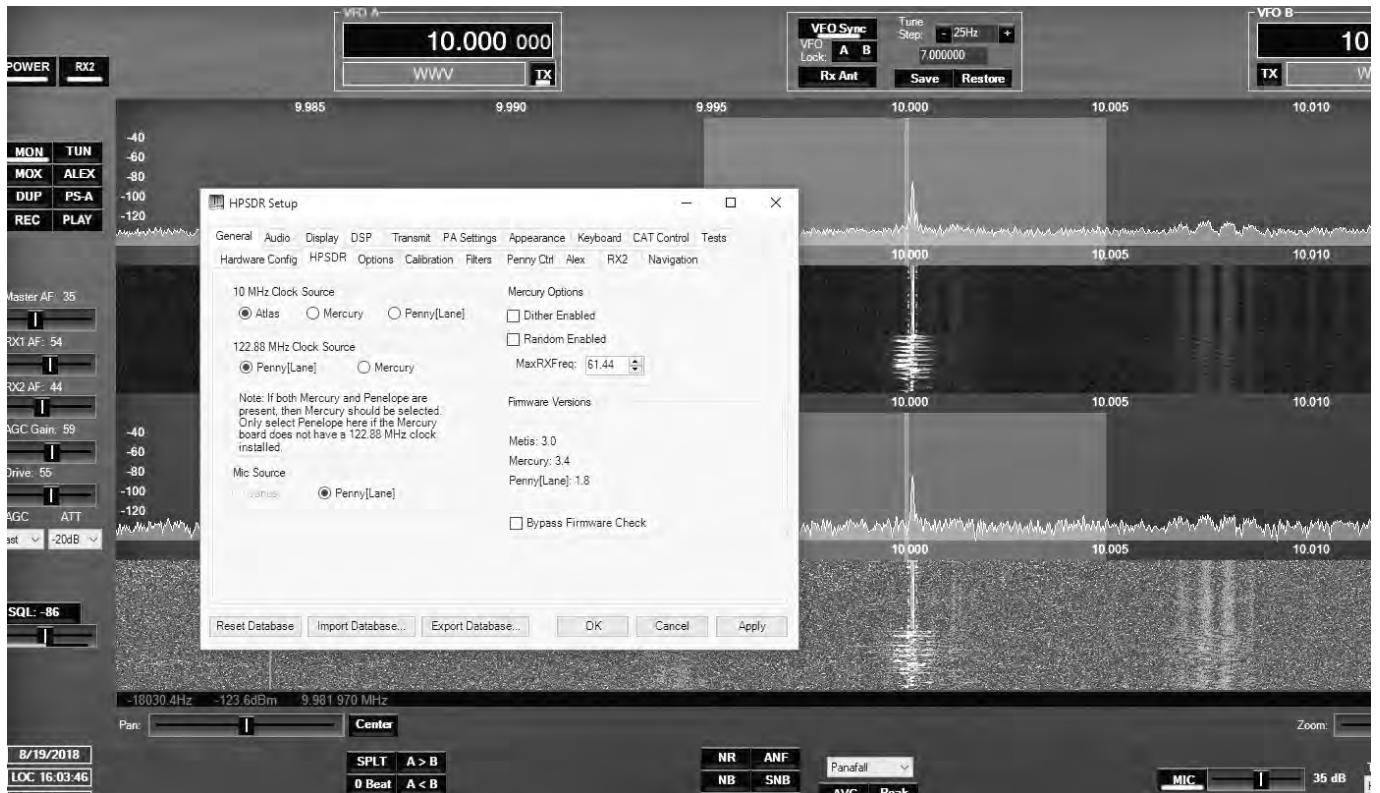


Figure 9 — The Atlas bus selected as the Themis 10 MHz clock reference in PowerSDR.

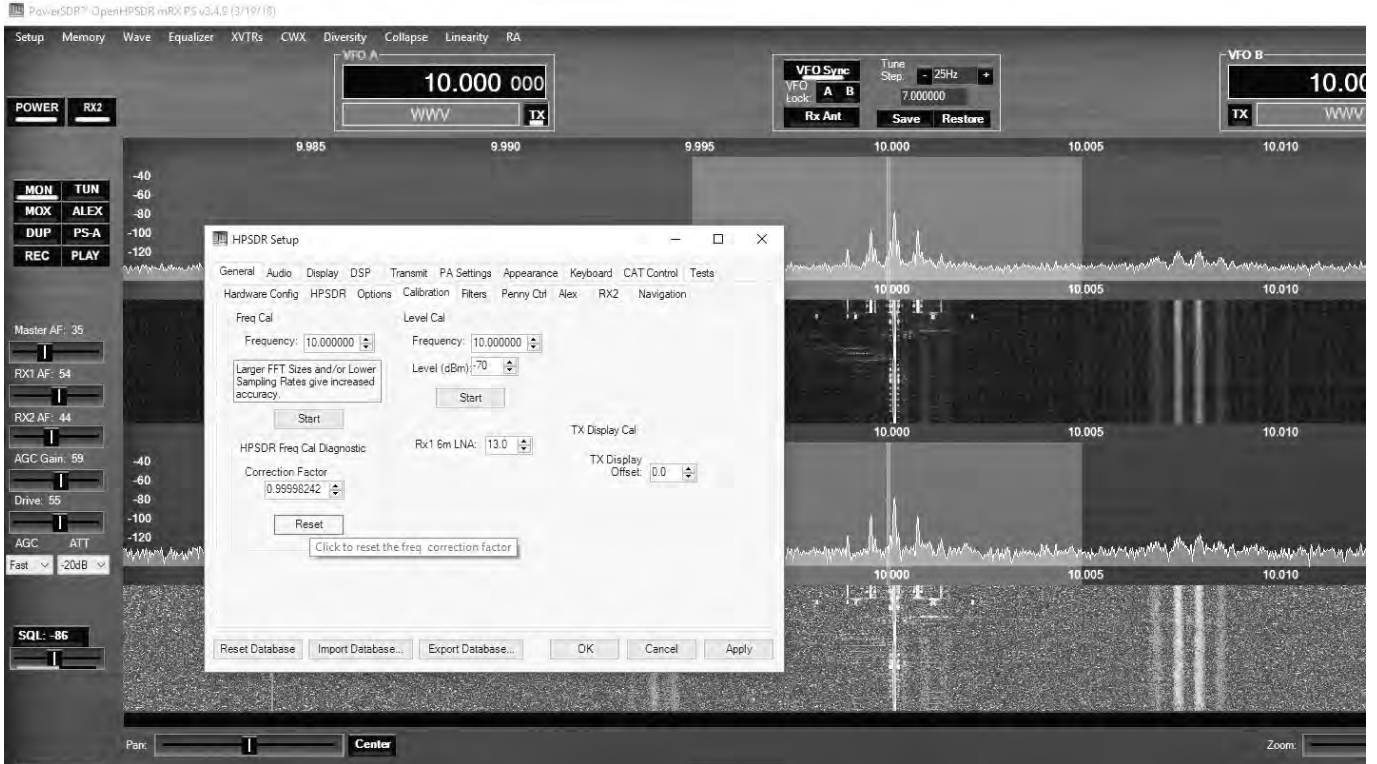


Figure 10 — The frequency calibration returned (notice the correction factor) before switching to Themis.



Figure 11 — The results after using the Themis GPSDO as the 10 MHz clock input.

using a 3rd party utility application that will take the data from the GPS USB output and set the clock on the PC.<sup>22</sup>

Figure 13 shows a capture from a debug session on Themis with the PWM DAC on the left hand side (LHS) and the inputs to the HRCAP register on the right hand side (RHS). The square-wave-like upper waveform on the left is the signal fed to the PWM DAC and the constant waveform below it is the EFC voltage. On the right is the output from the ECL AND gate in the upper dashed waveform, and the wide-dashed waveform on the bottom right is the signal from the GPS Engine. In the com port window on the left is the output from the Bluetooth module and on the right is debug data regarding the debug PID running on Themis.

Timing has been checked with frequency counters from two major manufacturers and differential signaling has also been checked using differential probes, and all looks good enough at the time of this writing to be used in the OpenHPSDR Atlas bus.

Measurements such as phase noise<sup>23</sup>, jitter, Allen deviation<sup>24</sup>, and so on, will be done at a future date when the author's budget allows for it. However, the chosen OCXO will largely determine the values for all these types of measurements.

## Physical Project Development

I discussed Themis with many people. I did the schematic capture, board layout, simulations in LTSpice<sup>25</sup> and Spice<sup>26</sup> in Altium<sup>27</sup>, created the Gerber files for PCB manufacture, bill of materials, and assembly package, and submitted to a very helpful local board shop that did the PCBA fabrication, assembly, and electrical testing. The initial results from Themis have been good.

I must mention that it is essential to set up a GPS timing base station, one that includes a good quality GPS antenna, see Figure 14, specifically designed<sup>28</sup> for timing applications. Also, good RF cabling and protection equipment such as a Polyphaser<sup>29</sup> surge suppressor are essential.

## Future Improvements

Some areas and ideas for improvement for Themis include the following.

- Lower power OCXOs are becoming commercially available, it will be interesting to see the real performance of those devices.
- ECL uses quite a bit of power and generates heat — minimizing the amount of ECL on the board is a priority even though ECL provides good timing results.

- Themis is a good experimenter's platform with lots of options. Maybe subsequent designs will be smaller and focus only on specific options.
- Powering Themis from the Anderson Powerpole<sup>®</sup> option is currently preferable due to the high starting current of the board. Getting start-up current requirements minimized is a future design goal but is dependent on the start-up current of the selected OCXO.
- Some newer OCXOs control EFC via I2C, SPI, or an alternate control bus. Adapt Themis to work with these types of OCXOs as appropriate.
- At the time of this writing, the GPS Packet, I2C and 1PPS features over the Atlas Interface have not been verified but are functional.

Finally, can Themis perform at a Stratum-II level<sup>30</sup> or better on a sub-US\$1,000 budget?

## Closing Thoughts

Working on Themis took me on a journey of seemingly endless discovery.<sup>31</sup> The topics covered the depth and breadth of the information. The people who have worked on this issue provided me with guidance. This was in some ways the most satisfying part of the project design. Of course, to see Themis

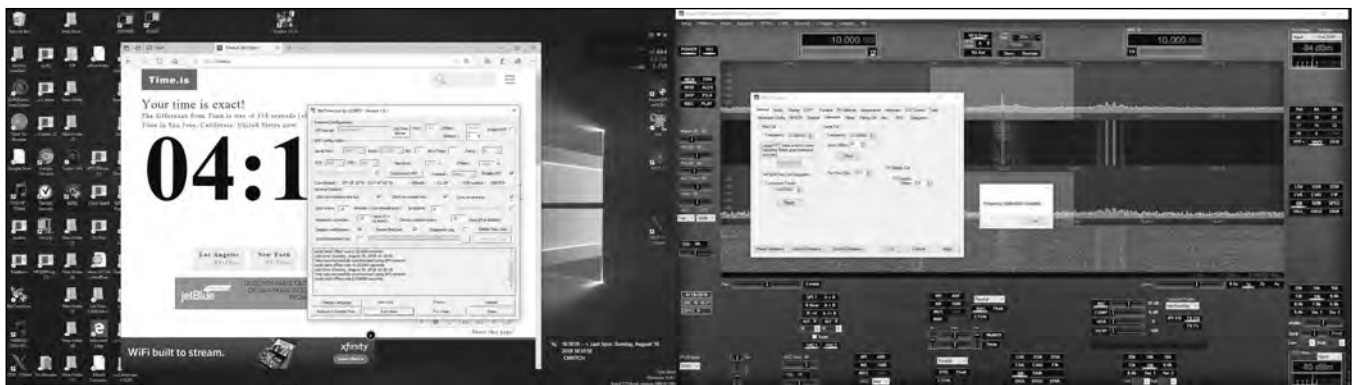


Figure 12 — A 3rd party utility application takes the GPS USB data output and sets the PC clock.



Figure 13 — A capture from a debug session on Themis with the PWM DAC on the Left Hand Side and the inputs to the HRCAP Register on the Right Hand Side.



Figure 14 — GPS timing antenna.

actually working in an Atlas bus is rewarding as well. It seems there's always something new to learn, something new and different to try, some new method and technique to try. That is why Amateur Radio is such a rewarding and satisfying hobby.

### Special Thanks

The disciplining engine required much thought and design work. I especially want to thank Phil Harman, VK6PH (formerly VK6APH), for his numerous discussions and inputs on this vast subject. I also want to thank Bryan Milliren of MTI-Milliren who provided invaluable input on OCXOs and some of the intricacies involved in the discipline of OCXOs and for his initial reviews of the project.

For some of the PID specific issues including advice on PID tuning, I want to thank Richard Poley. Richard and I had many chats over internet messaging, and he was a big help in getting some of the issues I was having with TI's DCL library running efficiently on Themis. It was an honor and joy on my part to collaborate with someone so experienced in the field of control theory.

A special thanks goes out to Casey Stys at On Semiconductor for his help and assistance with ECL issues and simulation questions I had early in the project development cycle.

A special thank you also goes out to Bert Kehren, formerly WB5MZJ, for our

numerous Friday afternoon discussions regarding timing, GPS, and some of the early ideas for the Themis project. Bert's knowledge is as broad and vast as anyone I've ever discussed the subject with; it was a true joy to discuss this subject with him.

I would also like to thank u-Blox for doing two complete Engineering Reviews of Themis, one when the schematic was complete and then again once the layout and PCB fab and assembly were complete. I am grateful to them for voluntarily performing the design reviews. U-Blox also did GPS performance reviews of data and metrics gathered from data I sent them from the THEMIS GPSDO LEA-6T modules once I had basic functionality, which showed good performance.

During the early days of the project when we were discussing Khronos I talked with Said Jackson of Jackson Labs. I owe a debt of gratitude to Said for his assistance in the early days of this project and also in piquing my curiosity as to how GPSDOs work, which ultimately led to the development of Themis.

### Themis Technical Addendum — Timing Discussion

Themis was designed to maintain timing specifications over temperature with temperature compensated ECL, so timing delays from the GPS receiver and from the OCXO to the disciplining engine can be

deterministically measured and controlled. With this feature, it's possible to achieve accurate timing with respect to the received signal from the GPS satellite constellation within an accurate and measurable resolution.

The governing expressions are below.

$t_{delayGPS}$  = propagation delay of GPS output into the GPSDO disciplining engine

$t_{delayOCXO}$  = propagation delay of OCXO output into the GPSDO disciplining engine

$PID_{SPideal}$  = biased PID set-point to align OCXO leading edges with actual GPS signal

Once digital lock has been achieved, a technique that I call 'PID-biasing' can be used to time-correct the leading edge of the OCXO clock so that it is in alignment with actual GPS time. Taking advantage of the Boolean characteristics of the circuit's ECL AND gate, the PID SP can be adjusted to compensate for the time delay of the received GPS signal plus the on-board propagation delay of the OCXO signal into the disciplining engine. Since the OCXO is already digitally locked, adjusting the PID slightly will cause the OCXO timing to lead the on-board GPS timing reference. By adding the delays of the GPS signal and the OCXO we get the following equation.

$$PID_{SPideal} = 48_{HRCAPclks} - (t_{delayGPS} + t_{delayOCXO}) \quad (A1)$$

To keep the OCXO edge aligned, a boundary condition is that the PID adjustment be within one-half of the HRCAP clock count we're using from the disciplining engine.

$$(t_{delayGPS} + t_{delayOCXO}) < \frac{48_{HRCAPclks}}{2} \quad (A2)$$

If it's necessary to adjust more than one-half of the ideal HRCAP clock count, then the OCXO can wrap. That is, instead of leading, the OCXO could be lagging, and that is an incorrect condition. By maintaining the boundary condition, the OCXO will always lead and will compensate for the aggregate delays, and will be in alignment with actual GPS time.

The experimenter is always open to the options of changing the timing characteristics by adjusting the GPS timing signal since Themis allows for almost all variables to be changed in the programming, except for the OCXO, of course. The EFC control of the OCXO will keep the output of the OCXO within its respective specifications for the normal life of the OCXO. Biasing the PID will not change that.

The maximum biasing amount that we have available with the timing represented is,

$$\frac{1}{2} HRCAP_{CLKS_{ideal}} = 24 HRCAP_{CLKS} > 200 \text{ ns} \quad (A3)$$

Most of the ECL devices used in the design has propagation delay on the order of 1 nanosecond per device, so, this resolution is well within what we can program in the PID control.

To demonstrate this concept let,

$$t_{delay_{GPS}} = 70 \text{ ns}$$

$$t_{delay_{OCXO}} = 30 \text{ ns}$$

which gives,

$$HRCAP_{clks} = \frac{100 \text{ ns}}{8.33 \text{ ns}} = 12 HRCAP_{clks}$$

and

$$PID_{sp_{ideal}} = (48 - 12) HRCAP_{clks} = 36 HRCAP_{clks}$$

The cardinal boundary condition is therefore met. Of course, these numbers are large, but it illustrates the flexibility in the adjustment range possible.

The following Figures are of oscilloscope

captures that demonstrate the PID-biasing concept. In Figure 15 the upper trace is taken immediately from the output of the first ECL driver on Themis, and the bottom trace is taken directly from the output of the 10 MHz OCXO. In Figure 16 the PID is biased by 12 from the ideal calculation. It is the logical AND of the bottom trace with the 10 MHz OCXO. The new SP for the PID is 36, so the PID will run with this SP until a new SP is set. In Figure 17, the upper trace shows the biasing of the OCXO that compensates for the propagation delays of the GPS and the OCXO.

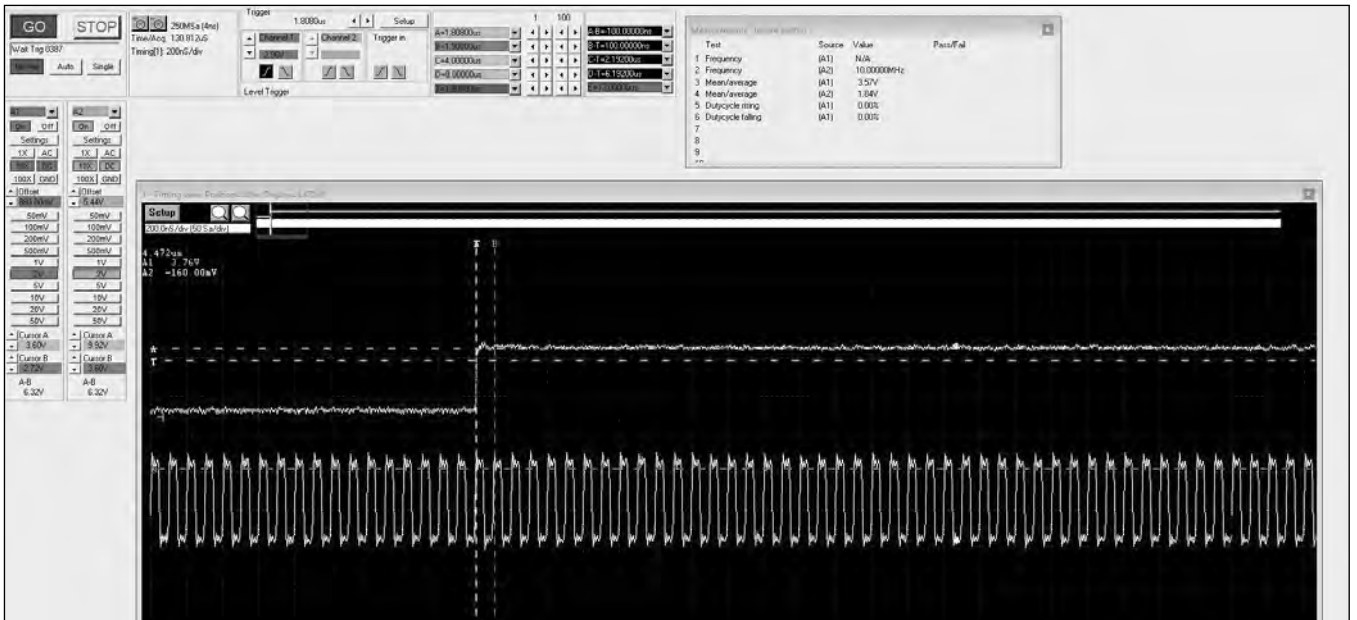


Figure 15 — The upper trace is the GPS 1PPS signal and the bottom is the 10 MHz OCXO.



Figure 16 — The upper trace is the logical AND of the bottom trace with the 10 MHz OCXO.

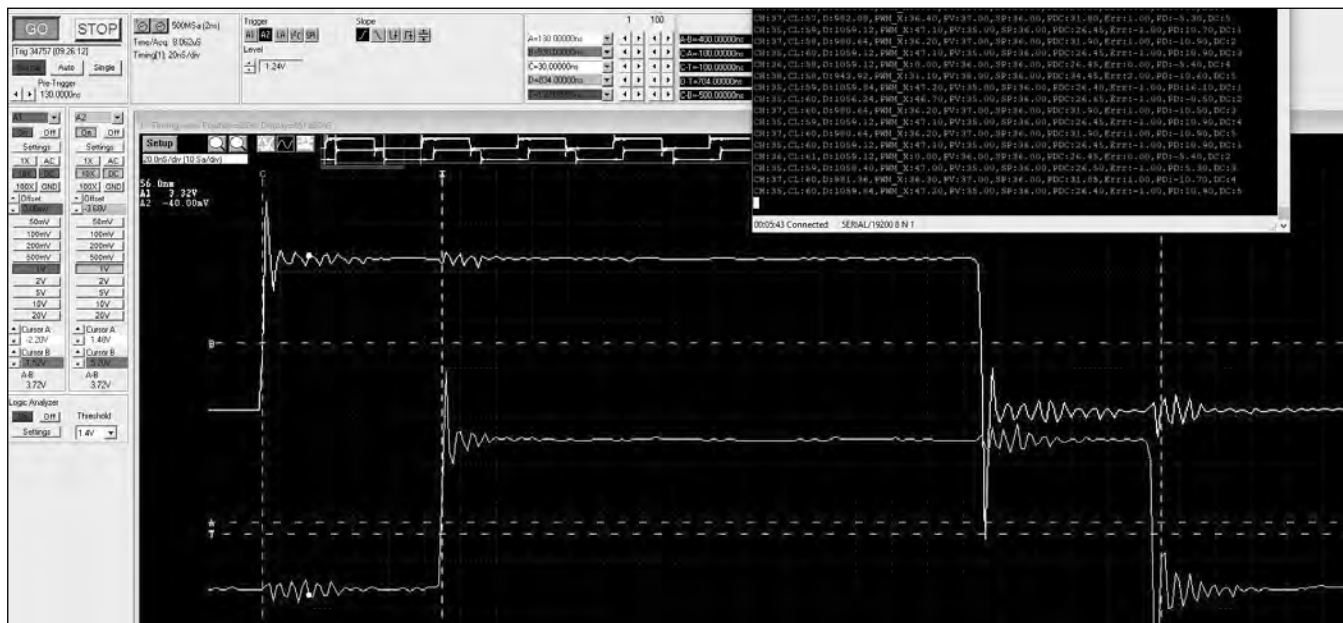


Figure 17 — The upper trace is OCXO input into the SYNC (the HRCAP input) circuit and the bottom trace is from the GPS.

John C. Westmoreland, AJ6BC, received the Technicians license, KJ6HCV, in April 2010, and his General and Amateur Extra licenses in 2011. In the early 1980s, while serving in the US Merchant Marine on the USNS Yukon, he constructed his first Yagi antenna per plans from the ship's radio operator. He had been interested in radio prior to this; but building that antenna from scratch, mounting it, and seeing what the performance increase was for our ship's radio systems got him hooked on radio. He became interested in the OpenHPSDR initiative and set up his first Software Defined Radio. John is also a Volunteer Examiner for the ARRL and has participated with local VE groups and on-site exams at the local annual Maker-Faire.

John received his BSEE degree from Lamar University of Beaumont, TX in May, 1988 and has been a licensed Professional Engineer in Electrical Engineering in California since 2002. He's had a consulting business that specializes in embedded systems design and firmware development for over 10 years. John is the inventor on US Patent 5,325,071, "Operational amplifier with digitally programmable gain circuitry on the same chip."

## Notes

<sup>1</sup>Westmoreland, AJ6BC, "High Performance Software Defined Radio", Pacificon 2014, Santa Clara, CA; [openhpsdr.org/doc/PacificCon2014/High%20Performance%20Software%20Defined%20Radio%20-%20Pacificon%202014.pdf](http://openhpsdr.org/doc/PacificCon2014/High%20Performance%20Software%20Defined%20Radio%20-%20Pacificon%202014.pdf).

<sup>2</sup>Links to Themis Schematic: [openhpsdr.org/themis.php](http://openhpsdr.org/themis.php).

<sup>3</sup>Atlas bus: The backplane for the OpenHPSDR platform using a connector of 3 columns of 32 pins for a total of 96 pins: [openhpsdr.org/atlas.php](http://openhpsdr.org/atlas.php).

<sup>4</sup>Rubidium Standard example: <https://www.thinksrs.com/products/prs10.html>.

<sup>5</sup>B. Bourke and B. Penrod, "An Analysis of a Microprocessor Controlled Disciplined Frequency Standard", Austron, Inc., 37th Annual Symposium On Frequency Control, IEEE, June 1983.

<sup>6</sup>See, <https://www.nist.gov/pml/walk-through-time-nist-time-services>.

<sup>7</sup>u-Blox LEA-6T: <https://www.u-blox.com/en/product/neolea-6t>.

<sup>8</sup>u-Blox u-center software: <https://www.u-blox.com/en/product/u-center>.

<sup>9</sup>High Resolution Capture (HRCAP), TMS320x2806x Piccolo Technical Reference Manual, Literature Number: SPRUH18G Jan. 2011—Revised Apr. 2017, Texas Instruments, pp.405-424.

<sup>10</sup>Texas Instruments TMS320F28069 Piccolo™ 32-bit MCU with 90 MHz, FPU, VCU, 256 KB Flash, CLA, [www.ti.com/product/TMS320F28069?keyMatch=tms320f28069&tisearch=Search-EN-Everything](http://www.ti.com/product/TMS320F28069?keyMatch=tms320f28069&tisearch=Search-EN-Everything).

<sup>11</sup>High-Resolution Pulse Width Modulator (HRPWM), TMS320x2806x Piccolo Technical Reference Manual, Literature Number: SPRUH18G Jan. 2011 – Revised Apr. 2017, Texas Instruments, Inc., pp. 373-404.

<sup>12</sup>MEMS: <https://abracon.com/product-lineup/timing-synchronization/mems>.

<sup>13</sup>HRCAP Calibration Library: TMS320x2806x Piccolo Technical Reference Manual, Literature Number: SPRUH18G January 2011—Revised Apr. 2017, Texas Instruments, Inc., pp.417-424.

<sup>14</sup>Q (Integer Quotient) Number Format: [processors.wiki.ti.com/images/8/8c/IQMath\\_fixed\\_vs\\_floating.pdf](https://processors.wiki.ti.com/images/8/8c/IQMath_fixed_vs_floating.pdf).

<sup>15</sup>EFC example, Pin 1 of the OCXO in the following: [mti-milliren.com/pdfs/270.pdf](http://mti-milliren.com/pdfs/270.pdf).

<sup>16</sup>C – The universal ubiquitous programming language, [https://en.wikipedia.org/wiki/The\\_C\\_Programming\\_Language](https://en.wikipedia.org/wiki/The_C_Programming_Language).

<sup>17</sup>C2000 Digital Control Library, Version 3.0, User's Guide, May 2018, Texas Instruments, Inc.; [www.ti.com/tool/c2000-digital-control-library](http://www.ti.com/tool/c2000-digital-control-library).

<sup>18</sup>TI DSP/MCU IDE (Integrated Development Environment): Code Composer Studio, [www.ti.com/tool/CCSTUDIO](http://www.ti.com/tool/CCSTUDIO).

<sup>19</sup>FreeRTOS, Free Real-Time-Operating System, <https://www.freertos.org/>.

<sup>20</sup>Grass-roots PID controller: starting point based largely on a post on this site: <https://control.com/thread/996485795>.

<sup>21</sup>Wireless Module Connector, p. 8 Themis Schematic (See Note 2).

<sup>22</sup>An example of a PC App that will work with the GPS data stream from Themis: [www.maniaradio.it/en/bkktimesync.html](http://www.maniaradio.it/en/bkktimesync.html).

<sup>23</sup>Allan deviation: [https://en.wikipedia.org/wiki/Allan\\_variance](https://en.wikipedia.org/wiki/Allan_variance).

<sup>24</sup>Phase noise: [https://en.wikipedia.org/wiki/Phase\\_noise](https://en.wikipedia.org/wiki/Phase_noise).

<sup>25</sup>LTspice: [www.analog.com/en/design-center/design-tools-and-calculators/ltspice-simulator.html?gclid=EALalQobChmLliobDgt\\_73AIvhcVhCh1KxAoEEAAYA\\_SAAEgJq-fD\\_BwE](http://www.analog.com/en/design-center/design-tools-and-calculators/ltspice-simulator.html?gclid=EALalQobChmLliobDgt_73AIvhcVhCh1KxAoEEAAYA_SAAEgJq-fD_BwE).

<sup>26</sup>Spice Simulation within Altium: [wiki.altium.com/pages/viewpage.action?pagelid=3080273](http://wiki.altium.com/pages/viewpage.action?pagelid=3080273).

<sup>27</sup>Altium PCB Design: <https://www.altium.com/>.

<sup>28</sup>EndRun Technologies Timing Antenna, <https://www.endruntechnologies.com/antennas.htm#kitTFS>.

<sup>29</sup>DGXZ+06NFNF-A, Hybrid ±6 V dc Pass RF Protector <https://www.polyphaser.com/products/rf-surge-protection/dgxz-plus-06nfnf-a>.

<sup>30</sup>Stratum Levels Defined, American National Standards Institute (ANSI), "Synchronization Interface Standards for Digital Networks" (ANSI/T1.101-1987), 1987, [www.raltron.com/wp-content/uploads/2016/08/sync\\_an02-stratumleveldefined.pdf](http://www.raltron.com/wp-content/uploads/2016/08/sync_an02-stratumleveldefined.pdf).

<sup>31</sup>This USCG site, as one example: <https://www.navcen.uscg.gov/>.

# A Different Look at the Phase Locked Loop

*A qualitative analysis of the Phase Loop reveals its utility.*

We take a somewhat different approach to the Phase Lock Loop (PLL) here. Rather than going into design details we discuss mainly the loop characteristics. Thus, this is a qualitative rather than quantitative analysis using salient data from the literature. The design details are covered in the referenced articles. The basic PLL is a negative feedback circuit where the phase of the RF output is locked to the phase of a reference oscillator. It is more accurate than an Automatic Frequency Control (AFC) since, while there may be some residual phase error, the frequency remains the same.

Among other applications, the basic PLL can be looked upon as either an RF power amplifier or an RF frequency multiplier. While this may be considered a strange definition, it will be shown that the PLL can perform either function with a more efficient circuit than with conventional methods. However, certain characteristics must be considered in optimizing its design. From these basic configurations other applications such as FM demodulators, frequency synthesizers, tracking filters, carrier extraction and others can be derived, as shown in the literature.

## Power Amplifier

The power amplifier version of a PLL is the basic form shown in Figure 1. It consists of a crystal oscillator (XO), a phase comparator, a voltage controlled oscillator (VCO) and a filter/integrator. It can provide a high output power at the frequency and accuracy of the low power XO, thus a high equivalent power gain can be realized.

A small sample of the output is phase-

compared with the phase of the XO in the phase comparator. Any error produces a correction voltage  $V_c$  after passing through the low-pass filter/integrator. This voltage is then applied to the VCO to bring it in phase with the XO. Thus the VCO output is at the exact frequency of the XO but at a much higher power level.

## Frequency Multiplier

With the addition of one more component, a frequency divider, as shown in Figure 2, the PLL becomes a frequency multiplier. The output frequency is multiplied by the same factor that the divider divides it. In just one

step, very high frequency multiplication can be obtained without the need of filtering that would otherwise be necessary to eliminate unwanted XO harmonics in conventional multiplier circuits.

## Basic PLL Characteristics and Definitions

PLL is basically a negative feedback circuit and thus it is prone to unwanted oscillations if care is not taken in its design.

### Type and Order

Both type and order are determined by the low-pass/integrator. The Type-1 PLL uses a passive low-pass filter and Type-2

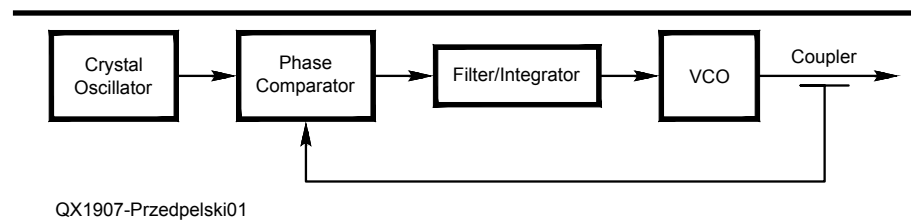


Figure 1 — The power amplifier version of a PLL.

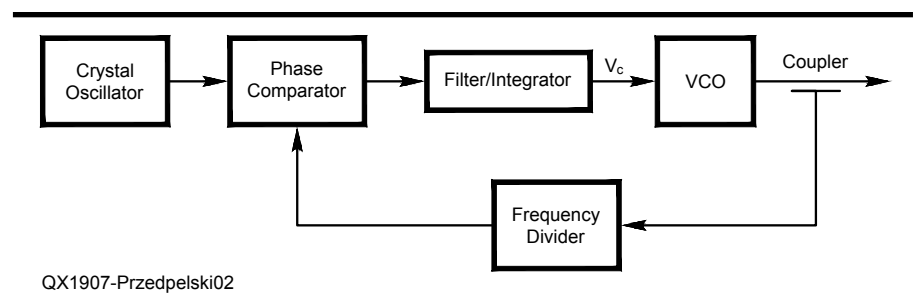


Figure 2 — The PLL as a frequency multiplier.





# Get Started with 3D Printing

*Design and build project boxes and other objects using easily modified 3D printer code.*

I recently received a hand-me-down Bukobot 3D printer (Figure 1). I have been interested in 3D printing for some time, but hadn't yet thought of an application that would cause me to actually buy one. After setting up the printer and printing a few sample objects that I downloaded from **Thingiverse.com**, the time had come to design something for myself. One thing that I had found on **Thingiverse** and printed was a simple knob. I had a variable capacitor with a 3/8" shaft, and I didn't happen to have any knobs like that in my junk box. The knob was created using a programming language called *OpenSCAD* that allows one to describe the geometry of a 3D part. Because it is a programming language, one can have user-modifiable parameters that determine the shape of the part. I was able to change a number to modify the size of the hole in the knob. This is not the only way to create objects for 3D printing. Many 3D modeling software programs exist and several of them are free.

## An L Bracket Starts as a Box

I have since become almost addicted to *OpenSCAD*. I have written programs for many different types of parts. One of my first programs for a simple L bracket is shown in Figure 2.

It starts out as a box (the *OpenSCAD* command to make a rectangular object is 'cube') out of which is removed another box so as to leave just the L bracket. The remainder of the code removes, using the difference command, three cylinders to make holes. The full *OpenSCAD* code for the "L Bracket" is on the [www.arrl.org/QEXfiles](http://www.arrl.org/QEXfiles) web page.

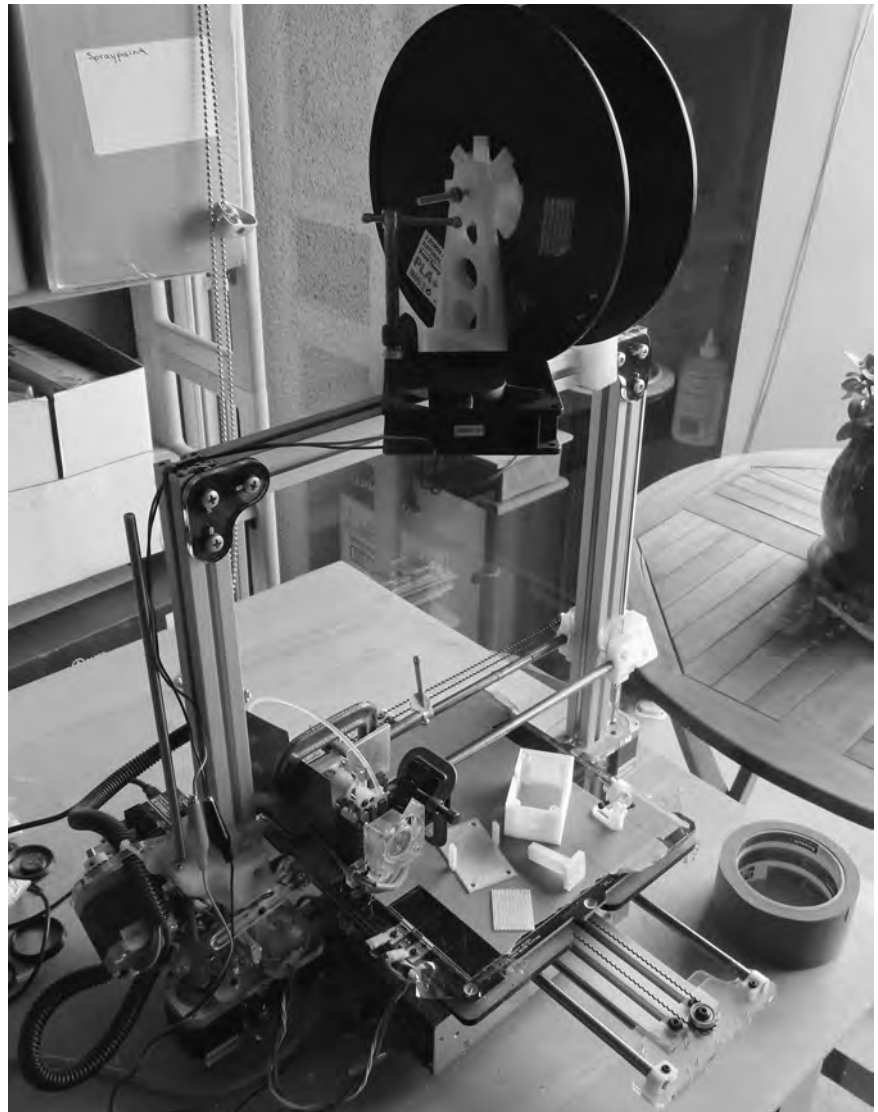


Figure 1 — Bukobot 3D printer with some example 3D-printed parts.

## Box and Lid

After my success with the L bracket, I designed a plastic project box, see Figure 3. For the project box, the user can change the 'wall\_thickness', 'inside\_width', 'inside\_length', 'inside\_depth', 'top\_plate\_thickness', 'support\_diameter', 'support\_hole', 'support\_hole\_depth', 'lid\_hole', 'hole1x', 'hole1y', 'hole1z',

'hole1diameter', 'hole2x', 'hole2y', 'hole2z', and 'hole2diameter'. The "Box&Lid" *OpenSCAD* code is on the [/QEXfiles](#) web page.

Saving the model or hitting the *OpenSCAD* preview button will update the screen with the new box design. If you don't like the holes in the sides, you can set 'hole1diameter' and/or 'hole2diameter' to 0.

The variable 'printphase' tells the

*OpenSCAD* code whether to display the box or the lid or both (this is for debugging only). I did this so that the box and lid would be in the same file and use the same exact dimensions. Before printing, set 'printphase' to 1 to render the box bottom, and then export it to an *stl* file. I then set 'printphase' to 2 to render the lid and export it to another *stl* file. What happens next depends upon the software that you use for your 3D printer. I

Figure 2 — *OpenSCAD* rendering of the L bracket.

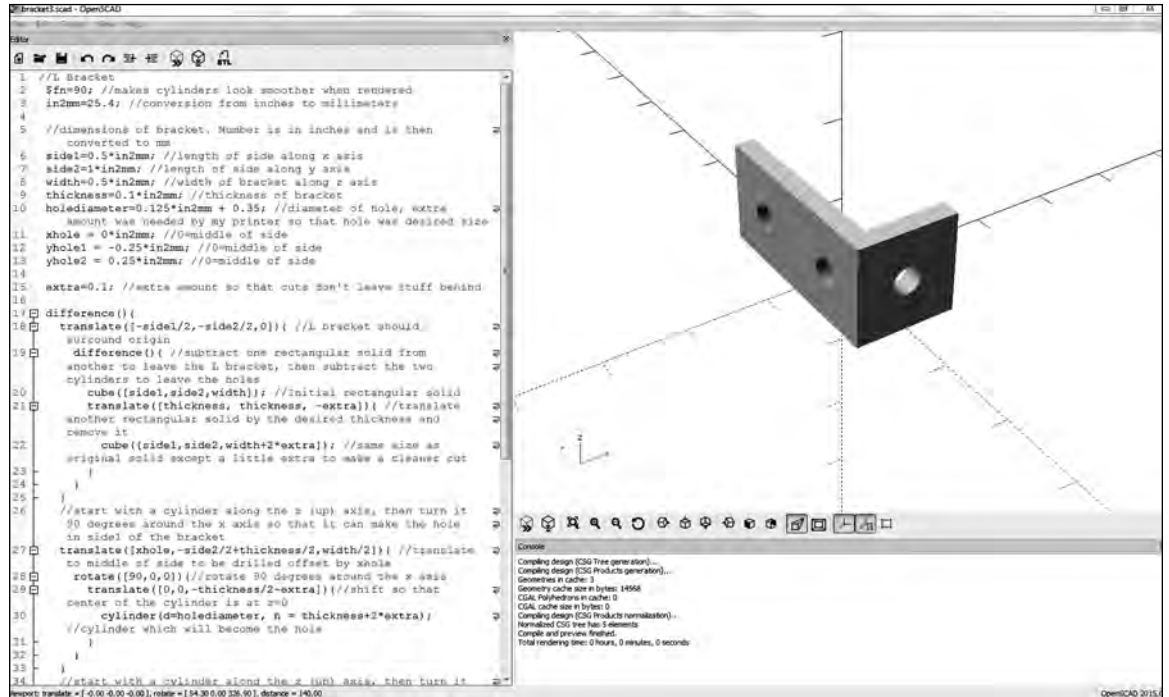
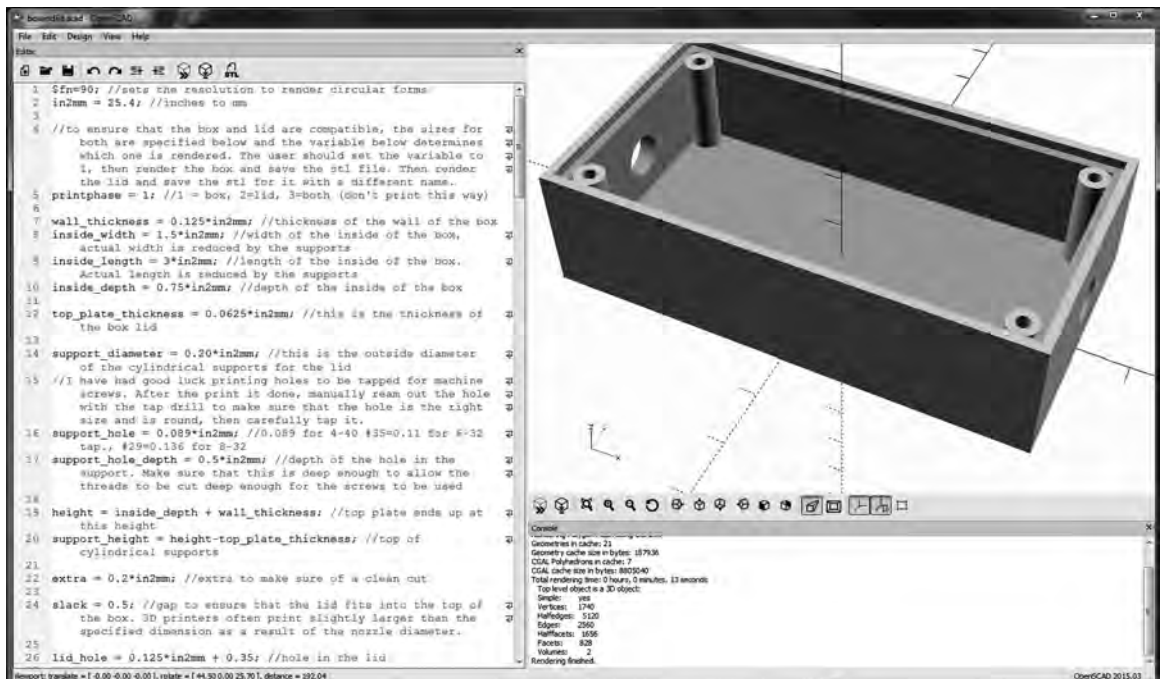


Figure 3 — *OpenSCAD* showing the bottom of the project box.



use *Repetier-Host* with the *Cura* slicer, so I load the *stl* file into *Repetier-Host*, then go to the *Slicer* tab and press slice. Next I select ‘start print’ and watch it go.

Printing a project box takes approximately 2 hours, so I usually just leave the 3D printer going all night and find the completed box sitting on the 3D printer bed when I wake up. Since you can design the box with all the holes in the right places, the only thing left to do is to attach the parts. I find that the entire process takes much less time than in the past when I went to my neighborhood electronics store to buy a box, mark the location of the required holes, and drill the holes. If your project requires rectangular holes or hexagonal holes — no problem — same for boxes shaped like cylinders or polygons.

A second project box holds a small mixer circuit to allow me to use my SDR dongle on the HF bands (Figure 4). I built a third box to hold a small power supply circuit, shortening the posts so that they support the circuit board (Figure 5). Figure 6 shows a 3D printed box, lid, an L bracket and a perforated board.

I plan to experiment with conductive paint to make shielded boxes. However, there is already a 3D printer that can print plastic parts with embedded metallic layers.

### 3D Printing Tips

Here are some 3D printing tips based on my experiences.

(1) Like most people I started with PLA for the print material. I have also printed with ABS, but ABS emits unpleasant fumes. So with ABS use an enclosed printer with an air filter, or print in a well ventilated place.

(2) Make sure that the nozzle is clean before starting to print. It is possible to pause a print, clean the nozzle and restart, but the print won’t be as strong at the joint.

(3) Make sure that the print bed surface is prepared to allow the filament to adhere well. For PLA, you can cover the print bed with blue painter’s tape. This technique has worked well for me. For ABS, I covered the bed with Kapton® tape and turned on the print bed heater.

(4) Make sure that the spacing between the nozzle and the print head is the same at all points. Some printers have self-leveling beds, but others will require you to move the print head to various points on the bed and adjust two or three thumbscrews. The idea is that when printing the first layer, the gap between the nozzle and the bed should be about the thickness of a normal piece of paper. If it is too tight, insufficient filament will be extruded to stick well to the bed. If it is too loose, the filament will just sit on the bed and not stick. There needs to be just the right amount of “squish.”

(5) For large items a “brim” might help

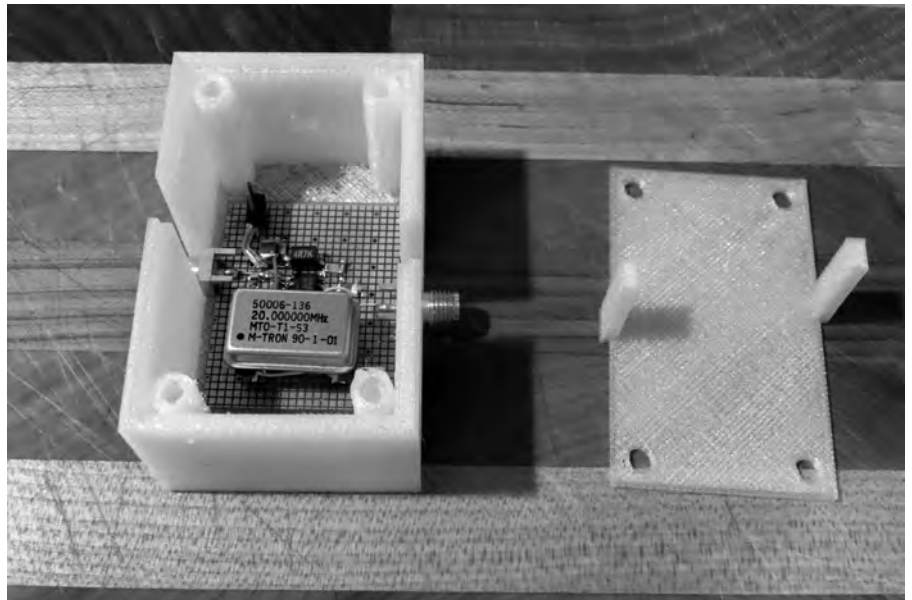


Figure 4 — A second project box holds a mixer circuit.

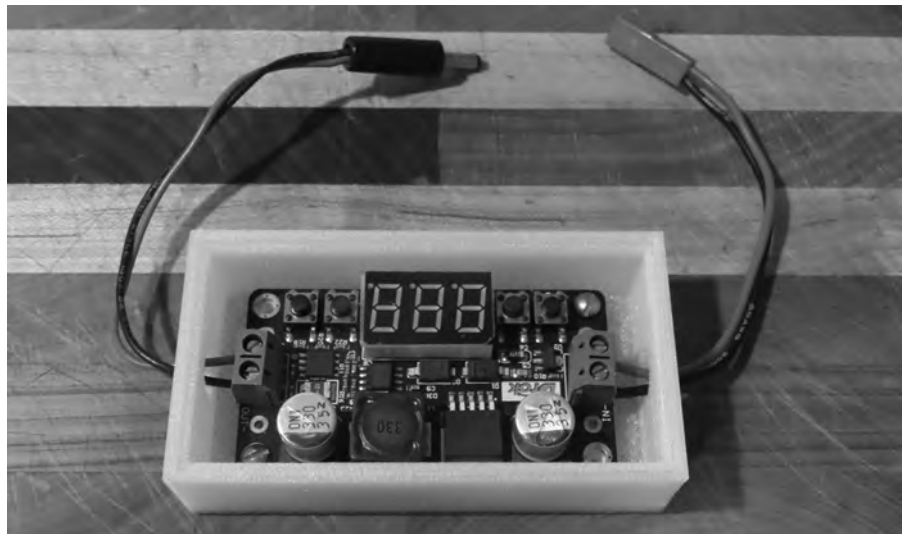


Figure 5 — A third project holds a small power supply circuit board.

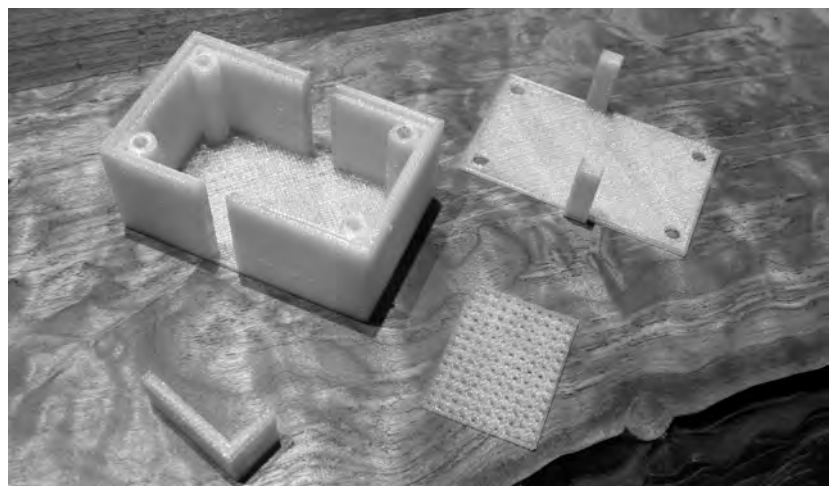


Figure 6 — A 3D printed box, lid, an L bracket, and a perforated board.

to avoid warping. A brim is a thin flat area surrounding the part to be printed like the brim of a hat. It helps hold the object tight to the print bed avoiding warping. Circular holes in the side of the box might not need support, but rectangular holes probably will. Support is a low density scaffolding that the slicer generates to allow the printer to print things that hang out into space like the eaves of a roof edge. You must cut away the support manually. Someday I hope to use a two-nozzle 3D printer to print both PLA filament and a water soluble filament for the support scaffolding at the same time.

(6) Holes must be made slightly larger than desired because the finite printer resolution could result in holes that are too small and perhaps out of round. I gently clean out holes with a drill bit if this happens.

(7) Monitor the printing from time to time to make sure that the filament is moving smoothly. If not, try slowing down the printing. Check the estimated time for completion before changing the speed. If the difference between the old and new times is larger than you have already been printing, just abort the print, clean the printer, and start again.

(8) Parts have a grain like wood and are quite strong along the direction that the filament was extruded, but much weaker from layer to layer. In one case, I printed small holes in the part and sewed Kevlar® thread through the layers to add tensile strength.

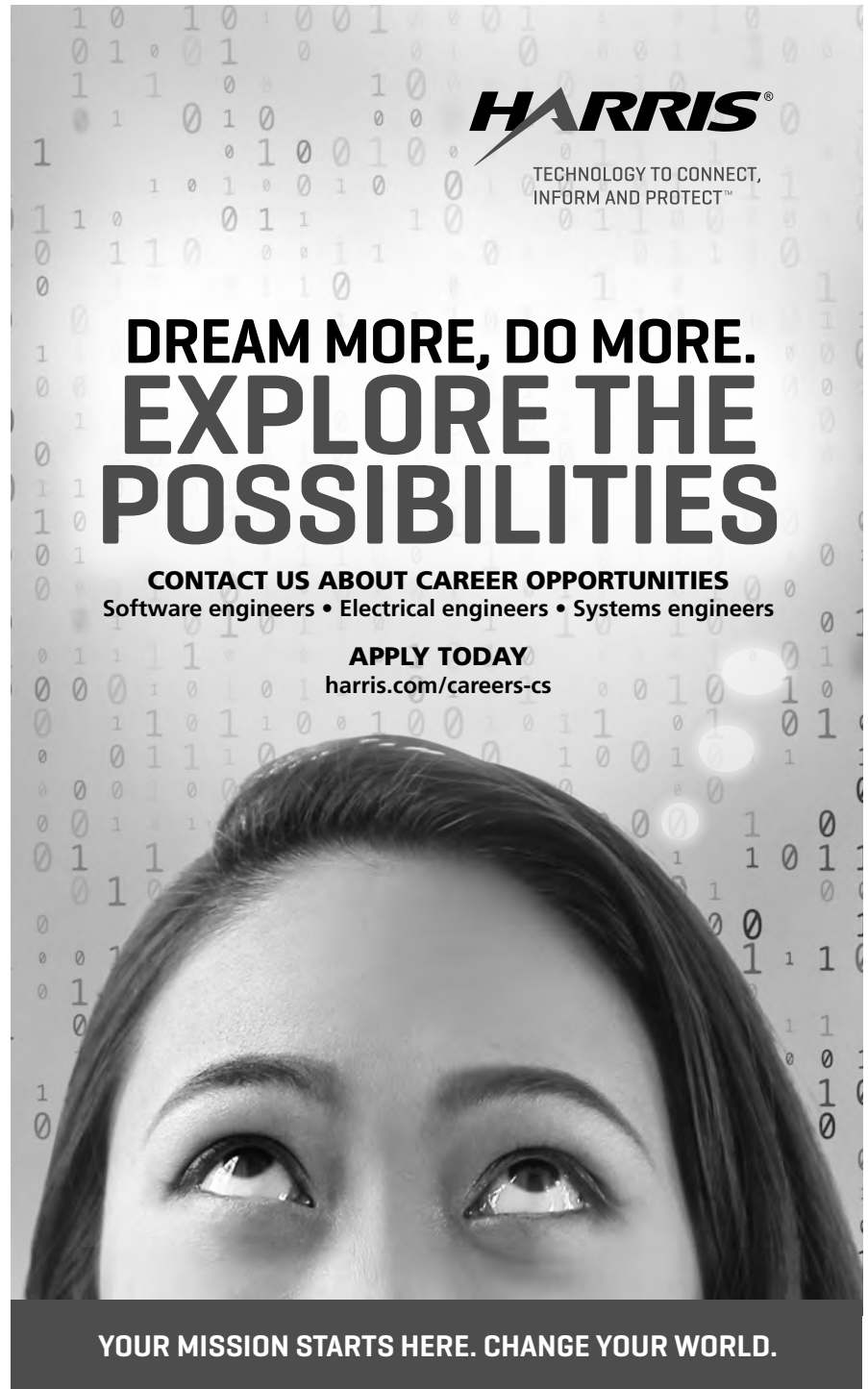
### Final Comments

The price of 3D printers is going down every day. If you aren't ready to buy one for yourself, check out your local makerspace to see if they have one you can use. I initially thought that 3D printing was useful only if one wanted to make more than one instance of an object. I thought that it would take me a long time to learn the CAD tools to design the parts. I also thought that it would take longer to design and print a part than to make it some other way. All of these assumptions turned out to be untrue. I learned how to use *OpenSCAD* very quickly. If you are more visually oriented, there are many easy-to-use 3D modeling programs. It took me a little while to make the first model, but now I can quickly customize it for different purposes. There are many enthusiastic people designing all kinds of things and posting them on **Thingiverse.com**.

This reminds me of the mid 1970s when people were first experimenting with personal computers and freely sharing their software creations. The big difference now is that people are making programs to create hardware, not software.

*Joseph Pingree, WB2TVB, was first licensed as WN2TVB in 1974 and received his present call sign when he upgraded to General Class license in 1976. He received a BS degree from the Massachusetts Institute of Technology in physics, an MS degree from the California Institute of Technology in planetary science, and a PhD in electrical engineering from Cornell University. Since then he has worked*

*as a radar systems engineer for Rockwell International and Boeing. He is married to Karen Kensek, KG6CUK, who helped to polish the manuscript for this article. Joe enjoys casual contest operating, and experimenting with new technology. When he is not working on an electronic project he might be observing the stars or flying model airplanes or rockets.*



**HARRIS**  
TECHNOLOGY TO CONNECT,  
INFORM AND PROTECT™

**DREAM MORE, DO MORE.  
EXPLORE THE  
POSSIBILITIES**

**CONTACT US ABOUT CAREER OPPORTUNITIES**  
Software engineers • Electrical engineers • Systems engineers

**APPLY TODAY**  
[harris.com/careers-cs](http://harris.com/careers-cs)

**YOUR MISSION STARTS HERE. CHANGE YOUR WORLD.**

# Pi Networks With or Without Inductor Loss — Part 1

## *Network synthesis — a tale of many Qs*

A controversy on the definition of the correct total  $Q$  for Pi filters in Bill Kaune's, W7IEQ, *QEX* articles<sup>1,2</sup> is resolved by closer examination of the effect of input terminations on the Pi network. For the case of the networks with inductor loss, some approximate formulas used in an excellent DOS based program by the late Reg Edwards, G4FGQ, are clarified. I show that they are similar to but more accurate than those first propounded by Everitt in 1931. These approximations including one I shall propose here are accurate for the efficiency to within a few percent but are significantly wrong in predicting the component values in some cases. New formulas are obtained based on several design input parameter options. As a prelude to a follow-on article, I shall also provide exact formulas for the power transfer functions for two common input terminations. All these formulas can be easily incorporated into Excel spreadsheets and graphed by the user.

### 1. Introduction

The recent *QEX* articles [*op. cit.*<sup>1,2</sup>] by Bill Kaune, W7IEQ, prompted me to look back into my own notes on the subject and in particular to re-examine an excellent program<sup>3</sup>, I inherited from Reg Edwards, G4FGQ, almost two decades ago. My findings are rather interesting and are reported in this paper.

The subject concerned is an old one. I note that early references date back to Everitt (1931)<sup>4</sup> and the excellent summary in the *Radio Engineers Handbook* by Terman (1943)<sup>5</sup>. Of less antiquity are the articles<sup>6</sup> by

Hewes, G3TDR, and Jessop, G6JP, who have derived many of the results given in Kaune in their RSGB data reference book, albeit with some misprints. Also, there are excellent articles by Lord Butler, VK5BR, a prolific Australian author with many interesting articles on the subject<sup>7</sup>, in particular the one on output coupling of RF transmitter power amplifiers<sup>8</sup> using Pi and T networks. Formulas of VK5BR for the lossless inductor have been rederived by Kaune in his recent second article. The VK5BR formulas are much more convenient for design purposes than those by Hewes, G3TDR, and Jessop, G6JP, [*op. cit.*<sup>6</sup>], and Bill Kaune, W7IEQ, [*op. cit.*<sup>1</sup>]. However, even simpler formulas are available such as those given in the *Radio Engineers Handbook* by Terman (1943), which I shall call the traditional phase shift based formulas. They unfortunately cannot be generalized to the lossy case easily. Wes Hayward<sup>9</sup> also gave simpler formulas for the Pi network but it must be noted that his  $Q$  should really be  $Q_2$  in the notation here and as in [*op. cit.*<sup>1,6</sup>] and should not be confused with the total network  $Q$  of the Pi network. Wes unfortunately omitted much of the theory behind his discussions, nor did he explain why he chose the  $Q_2$  formulas in his book, among all the others, making this article all the more necessary for those wanting more knowledge. Also, Kaune [*op. cit.*<sup>1</sup>] raised questions about other formulas for the total network  $Q$  — see his equation (5) — which are in the 2013 and 2015 *ARRL Handbooks*. As we shall see, for large  $Qs$  these are reasonably good for bandwidth and harmonics but they are only approximate. At the same time, Kaune [*op. cit.*<sup>1</sup>] seems to

think that there should be factor of one-half in the correct formula for total network  $Q$ . However, I shall show that this is valid only if the input is terminated with a physical resistance  $R_s$  of the same value as the input image resistance. For the unterminated input, there should be no factor of a half. Kaune has also provided interesting numerical results for Pi networks and cascades on bandwidth, harmonic attenuation and their dependence or independence on  $Q$ , but he has provided little theoretical explanations for the response behavior. This shows that there are still many areas of misunderstanding or at least of insufficient understanding which I hope I will be able to clarify for readers interested in the use of these important networks. Although the circuit concerned has only three simple components — a coil and two capacitors — there is much more than meets the eye. A good understanding is necessary in order to avoid some of the pitfalls. As noted by VK5BR [*op. cit.*<sup>8</sup>], Pi networks are useful for matching vacuum tube and modern FET RF power amplifiers, but for transistors (except at low power levels), due to their lower output impedances, the T network should be used instead, [*op. cit.*<sup>8</sup>], as for Pi networks, capacitors of abnormally large values at the input are impractical.

Readers can also save themselves a lot of trouble, due to the generosity of Reg Edwards, G4FGQ, who had earlier on provided many useful resources on his website [*op. cit.*<sup>3</sup>]. To explore this program, just follow the links to download the DOS executable program *pi\_tank.exe*. This will run automatically under Windows 7 and 32 bit architectures. For Windows 10 and 64 bits architectures, users

must install a Virtual DOS interface to open the program. The software was originally written in DOS Basic and compiled with no source code or documentation available. The Rev. George Dobbs, G3RJV, had written<sup>10</sup> an excellent background on Edwards' website and history. These sites are now maintained by Thom La Costa, K3HRN, and include useful Pi, Pi-L networks, bandwidth, efficiency and harmonic rejection calculators. Unfortunately, Edwards did not provide any information on the formulas he had used in his programs considering how useful they are. Most of them are no more than 40 KB in length, and capable of providing answers to many important questions. There are now many Pi network calculators available on the internet and Amateur Radio journals, but they are not as comprehensive as Edwards', nor do they provide sufficient justification for their formulas and approximations, see for example the Robinson, G3MPO, spreadsheets<sup>11</sup>. Especially important other than design is the issue of the frequency response. Most articles do not provide sufficient information, or at best only numerical results on the frequency response. The exact formulas provided here will advance one's knowledge considerably. However, it is important to note that Edwards' program is based on approximate formulas, in some cases accurate, in others not so much. I shall clarify these issues as we proceed.

In the beginning, I first noted that Edwards' inductor loss formula seems to date back to the original Everitt article of 1931 [op. cit.<sup>4</sup>] and in the *Radio Engineers Handbook* by Terman (1943), but to actually prove it was another matter. As it turned out, this was not the case, it was in fact a better approximation for the efficiency, though not exact. As Edwards' formulas were based on the original phase-angle Terman handbook formulas [op. cit.<sup>5</sup>] I at first attempted to generalize them to the lossy case. This led to failure and some frustrations, although some useful formulas emerge but they are too complex to be of value.

Quite remarkably, I later found that exact

results can be obtained by extending instead Hayward's  $Q_2$  based formulas [op. cit.<sup>9</sup>] but to retain the exact phase angle explicitly from an analytical solution does not seem possible. However, the modern Excel spread sheet came to my rescue and one can program it to tune the phase and calculate component values that are not straightforward otherwise. I shall show that while the Everitt's and Edwards' approximations and one other I shall propose later are good — within a few percent — for the efficiency, they are badly wrong for component values. From my equations it is now straightforward to deduce the retuning factors for the various components.

Finally, I shall provide the power transfer functions for the Pi network with lossless inductor as a prelude to a future article. I shall provide universal formulas for two common input terminal conditions. The first is double termination for an ideal input voltage source with internal resistance  $R_s$  same as Kaune's in [op. cit.<sup>1</sup>]. The second is single termination for an ideal input current source of zero internal resistance, appropriate approximately for the output terminal of a transmitter amplifier as mentioned by Hayward<sup>12</sup>. Harmonic attenuation properties and bandwidths can be deduced from these formulas as in Edwards' program but a comparison with his and other approximation methods will have to be postponed to a future article.

## 2. Single and Double Terminations

Let me start by providing a simpler derivation of the results of Bill Kaune, W7IEQ, and take a preliminary look at the frequency response of the Pi network near resonance. Figure 1 shows the standard Pi network. Inductor loss is in the form of a series resistor to the inductor.

Without loss of generality we shall assume a low to high transformation circuit with  $R_L > R_s$ , since the Pi network is reversible. We can first transform the loaded end  $X_{C2}$  and  $R_L$  of the Pi network in Figure 1 into a series LCR circuit at the output end with  $X_{C2}'$  and  $R_L'$  see Figure 2, which is the right half of Kaune's Figure 5. Note that we leave the

input  $R_s$  and  $C_1$  end alone. The equations for these series/parallel type transformations and vice versa are well-known and are given in, for example [op. cit.<sup>1-6</sup>].

Next we transform this series LCR circuit into a parallel  $R_p$  and  $X_p$  network (Figure 3) where:

$$R_p = \frac{(R_L')^2 + (X_L + X_{C2}')^2}{R_L'} \quad (1)$$

and

$$X_p = \frac{(R_L')^2 + (X_L + X_{C2}')^2}{(X_L + X_{C2}')} \quad (2)$$

where  $X_{C2}'$  and  $R_L'$  are given by, see Eqn (8) in [op. cit.<sup>1</sup>], for example:

$$X_{C2}' = X_{C2} \frac{R_L^2}{(R_L^2 + X_{C2}^2)} \quad (3)$$

and:

$$R_L' = R_L \frac{X_{C2}^2}{(R_L^2 + X_{C2}^2)} \quad (4)$$

Eqn (2) shows that we can split this  $X_p$  into a parallel pair of  $L_p$  and  $C_p$ , since

$$\frac{1}{X_p} = \frac{1}{X_{Lp}} + \frac{1}{X_{Cp}} \quad (5)$$

where obviously:

$$X_{Lp} = \frac{R_L^2 + (X_L + X_{C2}')^2}{X_L} \quad (6)$$

and, see Figure 3,

$$X_{Cp} = \frac{(R_L')^2 + (X_L + X_{C2}')^2}{X_{C2}'} \quad (7)$$

The circuit is now an equivalent parallel RLC circuit (at the zero phase design resonance frequency) with capacitances  $C_1$ ,  $C_p$ ,  $L_p$ ,  $R_p$ , and  $R_s$  all in parallel. Now at the design frequency we must have maximum power transfer and also zero phase shift for the image impedance  $Z_{I1}$  i.e. only a real component at  $\omega_0$ . Therefore:

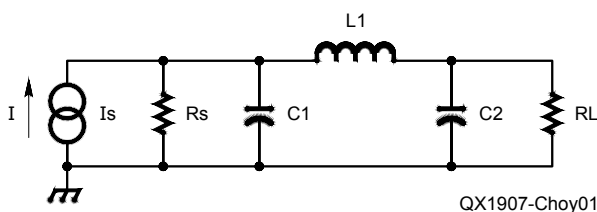


Figure 1 — The standard Pi network. Inductor loss is in the form of a series resistor (not shown) to the inductor.

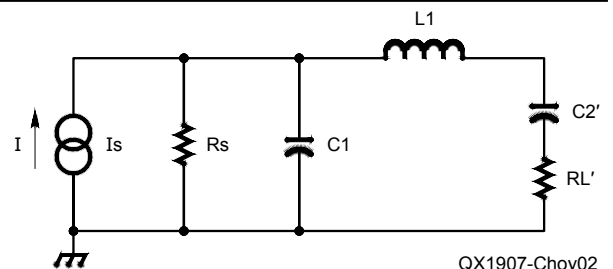


Figure 2 — Equivalent circuit of Figure 1 after a parallel-to-series transformation at the output end.

$$R_p = R_s \text{ and } \frac{1}{X_p} = \frac{1}{X_{Lp}} + \frac{1}{X_{Cp}} = -\frac{1}{X_{C1}} \quad (8)$$

In view of this result one may expect that the formula for the -1 dB and -3 dB bandwidth of an RLC circuit with the same network  $Q$  should predict fairly accurately the -1 dB and -3 dB bandwidth of the Pi network. This is what Edwards' program does but as we shall see in a future work, there is more to it than that. A number of useful results now follow from this transformation. Firstly, the question of the existence of the one-half factor in Kaune's  $Q$  formula — see his equation (6) — versus that of Hewes and Jessop [*op. cit.*<sup>6</sup>] their equation (10), and the *QST* article by Wingfield<sup>13</sup> becomes resolved in this picture. This follows from whether the circuit under consideration is doubly or singly terminated. In the former case  $R_s = R_p$  is physically present at the input but in the latter case  $R_s$  is physically absent being just the image impedance transformed back from the load to the source, as appropriate for a driving current source. This case is the usual one for output coupling of RF power amplifiers to antennas for example so that the network  $Q$  is:

$$Q = \frac{R_p}{X_{Lp}} = \frac{X_L}{R_L} = \frac{R_p}{X_p} - \frac{R_p}{X_{Cp}} \quad (9)$$

$$= Q_1 + Q_2 \text{ [singly terminated]}$$

where

$$Q_1 = \frac{R_s}{|X_{C1}|} \text{ and } Q_2 = \frac{R_L}{|X_{C2}|}$$

For the case of double termination, as for example when connecting the filter to a signal source with an internal resistance  $R_s$ , then the input now has two resistors of the same value effectively in parallel, so that:

$$Q = \frac{R_p}{2X_{Lp}} = \frac{1}{2}(Q_1 + Q_2) \quad (10)$$

[doubly terminated]

These results were already proven in [*op. cit.*<sup>1,6</sup>], but the reader can easily re-derive them using the above equations. The issue of the factor of half is therefore not fundamental for the design, but a consequence of the termination. The primary design parameters are  $Q_1$  and  $Q_2$  which we shall continue to use. The termination and therefore total network  $Q$ , does however affect the circuit response as double termination has a broader response, see later. These characteristics have been discussed long ago, see Hayward [*op. cit.*<sup>9</sup>] and his Figure 4.20 in particular. Remember that all  $Q$ s should be defined only at the design zero-phase frequency  $\omega_0$  and all frequencies in the expressions for the

$Q$ s must be set at the same design frequency  $\omega_0$ . Strictly speaking  $\omega_0$  is only one of several resonance frequencies, here it is the zero-phase frequency for the input image impedance  $Z_{11}$ , a fact well known to workers in the study of quartz crystal behavior, see Bloom Notes<sup>14,15</sup> as cited by me<sup>16</sup>. Another definition for resonance frequency is that for the power gain peak, which need not be the same as  $\omega_0$ . At the design frequency  $\omega_0$  we can show that the power transfer function, if defined correctly, will be unity (i.e., 0 dB) in the lossless case or is in fact  $\epsilon$  in the lossy case, where  $\epsilon$  is the overall circuit power efficiency. However, the peak need not always occur there, and at a frequency away from  $\omega_0$  the input impedance can be complex, see Eqn (14) later.

Now, the above equations and relations derived from them, can be used as design equations using any three parameters as input, since we have three unknown components. A useful relation, easily derived from these equations is in [*op. cit.*<sup>6</sup>], see also Appendix 1.2:

$$\frac{R_L}{R_s} = \rho_L = \frac{1 + Q_2^2}{1 + Q_1^2} \quad (11)$$

Hewes and Jessop [*op. cit.*<sup>6</sup>] use the total  $Q$  as input parameter (or  $2Q$  if doubly terminated) and Eqn (11) provides a solution for  $Q_1$  as a quadratic equation in terms of the transformation ratio  $\rho_L$  and  $Q$  (since  $Q_2 = Q - Q_1$ ). This is essentially also the design method of Kaune [*op. cit.*<sup>1</sup>], but if one prefers what Hayward has done [*op. cit.*<sup>9</sup>] one can choose  $Q_2$  as the third design parameter instead. Any possible choice of three parameters will do for the design but it is common to fix  $R_L$  and  $R_s$ , after all, one of the purpose of using the Pi network is for impedance transformation, plus one other parameter such as  $X_{C1}$ ,  $X_L$ ,  $Q$ ,  $Q_2$ , etc., as in [*op. cit.*<sup>1,4,6,9</sup>] respectively. However, in Edwards, G4FGQ's software [*op. cit.*<sup>3</sup>], it is the phase-lag angle  $\beta$  for the voltage transfer function  $H_V$  at  $\omega_0$  that is the third parameter. The equations he had used have been derived previously throughout the literature, see [*op. cit.*<sup>5</sup>], so I shall merely state them later, they will become transparent in a future article. The advantage of the

$\beta$  equations is that they are very useful in studying cascading networks, for the total voltage transfer function at  $\omega_0$  is given by the product of all the magnitudes  $|H_i|$  times an exponential whose total phase angle  $\beta$  is the sum of all the individual phases  $\beta_i$ , see [*op. cit.*<sup>5</sup>]. In his paper Kaune also cited formulas for  $Q$  — see his equation (5) — which are in the older 2013 and 2015 *ARRL Handbooks*. We can see that these formulas can only be approximate, valid for large  $Q$  where either  $Q_1$  ( $R_L < R_s$ ) or  $Q_2$  ( $R_L > R_s$ ) is the larger dominant component.

Having established the equivalence to a parallel RLC tank circuit at resonance only, a quick look at the results for harmonic attenuation for the RLC network shows that the exact form of the impedance function at the  $n$ -th harmonic frequency is given by the expression:

$$\left| \frac{Z_{11}(jn\omega_0)}{Z_{11}(j\omega_0)} \right| = \frac{1}{\sqrt{1 + Q^2 \frac{(n^2 - 1)^2}{n^2}}} \quad (12)$$

a result that is independent of the ratio of the source to load resistances<sup>17</sup>. In the large  $Q$  limit, Eqn (12) reduces to:

$$\left| \frac{Z_{11}(jn\omega_0)}{Z_{11}(j\omega_0)} \right| \approx \frac{n}{Q(n^2 - 1)} \quad (13)$$

a result already given by equation (3.4-12) on page 82 of [*op. cit.*<sup>17</sup>]. Furthermore, the use of the approximate Eqn (13) only underestimates the exact attenuation Eqn (12) by about 1% for the second harmonic for  $Q = 5$ . We will see how these results change for the Pi network later as the above formulas are in fact quite inaccurate. Edwards seemed to have realized this and he had used an approximation that we will discuss in a follow-on paper.

Our equivalent circuit Figure 3 corresponds to a conventional RLC circuit exactly only at  $\omega_0$ . In fact the exact input impedance function for the Pi network differs from a conventional RLC circuit, see page 25 in [*op. cit.*<sup>17</sup>], and is given by Clarke and Hess<sup>18</sup> page 441 (after correcting for some of their misprints):

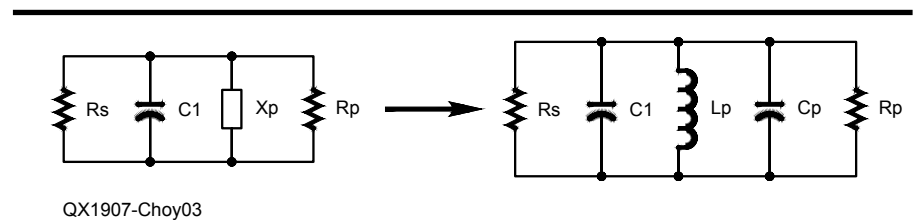


Figure 3 — Equivalent parallel RLC circuit of Figure 1 after a series-to-parallel transformation of Figure 2 including the inductor. The current sources have been removed here for clarity.



$$Z_{11}(z) = \frac{z^2 + \frac{z\omega_0}{Q_2} + \omega_2^2}{C_1 \left( z^3 + \frac{z^2\omega_0}{Q_2} + z[1+N]\omega_2^2 + \frac{\omega_2^2 N \omega_0}{Q_2} \right)} \quad (14)$$

where  $z$  is the complex frequency,

$$Q_2 = R_L / |X_{C2}| = \omega_0 C_2 R_L \text{ and,}$$

$$\omega_2^2 = 1 / (LC_2) \neq \omega_0^2 \text{ and}$$

$$N = C_2 / C_1$$

The formula Eqn (14) is a classic manifestation of the famous Forster's reactance theorem<sup>19</sup>, that dates back to 1924 see for example Terman, [op. cit.<sup>5</sup>]. We need not go into deriving this formula here, the details will be shown in a follow-on work, except to note that for large  $Q_2$ , when  $\omega_2$  is approximately  $\omega_0$  we have zeroes at

$$z = \pm j\omega_2$$

and poles at

$$z = \pm j\omega_2 \sqrt{(1+N)} \text{ and at the origin.}$$

This differs from a conventional RLC which have poles at

$$z = \pm j\omega_0$$

and a single zero at the origin, see for example page 27 of [op. cit.<sup>17</sup>]. As noted by Clarke and Hess [op. cit.<sup>18</sup>], these poles are troublesome for capacitance ratios  $N = 3, 8, 15, \text{ etc.}$ , because they can lead to resonant harmonic currents close to the second, third and fourth harmonics, etc., which don't show up in the voltage transfer functions, but may damage an active device and cause undesired interference. This is a reminder that there is more than meets the eye for the Pi network. I hope to return to these issues in a future article to avoid further digression. The voltage and therefore the power transfer functions though are fortunately simpler to evaluate as will be shown in a follow-on work, which will enable us to test the simpler approximations used by the G4FGQ program. Let us now take a look at the G4FGQ software which I shall follow by a discussion of the assumptions in his program and their validity.

### 3. G4FGQ Pi Network Program and Design Equations.

The G4FGQ *pi\_tank.exe* program [op. cit.<sup>3</sup>] gives a meager introduction to the features, see Figure 4, telling the user

essentially how to run the program. Do not expect very much in terms of background physics or references to original papers nor a discussion of the validity of the approximate equations. It is, however, a marvelous piece of code for its time, only about 40 KB long and it can model Pi networks with both pure or lossy inductors. As it was designed for RF transmitter outputs, the program will ask for the input parameters, which are:

(1) Design Frequency  $\omega_0$ , (2) Peak voltage of the active device:  $V_{pk}$ , (3) Instantaneous output RF power  $P$ , (4) Output termination, which must be a pure resistance  $R_L$ , (5) the phase lag angle  $\beta$  which must be between  $90^\circ$  and  $180^\circ$  and finally the coil  $Q$  factor  $Q_L$ . The program deals only with single terminations so the input image resistance  $R_s$  is calculated from:

$$R_s = \frac{V_{pk}^2}{2P}$$

Item number (1) is actually the designed zero-phase resonance frequency as discussed earlier. The design equations are the standard ones from network theory which for pure

reactances, will yield the correct real matching input and output resistance value, see [op. cit.<sup>45</sup>],

$$X_{C1} = \frac{R_s R_L \sin \beta}{R_L \cos \beta - \sqrt{R_s R_L}} \quad (15)$$

$$X_{C2} = \frac{R_s R_L \sin \beta}{R_s \cos \beta - \sqrt{R_s R_L}} \quad (16)$$

$$X_L = \sqrt{R_s R_L} \sin \beta \quad (17)$$

The lossless Pi network  $Q$  which I shall now denote as  $Q_u$  following the convention used by Hayward<sup>20</sup>, is calculated by the program from the formula:

$$Q_u = \frac{1}{\sin \beta} \left\{ \sqrt{\frac{R_s}{R_L}} + \sqrt{\frac{R_L}{R_s}} - 2 \cos \beta \right\} \quad (18)$$

Although the phase lag  $\beta$  is of no interest in most Amateur Radio applications, as we

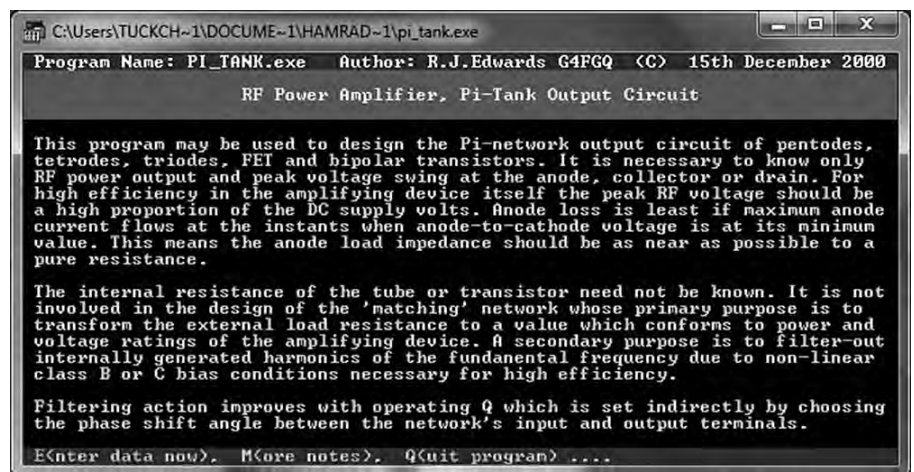


Figure 4 — The G4FGQ *pi\_tank.exe* program user DOS-era interface.

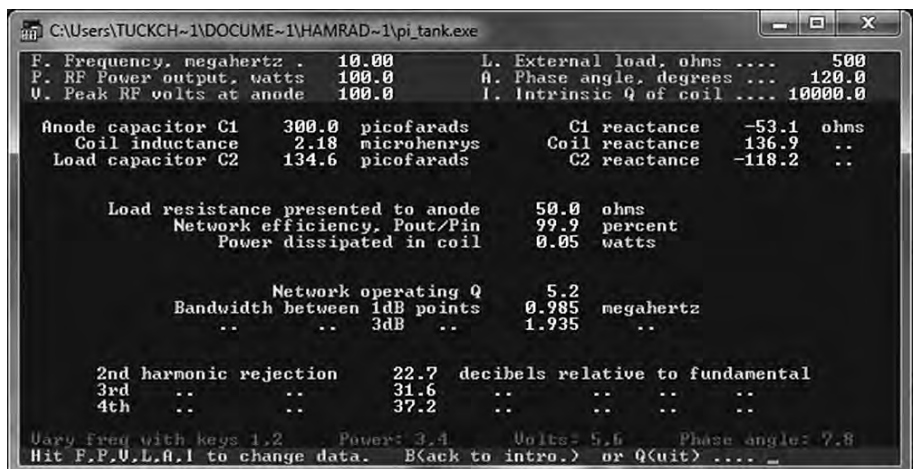


Figure 5 — An example using the *pi\_tank.exe* program for a very high  $Q$  (essentially lossless) inductor.

can see, it is connected with network  $Q$ , and may be important in some applications. As an example I shall provide the page for the output based on a model Pi network at 10 MHz, see Figure 5 below, first for a very large coil  $Q_L = 10,000$  — essentially a lossless coil — and then Figure 6 for a realistic coil with a  $Q_L$  of 12.

As can be seen, a change of  $Q_L$  from 10,000 to 12 (values that cover a practical range of coils) does not alter the reactance values in this program at all, nor the harmonic suppression characteristics significantly. However, the total network  $Q$ , power efficiency, and 3 dB bandwidth drop by almost 30%.

Now here are some of the questions that one can now ask: a) Is this program accurate? Specifically, b) What are the actual changes to the components values if we want to maintain the same phase angle as the lossless inductor which Edwards' program requires? c) Can Edwards' approximation be improved? d) For fixed  $R_s$ ,  $R_L$  and  $Q_L$

what value of  $X_L$  will give the maximum power efficiency and what is this maximum efficiency? The last question was first posed by Everitt [*op. cit.*<sup>4</sup>], and he answered it using his approximations. There are many other similar questions, which I hope the readers can resolve by themselves using the formulas I shall provide. I can now answer immediately question a) after my extensive investigations. The program is certainly accurate for lossless coils but for  $Q_L$  in the range 10 to 20 the results are only approximate and must be used with some caution. Fortunately, the inaccuracies in the program can now be improved upon without much effort, as we shall see. Later in this paper, I shall also be able to provide answers to questions b) and c), while d) is left as an exercise for the reader.

#### 4. The Everitt and Edwards Approximations.

For an inductor with finite  $Q_L$ , as noted by Terman Note [*op. cit.*<sup>5</sup>], the design Eqns (15) to (18) become invalid, since they hold only for a network with only reactive elements. One could use the  $R_V$  model discussed by Kaune [*op. cit.*<sup>2</sup>], but unfortunately that model followed a rather specific design path for partitioning the network into back-to-back L networks, in which the power efficiency  $\varepsilon$  and coil resistance  $r_L$  must also be specified in advance. Here I shall take the opportunity to re-derive the equivalent model that does not depend on any specific repartitioning of the Pi network and therefore quite general. We return to Eqns (1) through (7) and insert the inductor loss as a resistor  $r_L$  in series with  $L$ . This merely adds the inductor loss resistance  $r_L$  to the transformed resistor  $R_L'$  in the next step. From now on, all quantities

in Section 2 shall refer to the lossless inductor case and in particular all  $Q$ s there will bear the superscript 0 when we refer to them, while all  $Q$ s without superscripts shall be referred to the lossy inductor case here. Thus, the modified equations are:

$$R_p = \frac{(r_L + R_L')^2 + (X_L + X'_{C2})^2}{r_L + R_L'} \quad (19)$$

and

$$X_p = \frac{(r_L + R_L')^2 + (X_L + X'_{C2})^2}{(X_L + X'_{C2})} \quad (20)$$

where  $X_{C2}'$  and  $R_L'$  are given by the same form as before, i.e., Eqn (3) and (4), which remain unchanged. Thus, although some of these equations are identical, others are not, so the design component values will change in general. The equations for the components' reactance of the parallel equivalent circuit are now:

$$X_{Lp} = \frac{(r_L + R_L')^2 + (X_L + X'_{C2})^2}{X_L} \quad (21)$$

and

$$X_{Cp} = \frac{(r_L + R_L')^2 + (X_L + X'_{C2})^2}{X'_{C2}} \quad (22)$$

with Eqn (8) still defining the maximum power transfer and the zero phase frequency conditions. Now comes the interesting part. The total network  $Q$ , which we shall designate as  $Q_{Net}$  is easily written down for the equivalent parallel tuned circuit at  $\omega_0$  resonance (remember, for single termination there is no factor of two):

$$Q_{Net} = \frac{R_p}{X_{Lp}} = \frac{X_L}{r_L + R_L'} \quad (23)$$

and from this we obtain:

$$\frac{1}{Q_{Net}} = \frac{r_L + R_L'}{X_L} = \frac{1}{Q_L} + \frac{1}{Q_u} \quad (24)$$

where  $Q_L$  is the coil  $Q$  and  $Q_u$  (with no superscript 0) is the unloaded  $Q_u$  at zero-phase resonance, but its value is not the same as  $Q_u^0$  before. The equation for  $Q_u$  is given by:

$$Q_u = \frac{X_L}{R_L'} = \frac{X_L}{R_L} (1 + Q_2^2) \quad (25)$$

Here I shall continue to define

$$Q_1 = \frac{R_s}{|X_{C1}|} \quad \text{and} \quad Q_2 = \frac{R_L}{|X_{C2}|}$$

but note that these do not have the same values as those in Section 2, which we shall designate as

$$Q_1^0 = \frac{R_s}{|X_{C1}^0|} \quad \text{and} \quad Q_2^0 = \frac{R_L}{|X_{C2}^0|}$$

as mentioned earlier. Eqn (24) is a general result for dissipative circuits for either series or parallel resonant systems, as mentioned by Wes Hayward [*op. cit.*<sup>20</sup>].

Now the power efficiency  $\varepsilon$  can be immediately written down since following Kaune [*op. cit.*<sup>2</sup>] we have:

$$\begin{aligned} \varepsilon &= \frac{R_L'}{r_L + R_L'} = \frac{1}{1 + \frac{r_L}{R_L'}} = \frac{1}{1 + \frac{r_L}{X_L} \frac{X_L}{R_L'}} \quad (26) \\ &= \frac{1}{1 + \frac{Q_u}{Q_L}} = \frac{Q_{Net}}{Q_u} \end{aligned}$$

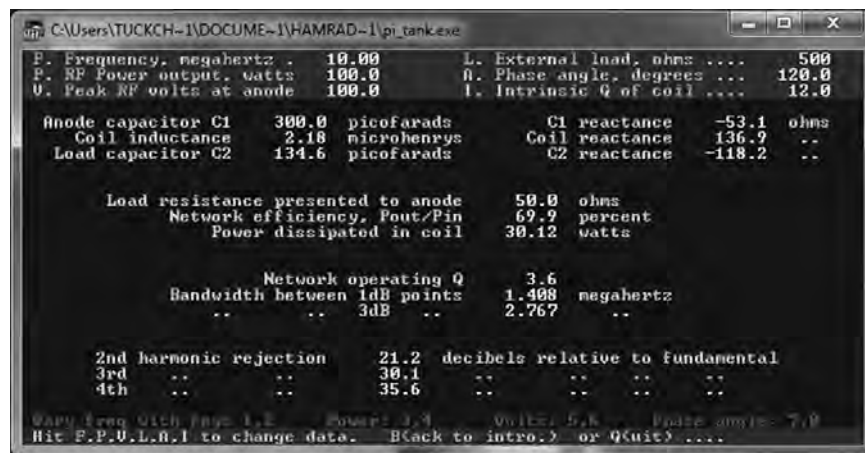


Figure 6 — Another example using the *pi\_tank.exe* program for a finite  $Q_L$  of 12 inductor. The Pi network components and reactance values output by the program do not change, but all the other output values do. This approximation is investigated in this paper.

which follows from Eqns (24) and (25) and has an obvious physical interpretation. The power efficiency  $\varepsilon$  is given by the ratio of the total network  $Q_{Net}$  divided by the unloaded network  $Q_u$  of Eqn (25), see Figure 2. If we specialize to a specific  $R_v$  model like Kaune [op. cit.<sup>3</sup>] it is not difficult to show that both Eqns (23) and (26) are equivalent to his Eqns (24) and (21) respectively, bearing in mind the factor of 1/2 for his double termination. The proof for this is in the Appendix 1.1. For now, let me mention Edwards' approximation [op. cit.<sup>3</sup>] as used in his program. It is in fact obtained by modifying Eqn (24) by assuming that  $Q_u$  is approximately  $Q_u^0$ , so that:

$$\frac{1}{Q_{Net}} \approx \frac{1}{Q_{NetReg}} = \frac{1}{Q_L} + \frac{1}{Q_u^0} \quad (27)$$

From this  $Q$  he can also obtain the approximate power efficiency from Eqn (26);

$$\varepsilon \approx \varepsilon_{Edwards} = \frac{1}{1 + \frac{Q_u^0}{Q_L}} = \frac{Q_{NetReg}}{Q_u^0} \quad (28)$$

Eqn (27) and (28) are the approximations used by Edwards' program for the calculation of network operating  $Q_{Net}$  and the network power efficiency  $\varepsilon$ , see Figure 6. For the example in that figure these give  $Q_0 = 3.6$  and  $\varepsilon_{Edwards} = 69.9\%$  respectively. Can these values be improved easily? The answer is affirmative, but before that, let me first discuss Everitt's [op. cit.<sup>4</sup>] approximation. Eqn set (19) to (24) and equations derived from them, furnish many different choices for the design of the Pi network. I shall outline a few examples.

#### Method (I)

If we specify  $R_s$ ,  $R_L$ ,  $\varepsilon$  and  $Q_2$  similar to Wes Hayward's formula [op. cit.<sup>20</sup>], but with a lossy inductor. Then immediately  $|X_{C2}|$  is known by definition and we can obtain  $Q_1$  from the following equation easily derived from the above equations, see Appendix 1.2.

$$\frac{R_L}{R_s} = \rho_L = \varepsilon \frac{1 + Q_2^2}{1 + Q_1^2} \quad (29)$$

This is just a simple quadratic in  $Q_1$  whose solution will immediately provide the value for  $|X_{C2}|$ . Next we can obtain  $Q_L$  from:

$$\varepsilon = \frac{Q_L - Q_1}{Q_L + Q_2} \quad (30)$$

another equation to be found in Appendix 1. Once that is done we can obtain  $Q_u$  from Eqn (26) and also  $Q_{Net}$  from Eqn (24). Also now  $X_L$  follows from Eqn (25) and the design is complete.

#### Method (II)

If we specify  $R_s$ ,  $R_L$ ,  $Q_L$  and  $Q_2$  then first

we can find  $|X_{C2}|$ , and so we can obtain  $Q_1$  by substituting Eqn (30) into Eqn (29), which also gives a quadratic in  $Q_1$  and from which we can find  $|X_{C1}|$ . Then we can obtain  $\varepsilon$  from Eqn (30),  $Q_u$  Eqn (26) and  $Q_{Net}$  from Eqn (24) and now also  $X_L$  follows from Eqn (25).

#### Method (III)

This method is the scheme of Kaune [op. cit.<sup>2</sup>]. We specify  $R_s$ ,  $R_L$ ,  $r_L$  and  $\varepsilon$ , then from his Eqn (21), that is,

$$\varepsilon = 1 - \frac{r_L}{R_v}$$

in our notation, we can obtain  $R_v$  from which all network elements will follow from his Eqn (15) changing his  $R_2$  to  $r_L$  in our notation here. Once all the elements are known, the calculation for  $Q_{Net}$  can follow from his Eqn (24) — removing the factor of 1/2 for single termination — or from Eqn (25) and (26) above.

#### Method (IV)

Here we specify  $R_s$ ,  $R_L$ ,  $Q_L$  (or  $r_L$ ) and  $X_L$  as used by Everitt who unfortunately did not realize that an exact solution is possible. This option is useful if one has a coil whose loss resistance or coil  $Q_L$  has been measured in advance and that it does not change significantly with inductance such as in high  $Q$  toroidal coils, but *not* air core coils as investigated by Kaune [op. cit.<sup>2</sup>] for reasons that we will not go into here. From Eqn (19) to (29), we can show that  $Q_2$  is given by the quadratic (see Appendix 2):

$$aQ_2^2 - 2bQ_2 + c = 0 \quad (31)$$

Here the coefficients are:

$$\begin{aligned} a &= r_L^2 + X_L^2 - r_L R_s \\ b &= R_L X_L \\ c &= (r_L + R_L)^2 - R_s (r_L + R_L) + X_L^2 \end{aligned} \quad (32)$$

From the solution of this quadratic, the appropriate root for  $Q_2$  is determined by its positivity and also by continuity from the lossless case  $r_L$  approaching 0, then  $|X_{C2}|$  is now determined. Now Eqn (25) gives  $Q_u$  and Eqn (26) gives the efficiency  $\varepsilon$  from which Eqn (29) now gives  $Q_1$ , and  $|X_{C1}|$  is finally obtained. Another useful choice for example is Method V.

#### Method V

Here we specify  $Q_1$ ,  $Q_2$ ,  $\varepsilon$  and  $R_L$ , which suits the universal response formulas and the original Butler method [op. cit.<sup>8</sup>], and so on. However, I shall mention that in his paper, Everitt first obtained an exact equation for the power dissipation by a different method. The argument is quite straight forward but different from what we have used here. The

input current  $I_{in}$  must by Kirchoff's law be split between the current in the capacitor  $I_{C1}$  and the inductor current  $I_L$ . The current  $I_{C1}$  is not dissipative by assumption and this should be a vector orthogonal to the input voltage  $V_{pk}$  which must be in phase with the vector input current  $I_{in}$  at resonance. From the Pythagorean theorem it follows that:

$$I_L^2 = I_{in}^2 + I_{C1}^2$$

and from this, the power dissipated in the coil must be:

$$\begin{aligned} P_{loss} &= I_L^2 r_L = I_L^2 \frac{X_L}{Q_L} \\ &= \frac{V_{pk}^2 X_L}{Q_L} \left( \frac{1}{R_s^2} + \frac{1}{|X_{C1}|^2} \right) \end{aligned} \quad (33)$$

From Eqn (33) it is straight forward to show that the power efficiency is identical with all our results here and in Kaune [op. cit.<sup>2</sup>]. The next step, however, is where Everitt [op. cit.<sup>4</sup>] made his bold approximation by substituting for  $|X_{C1}|$  the value  $|X_{C1}^0|$  from Eqn (15), presumably because he did not think an exact analytic solution was possible, which can be rewritten as:

$$X_{C1}^0 = \frac{-R_s X_L}{R_s + \sqrt{R_s R_L - X_L^2}} \quad (34)$$

Note here  $X_L$  is an input parameter in his design option, which is Method IV. This equation as stated earlier is valid only when all network elements are purely reactive. So, it is a very brave assumption. Everitt had made no comments about its validity in his paper. The power loss of Everitt has been tabulated in Terman [op. cit.<sup>5</sup>] and subsequent editions of his handbook, and probably used reliably for many generations of radio engineers. So what is it in our language, and is it better than Edwards' approximation? To connect Everitt's approximation to our formulas, one can show from Eqn (33) that his approximate loss fraction is in fact given by,

$$\begin{aligned} \delta_{Everitt} &= \frac{P_{loss}}{P_{in}} = \frac{X_L}{R_s Q_L} (1 + Q_1^{02}) \\ &= \frac{X_L \rho_L}{R_L Q_L} (1 + Q_1^{02}) \\ &= \frac{Q_u^0}{Q_L} \end{aligned} \quad (35)$$

Here I have used Eqns (11) and (25) in the last step taking care to include the superscript 0, so that:

$$\varepsilon_{Everitt} = 1 - \frac{Q_u^0}{Q_L} \quad (36)$$

Notice this is a first order expansion of Edwards' approximation Eqn (28) when

$Q_u^0/Q$  is small. The value for the power efficiency for our example of Figure 6 is:  $\varepsilon_{Everitt} = 56.9\%$  compared to Edwards' value or  $69.9\%$ , so Everitt's formula gives a relatively conservative estimate. Here I must admit that I have no idea where Edwards got his approximate formula Eqn (28) from, since he had left no documentation. Presumably it can be justified by some means but I did not pursue this further, since it is possible to obtain other approximate or exact results. Before discussing the exact results, I shall propose another approximation which will answer question (3). This is based on assuming  $Q_1$  is approximately  $Q_1^0$  and  $Q_2$  is approximately  $Q_2^0$  instead of  $Q_u$  approximating  $Q_u^0$  so that Eqn (3) becomes:

$$\varepsilon_{Ch} = \frac{Q_L - Q_1^0}{Q_L + Q_2^0} \quad (37)$$

The rationale here is that if we were to retain unchanged the component values as Edwards has done, then we must use only the approximate values of  $Q_1$  and  $Q_2$  alone in the formula to calculate the efficiency without other intermediaries. The value so obtained is,

$$\varepsilon \approx \varepsilon_{Ch} = 68.1\% \text{ with } Q_u \approx 5.61 \text{ and } Q_{Net} \approx 3.82.$$

These values are to be compared with Edwards', which are:

$$\varepsilon_{Edwards} = 69.9\% \text{ with}$$

$$Q_u \approx Q_u^0 = 5.17 \text{ and } Q_{Net} \approx 3.61$$

or with Everitt's, which are:

$$\varepsilon_{Everitt} = 56.9\% \text{ with } Q_u \approx Q_u^0 = 5.17 \text{ and } Q_{Net} \approx 2.94.$$

These  $Q$  values using formulas Eqn (39) and (40) below together with the exact results to be shown in the next section for the same phase angle are tabulated in Table 1.

Note however that the resultant approximate component values mean that the frequency response functions will and can differ significantly from the exact model. Also, because my approximate  $Q_u$  and  $Q_{Net}$  (rows 6 and 7 in Table 1) are closer to the exact values, can we expect that they will give better estimates for bandwidth and harmonic suppression? The above formulas enable question d) to be answered now, but it will be left as a useful exercise for the reader, as the details would take us too far from the main theme in this paper. However, I shall cite Everitt's [*op. cit.*<sup>4</sup>] result obtained in 1931. Everitt showed that the maximum

**Table 1.**

**Summary of the various approximations vs. the exact results as discussed in the text. Since the important  $Q_1$  and  $Q_2$  parameters in the various approximate models do not change, some component values remain the same as the lossless model. However,  $Q_u$  and  $Q_{Net}$  are different and therefore will give different predictions for the response and bandwidth.**

	Lossless	Everitt	Edwards	My approximation	Exact
Phase $\beta$	120°	117.9°	101.7°	104.8°	120°
$Q_L$	$\infty$	12	12	12	12
$Q_1$	0.94	0.94	0.94	0.94	0.87
$Q_2$	4.23	4.23	4.23	4.23	5.10
$Q_u$	5.17	5.17	5.17	5.61	6.44
$Q_{Net}$	5.17	2.94	3.61	3.82	4.19
$\varepsilon$	100%	56.91%	69.88%	68.13%	65.06%
$X_{C1}$	-53.05 $\Omega$	-53.05 $\Omega$	-53.05 $\Omega$	-53.05 $\Omega$	-57.35 $\Omega$
$X_{C2}$	-118.23 $\Omega$	-118.23 $\Omega$	-118.23 $\Omega$	-118.23 $\Omega$	-97.95 $\Omega$
$X_L$	136.93 $\Omega$	136.93 $\Omega$	136.93 $\Omega$	148.60 $\Omega$	119.10 $\Omega$

efficiency is approximately given by:

$$\varepsilon_{max} \approx 1 - \left( \frac{R_L + R_s}{Q_L X_{Lmax}} \right) \quad (38)$$

for the value

$$X_L = X_{Lmax} = \sqrt{R_L R_s}.$$

Readers who are motivated to do the above exercise can compare the exact maximum efficiency with Everitt's.

## 5. Finding the Exact $\varepsilon$ with the Same Phase Angle

At this stage the reader must be curious as to what the exact value for  $\varepsilon$  is, and how do the above approximations compare. To do this we need to exercise some care in the phase method. First two more useful formulas can be obtained from the above equations, they are (see Appendix 3):

$$Q_u = \frac{Q_1 + Q_2}{1 - \frac{Q_1}{Q_L}} \quad (39)$$

and

$$Q_{Net} = \frac{Q_1 + Q_2}{1 + \frac{Q_2}{Q_L}} \quad (40)$$

Notice that Eqn (40) differs from Kaune's  $Q_{Net}$  formula (19) of [*op. cit.*<sup>2</sup>] (without the factor of 1/2), which he wrote as  $Q_A + Q_B$  by putting all the loss in  $Q_B$ , but these are not the same as  $Q_1$  and  $Q_2$  here. Physically it seems more attractive to retain the definitions for  $Q_1$  and  $Q_2$  and designate how they change from the lossless values,  $Q_1^0$  and  $Q_2^0$  and how they must be combined to form  $Q_u$  and  $Q_{Net}$  as shown above. However, in comparing with Edwards' method, we need to note that the

input parameters we specify should be  $R_s$ ,  $R_L$ ,  $Q_L$  and phase angle  $\beta$ . We will call this Method VI.

### Method VI

Eqn (17) for the phase angle, which we shall rewrite in the form:

$$\begin{aligned} \sin \beta^0 &= \sqrt{\frac{1}{R_s R_L}} X_L^0 \\ &= \sqrt{\frac{R_L}{R_s}} \frac{Q_u^0}{1 + Q_2^0} \end{aligned} \quad (41)$$

is no longer valid. The correct equation must be derived from a network analysis of the voltage transfer function. The result is:

$$\begin{aligned} \sin \beta &= \sqrt{\frac{\varepsilon}{R_s R_L}} q_2 X_L \\ &= \sqrt{\frac{\varepsilon R_L}{R_s}} \frac{q_2 Q_u}{1 + Q_2^2} \end{aligned} \quad (42)$$

where

$$q_2 = 1 + \frac{Q_2}{Q_L}$$

Note that  $X_L$  and the  $Q$ s in Eqn (42) do not have the superscript 0. We must fix the phase angle to be identical to the loss free case,  $\beta = \beta^0$ , in this case 120°, as requested by Edwards' program. The resulting algebraic transcendental equations to obtain the component values are quite formidable. Fortunately, this task can now be solved by using the Method II spread sheet. Instead of using the angle as a parameter, I shall use Method II and input  $Q_2$  which I shall tune and adjust so that the calculated phase angle is the same as the original lossless value, in this case is 120°. The value of  $Q_2 = 5.1044$  will give the correct angle to three decimal places and a  $Q_u = 6.444$  with an efficiency of  $\varepsilon = 65.06\%$  as tabulated in Table 1. At last, this is the exact value for the same phase

angle with inductor loss. In addition, the component values are shifted as follows:

$$\frac{X_{C1}}{X_{C1}^0} = 1.081, \quad \frac{X_{C2}}{X_{C2}^0} = 0.828, \text{ and}$$

$$\frac{X_L}{X_L^0} = 0.870.$$

Thus, we can conclude that for these parameters, Edwards' component values are up to 20% out if we want to maintain the same phase angle. These results answer questions a), b) and c) in Section 3. Finally, a spread sheet can easily be written for Method I. This requires as inputs  $R_s$ ,  $R_L$ ,  $Q_2$  and  $\varepsilon$ , that is an insertion-based algorithm similar to Kaune [op. cit.<sup>2</sup>]. This spreadsheet can then calculate the coil resistance  $r_L$  that can also be used as input in Kaune's Method III above, and will allow a comparison with his algorithm. We find perfect agreement, as seen in Appendix 1.1.

I shall provide two further equations, which are for the power transfer functions in the lossless case. As discussed by Hayward [op. cit.<sup>12</sup>], the frequency response depends not just on the circuit component values, but also significantly on the terminations. In the case of a voltage source, doubly terminated as in Kaune [op. cit.<sup>1</sup>], the power response function is given by:

$$G_{term}^0(j\omega) = \frac{4R_s}{R_L} \left| \frac{V_{out}}{V_{in}} \right|^2 \quad (43)$$

$$= \frac{4(1+Q_1^2)(1+Q_2^2)}{C^2 + \omega^2 D^2}$$

where:

$$C = 2 + Q_1^2 + Q_2^2 - \omega^2 Q_u^2$$

$$D = 2Q_u + (1 - \omega^2)(Q_1 Q_2^2 + Q_2 Q_1^2)$$

Here all frequencies are normalized to the design frequency  $\omega_0$  and I have dropped all superscripts for convenience, in particular:

$$Q_u = (Q_1 + Q_2) = 2Q_{Net}$$

as discussed earlier. Next the expression for the power response function for the case of an unterminated Pi network driven by a current source is given by:

$$G_I^0(j\omega) = \frac{R_L}{R_s} \left| \frac{I_{out}}{I_{in}} \right|^2 \quad (44)$$

$$= \frac{(1+Q_1^2)(1+Q_2^2)}{E^2 + \omega^2 F^2}$$

where

$$E = 1 + Q_1^2 - \omega^2 Q_1 Q_u$$

$$F = Q_u + (1 - \omega^2)(Q_1 Q_2^2 + Q_2 Q_1^2).$$

However now

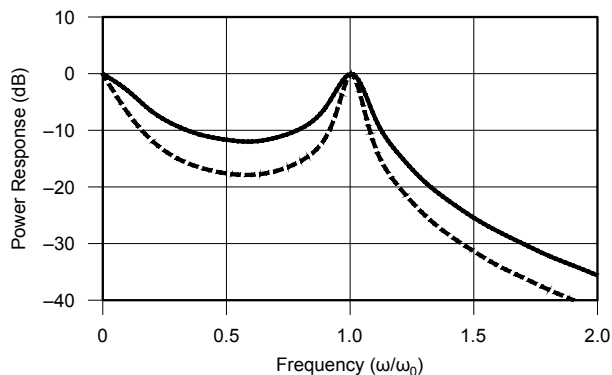
$$Q_u = (Q_1 + Q_2) = Q_{Net}$$

without the factor of 1/2 as discussed earlier. A number of limits can be easily checked. All response functions vanish at infinite frequency, and at zero frequency they are given by the appropriate resistance ratios. In addition, with a little algebra one can prove that they are indeed normalized for 0 dB at the design frequency  $\omega = 1$ . One can now easily plot these functions and for example verify that they agree with Figure 4.20 of Wes Hayward [op. cit.<sup>9</sup>]. This is shown in Figure 7 here.

Now we plot the response for the Pi filter of Figure 5, shown in Figure 8. In particular note that the peak for  $G_I^0(j\omega)$  need not be at  $\omega = 1$  for other terminations. Readers can easily check Eqns (43) and (44) against results of numerical simulations such as *LTSpice* or other numerical algorithms.

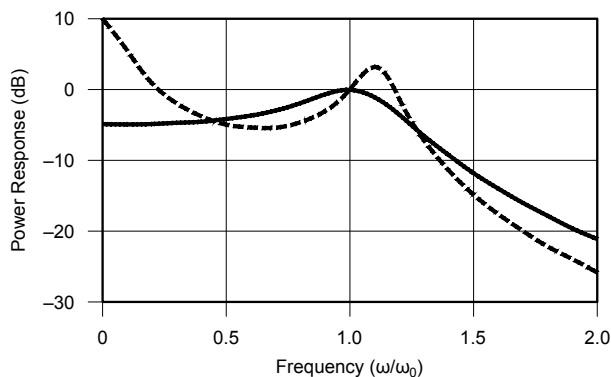
Finally, for those who are curious as to

how  $Q_u$  determines the response and hence bandwidth, see Eqns (43) and (44), which as far as I am aware had not appeared in any literature before. They show that the response functions for these terminations depend on only two parameters  $Q_1$  and  $Q_2$  even though there are three free design parameters:  $R_s$ ,  $R_L$  and one other parameter. However, if  $Q_u$  is chosen as the third parameter, as used by Hewes and Jessop [op. cit.<sup>6</sup>], then  $Q_1$  and  $Q_2$  are given by Eqn (11) as functions of  $Q_u$  (see comments following that equation) and the response is now fixed, so  $Q_u$  will directly determine the bandwidth BW, which answers Kaune's first question, although it will not be given by a simple formula  $BW = \omega_0/Q_u$ . For other design options, this is not the case, for example in Hayward's method it is  $Q_2$  and in Edwards' phase angle option Section 3 it is the angle  $\beta$  that will determine the bandwidth directly. Readers are encouraged to ponder how Eqns (43) and (44) are modified when the inductor loss comes into play.



QX1907-Choy07

Figure 7 — Universal power response in decibels for a lossless symmetrical Pi Network with  $Q_1=Q_2=10$ . The x-axis is normalized to the design frequency  $\omega_0$ . The solid curve is for double-termination Eqn (43) and the dashed curve is for single termination Eqn (44).



QX1907-Choy08

Figure 8 — Universal power response in dB for a lossless asymmetrical Pi Network with  $Q_1=0.942$  and  $Q_2=4.229$ . The x-axis is normalized to the design frequency  $\omega_0$ . The solid curve is for double-termination Eqn(43) and the dashed curve is for single termination Eqn (44).

## 6. Conclusion

Filter synthesis is a huge subject with many big names in the field including Forster, Zobel, Cauer, Belevitch, Darlington, Cocci, Guillemin, and others. This article barely touches the surface of the subject but I hope it will introduce the reader to the intricacies and enrich an understanding of Pi filters. In the planned future article I shall present the network analysis results for the frequency response functions to show how good Edwards' approximations are for bandwidth and harmonic attenuation. There the story becomes even more interesting.

## Appendix 1

### A1.1 Verification the $R_v$ model of Kaune [op. cit.<sup>2</sup>].

Our general expression for  $Q_{Net}$  reduces to Kaune's [op. cit.<sup>2</sup>] more specific model in which he assigns the inductor loss only to the second half of his L network. From the first part of Eqn (23):

$$\begin{aligned} Q_{Net} &= \frac{R_p}{X_{Lp}} \\ &= \frac{R_p}{|X_{C1}|} + \frac{R_p}{|X_{Cp}|} \\ &= \left( Q_1 + \frac{R_p}{|X_{Cp}|} \right) \end{aligned} \quad (45)$$

Now from Eqn (19) and (20), we can easily show that:

$$\frac{R_p}{|X_{Cp}|} = \frac{X'_{C1}}{r_L + R'_L} = \frac{Q_2}{1 + r_L / R'_L}$$

since

$$\frac{r_L}{R'_L} = \frac{r_L}{R'_L} \left( 1 + \frac{r_L}{R'_L} \right)$$

then it follows that:

$$Q_{Net} = \frac{R_s}{|X_{C1}|} + \frac{Q_2}{1 + \frac{r_L}{R'_L} (1 + Q_2^2)} \quad (46)$$

and from Eqn (26):

$$\varepsilon = \frac{1}{1 + \frac{r_L}{R'_L}} = \frac{1}{1 + \frac{r_L}{R'_L} (1 + Q_2^2)} \quad (47)$$

We can now use the third equation in equation (15) of Kaune [op. cit.<sup>2</sup>], and thus in our notation:

$$\frac{1}{Q_2^2} = \left( \frac{X_{C2}}{R_L} \right)^2 = \frac{R_v - r_L}{R_L + r_L - R_v} \quad (48)$$

where  $R_v$  is defined in his paper. After some algebraic manipulations, we have:

$$\frac{r_L}{R_L} (1 + Q_2^2) = \frac{r_L}{R_v - r_L} \quad (49)$$

Thus the power efficiency  $\varepsilon$  in Eqn (47) is:

$$\varepsilon = \frac{1}{1 + \frac{r_L}{R_L} (1 + Q_2^2)} = 1 - \frac{r_L}{R_v} \quad (50)$$

and for  $Q_{Net}$  in Eqn (46) we have:

$$\begin{aligned} Q_{Net} &= \frac{R_s}{|X_{C1}|} + \frac{Q_2}{1 + \frac{r_L}{R_L} (1 + Q_2^2)} \\ &= \frac{R_s}{|X_{C1}|} + \frac{R_L}{|X_{C2}|} \left( \frac{R_v - r_L}{R_v} \right) \end{aligned} \quad (51)$$

Eqns (50) and (51) are in full agreement with Eqns (21) and (24) in Kaune [op. cit.<sup>2</sup>] apart from the half factor in Eqn (51) since we are considering single termination, see Section 2.

### A1.2 Proof of Eqn (29)

Next, I shall sketch the proof of Eqn (29). We start by writing:

$$\begin{aligned} \frac{R_L}{R_s} &= \frac{R_L}{R_p} \\ &= \frac{R_L (r_L + R'_L)}{(r_L + R'_L)^2 + (X_L + X'_{C2})^2} \end{aligned} \quad (52)$$

where we have used Eqn (19) and by making use of Eqn (25) we now have:

$$\begin{aligned} \frac{R_L}{R_s} &= \frac{R'_L (r_L + R'_L) (1 + Q_2^2)}{(r_L + R'_L)^2 + (X_L + X'_{C2})^2} \\ &= \frac{\left( 1 + \frac{r_L}{R'_L} \right) (1 + Q_2^2)}{\left( 1 + \frac{r_L}{R'_L} \right)^2 + (Q_U - Q_2)^2} \end{aligned} \quad (53)$$

Now from Eqn (26) we have

$$\left( 1 + \frac{r_L}{R'_L} \right) = 1 + \frac{Q_U}{Q_L}$$

and from Eqn (39), which we shall prove in Appendix 3, it follows:

$$Q_U - Q_2 = Q_1 \left( 1 + \frac{Q_U}{Q_L} \right)$$

Substituting these results into Eqn (53) and using once again Eqn (26) proves the formula (29) in the text. Eqn (11) follows by taking  $\varepsilon = 1$  since this is the lossless case.

### A1.3 Proof of Eqn (30)

From Eqn (26) again, we have:

$$\frac{1}{\varepsilon} = 1 + \frac{Q_U}{Q_L} = 1 + \frac{1}{Q_L} \frac{(Q_1 + Q_2)}{1 - \frac{Q_1}{Q_L}} \quad (54)$$

from which Eqn (30) is proved.

## Appendix 2

### Proof of Eqns (31) and (32)

We first start from Eqn (19) and find that:

$$R_s (r_L + R'_L) = (r_L + R'_L)^2 + (X_L - |X'_{C2}|)^2 \quad (55)$$

Now as  $X_{C2}'$  and  $R_L'$  are given by the same form as Eqns (3) and (4), then substituting these quantities into Eqn (55) and using the definition of  $Q_2$  this becomes:

$$\begin{aligned} R_s \left( r_L + \frac{R_L}{(1 + Q_2^2)} \right) &= \left( r_L + \frac{R_L}{(1 + Q_2^2)} \right)^2 + \\ &\left( X_L - \frac{R_L Q_2}{(1 + Q_2^2)} \right)^2 \end{aligned} \quad (56)$$

Further straightforward algebraic simplifications show that this reduces to a quadratic equation in  $Q_2$  in the form of Eqn (31) with the coefficients defined by Eqn (32).

## Appendix 3

### Proof of Eqns (39) and (40)

To prove Eqn (39) we first find an equation for

$$Q_1 = \frac{R_s}{|X_{C1}|} = \frac{R_p}{|X_p|} \quad (57)$$

the latter follows from the conditions Eqn (8). From Eqn (19) and (20) it follows that:

$$\begin{aligned} Q_1 &= \frac{X_L - |X'_{C2}|}{r_L + R'_L} = \frac{\frac{X_L}{R'_L} - \frac{|X'_{C2}|}{R'_L}}{1 + \frac{r_L}{R'_L}} \\ &= \frac{Q_U - Q_2}{1 + \frac{Q_U}{Q_L}} \end{aligned} \quad (57)$$

The last denominator follows from Eqn (26). Thus by rearranging this equation we have a proof of Eqn (39). Now Eqn (40) can easily be proved using Eqns (24) and (39).

Tuck Choy, MØTCC, received his City and Guilds Amateur Radio certificate in 1971 after high school in Singapore. He then pursued a career in theoretical physics, first as a PhD student and post-doc in London, post-doc at Harwell, then Michigan, assistant professor at Rhode Island and then as a faculty member at Monash University in Australia in 1990. There he took his Morse exams, and took the call sign VK3CCA. His first published homebrew project was a QRP 80 m SSB/CW transceiver using ideas from Gary Breed and Drew Diamond. He won the best technical article award from the Wireless Institute of Australia in 1997. He is now retired but remains active in his professional work and hobbies. Tuck has published a new edition of his book "Effective Medium Theory", Oxford University Press in 2016. He and his wife Debra, who is a professor of linguistics at the Sorbonne in Paris, live in the south of France. In addition to pursuing the foundations of quantum theory, astronomy and ham radio, he has also been an occasional contributor to QEX.

## Notes

- <sup>1</sup>B. Kaune, "Quality Factor, Bandwidth, and Harmonic Attenuation of Pi Networks," QEX, Sep./Oct., 2015, pp. 29-35.
- <sup>2</sup>B. Kaune, "Pi Networks with Loss," QEX, Jan./Feb., 2017, pp. 33-44.
- <sup>3</sup>R. Edwards, G4FGQ, [Online]: [zerobeat.net/G4FGQ/#S102](http://zerobeat.net/G4FGQ/#S102).
- <sup>4</sup>W. L. Everitt, "Output networks for Radio-Frequency Power Amplifiers," *Proceedings of I.R.E.*, vol. 19, no. 5, pp. 725-737, 1931.
- <sup>5</sup>F. E. Terman, in, *Radio Engineer's Handbook*, NY, McGraw-Hill, 1943, pp. 206-215.
- <sup>6</sup>R. S. Hewes and G. R. Jessop, in *Radio Data Reference Book*, London, RSGB, 1995, pp. 61-66.
- <sup>7</sup>L. Butler, [Online]: [users.tpg.com.au/users/ldbutler/index.htm](http://users.tpg.com.au/users/ldbutler/index.htm).
- <sup>8</sup>L. Butler, [Online]: [users.tpg.com.au/users/ldbutler/OutputCoupling.pdf](http://users.tpg.com.au/users/ldbutler/OutputCoupling.pdf).
- <sup>9</sup>W. Hayward, *Introduction to Radio Frequency Design*, ARRL, 1994, p. 139-141, ARRL.
- <sup>10</sup>G. Dobbs, "QRP," *RadCom*, p. 55, Oct., 2013.
- <sup>11</sup>J. Robinson. G3MPO, "Designing ATUs using a Spreadsheet," *RadCom*, pp. 24-27, 1999.
- <sup>12</sup>W. Hayward (*op. cit.*), p. 140.
- <sup>13</sup>E. Wingfield, "New and Improved Formulas for the Design of Pi and Pi-L networks," *QST*, pp. 23-29, Aug., 1983.
- <sup>14</sup>A. Bloom, "Letters to the Editor," QEX, Sep./Oct., 2008, pp. 41-42.
- <sup>15</sup>A. Bloom, "Letters to the Editor," QEX, Jan./Feb., 2010, pp. 37-38.
- <sup>16</sup>T. Choy, "Letters to the Editor," QEX, Sep./Oct., 2014, p. 38.
- <sup>17</sup>K. K. Clarke and D.T. Hess, *Communications Circuits: Analysis and Design*, Reading, MA: Addison-Wesley, 1971, pp. 31-38.
- <sup>18</sup>K. K. Clarke and D.T. Hess, (*op. cit.*), "Pi Network," on pp. 439 to 444.
- <sup>19</sup>R. M. Foster, "A Reactance Theorem," *Bell System Technical Journal*, vol. 3, pp. 259-267, 1924.
- <sup>20</sup>W. Hayward (*op. cit.*), p. 57.

## Errata

In the errata of QEX May/June 2019 regarding Phil Salas, AD5X, "Low-Cost Low-Distortion 2-Tone Test Oscillator for Transmitter Testing", we miss-identified the issue date. It should be QEX Mar./Apr. 2019. In that errata, the audio output is mistakenly shown connected to the collector of the output transistor. Instead the output should be taken via the 0.1 µF capacitor from the junction of the emitter and the 3.3 kΩ resistor. Thanks to Lawrence Joy, WN8P, for spotting the issue date error.

In Maynard Wright, W6PAP, "Measuring Characteristic Impedance of Coax Cable in the shack - Another Approach." QEX May/June 2019 there is an errors in the second equation of the first column. The correct equation is,

$$\begin{aligned} Z_m &= jZ_0 \\ &= j(R_0 + jX_0) \\ &= -X_0 + jR_0 \end{aligned}$$

We regret the error.

# 2019 ARRL / TAPR

## Digital Communications Conference

**September 20-22  
Detroit, Michigan**

**Make your reservations now  
for three days of learning  
and enjoyment at the  
Marriott Detroit Metro  
Airport Hotel. The Digital  
Communications  
Conference schedule  
includes technical and  
introductory forums,  
demonstrations, a Saturday  
evening banquet and an  
in-depth Sunday seminar.**

**This conference is for  
everyone with an interest in  
digital communications—  
beginner to expert.**



**Call Tucson Amateur  
Packet Radio at:  
972-671-8277,  
or go online to  
[www.tapr.org/dcc](http://www.tapr.org/dcc)**

# Receiver Step Attenuator

*This step attenuator is an easy way to improve a receiver's handling of strong signals and to add signal diagnostic capability.*

Having been bitten by the software defined receiver (SDR) bug and experimenting with simple SDR 'dongles' and an HF converter, it didn't take long for me to start thinking of ways to improve this simple receiver. It was readily apparent that an HF receiver like this was wide open to strong signal overload from commercial broadcast signals and even from the ham across town. One way to deal with strong signal overload is to add a broadband attenuator between the receiver and the antenna. This article describes an HF step attenuator and control circuit that you can build for about US\$80.

My goal was to create a step attenuator that would allow me to set just the right amount of attenuation to reduce strong signals while still allowing weak signal readability. I wanted a front-end attenuator that was easily switchable in reasonable steps with known increments to maximize its usability. Of course, one of the steps should be 0 dB.

## What Others Have Done

Commercially available communications receivers frequently offer front-end RF attenuators, sometimes in conjunction with a preamplifier. For example, the Ten-Tec RX-340 provides a switchable 15-dB attenuator and a switchable 10-dB preamplifier. The RF Space NetSDR+ has a three-step attenuator providing 10, 20, and 30 dB. The Icom R70 and R71A have a front panel switch that allows selection of either a preamplifier, a single attenuator of about 20 dB, or neither. The newer R75 has separate switches for the preamp and single-stage 20-dB attenuator. By comparison, the top-of-the-line Icom R9500 receiver employs several receiving band dependent step attenuators. For the HF bands, attenuation up to 30 dB can be selected in 6-dB steps.

For VHF/UHF, the steps are 10, 20, and 30 dB. Above 1150 MHz only a single 20-dB attenuator may be selected. The venerable Kenwood R-1000 (c. 1980) had a step attenuator providing 0 to 60 dB in 20-dB steps. The later (c. 1990) Kenwood R-5000 receiver had a selectable 0 to 30dB attenuator in 10-dB steps.

RF step attenuators have frequently appeared in Amateur Radio literature. Bramwell<sup>1</sup> described a general purpose step attenuator that used a series of slide switches to bring any of 10 attenuator "pads" into the RF path. Attenuations between 1 and 71 dB in 1-dB steps were available. Bramwell relied exclusively on 1% metal film resistors rather than compromising on less-precise 5% values. Oñate and Fortuny<sup>2</sup> employed a two-stage step attenuator with relays to select each attenuator section in a software controlled preselector that provided 6, 12, and 18-dB of front end attenuation. A similar two-stage step attenuator was described in the *2019 ARRL Handbook*<sup>3</sup> using manual switches. Ostapchuk<sup>4</sup> described a rugged step attenuator that used a machined enclosure so each Pi-configured resistor network and DPDT toggle switch was in its own shielded compartment. He noted that an earlier iteration that did not employ this extensive shielding was a failure. He also used 1% metal film resistors. An earlier design by Shriner and Pagel<sup>5</sup> that used an enclosure made from PC board also employed shielded partitions between each attenuator section.

## Attenuator Design

I chose a step attenuator design that allows for selection of attenuation from 0 to 21 dB in 3-dB steps, with fast relay switching and a rotary binary coded decimal or "BCD" switch for attenuation selection. I chose 3-dB steps because it seemed more relevant than

any other step size. A 3-dB change is at the upper end of what most people can perceive<sup>6</sup> and it represents a half-power reduction, so each step should be immediately apparent to the ear and sound roughly equal. Also, a maximum attenuation of 21 dB should be sufficient in most cases and makes it easier to provide enough isolation between sections. Using relays also helps preserve section isolation. Each attenuator section is further isolated by ground plane routing and vertical shields.

Resistor values for these attenuator "pads" are widely available in the literature and online<sup>7</sup>. While the Pi- and T-network topologies are theoretically equal, most applications seem to rely on the Pi-network, probably because real resistors approximating the theoretical values are easier to find and implement for most common attenuations. I chose to use the Pi-network in my design.

The step attenuator circuit (Figure 1) has three sections providing 3-dB, 6-dB, and 12-dB attenuation respectively.

Each attenuation section is switched in or out of the signal line with NEC EC2-5NJ non-latching miniature DPDT relays. These relays are specifically designed for electronic switching and telecommunications service. They are very compact, very fast (rated operation time is approximately 2 ms) and should be adequate for use through the HF band. These relays are energized with +5 V applied to the relay coils at points A, B, and C. Table 1 shows how the relay points A, B, and C are switched to get 0 to 21 dB in 3-dB increments.

When all relays are un-energized, the signal passes through without attenuation — that is, the relays in their "normally closed" (NC) condition and correspond to the 0 dB setting. General purpose diodes (1N4001 or equivalent) bridge the relay coils to provide



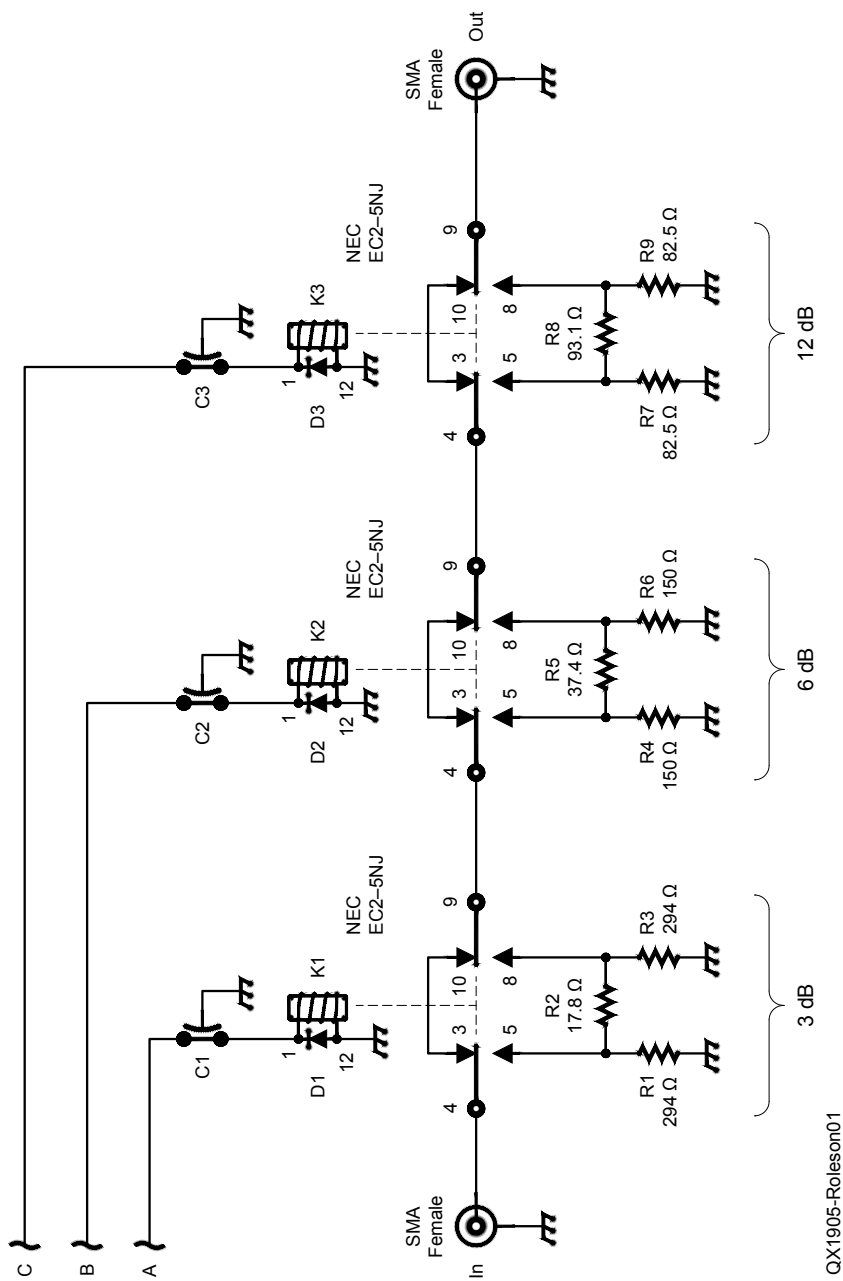


Figure 1 — Three-stage step attenuator schematic. Relays are shown in their non-energized state.

Table 1

Attenuation for activation of relay coils at points A, B, and C.

C	B	A	Atten., dB
0	0	0	0
0	0	1	3
0	1	0	6
0	1	1	9
1	0	0	12
1	0	1	15
1	1	0	18
1	1	1	21

discharge paths for inductive field collapse when the relays are turned off. These are sometimes called fly back diodes. Feed-through capacitors (0.01  $\mu$ F) shunt impulsive RF to ground that the relay switching might produce, and keep RF from getting into or out of the shielded attenuator assembly via the control lines.

For ease of construction, I chose to use 1/4 W axial-leaded resistors. While 5% resistors are arguably adequate for Amateur Radio use, I used my multimeter and dug into my stash of 5% resistors, selecting resistors that were as close as possible to theoretical values.

As others have described, the enclosure, shielding, and printed circuit board (PCB) layout are important especially when it comes to isolating the three attenuator sections. Figure 2 shows that each attenuator section on this compact 2-sided PCB (~2.2 inches square) is surrounded by ground plane. Since I needed only one of each PCB, I chose to make the boards myself, but I used the free *ExpressPCB* software for the layout. My preferred method is to print reversed black images of the PCB layers on clear plastic "overhead sheets" with a laser printer. I then lay this over the blank PCB, and cover with a thin cotton cloth (old T-shirt is ideal), and use a hot clothing iron to transfer the printer toner to the PCB. The toner then becomes the etchant resist. I used the same method to make the switching control dial, skipping the etchant step but instead coating the final product with a thin coat of clear acrylic.

Two section shields (Figure 3) were cut from 0.010 inch thick brass sheet, and were soldered onto the PCB to separate the attenuator sections. Brass sheet 0.010 inches thick (30 gauge) suitable for cutting into the attenuator section shields is typically available from hobby and some hardware stores. The K&S brand is often shown in displays where individual 4 inch by 10 inch sheets are available for purchase. This material is easily cut with sharp scissors or a metal nibbler.

The RF and control connections are all along one edge. The completed PCB

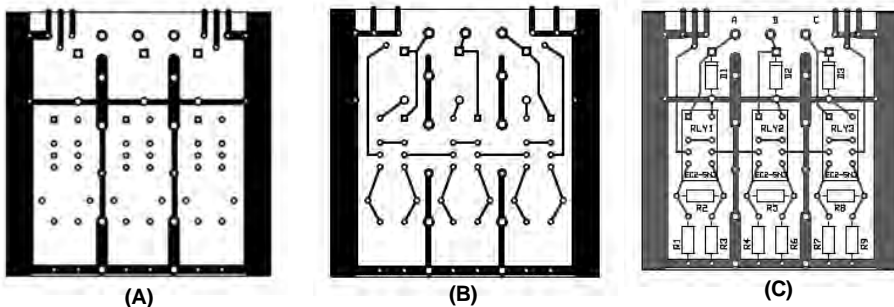


Figure 2 — Step attenuator PC board, (A) top layer, (B) mirrored bottom layer, (C) full layout. The board is 2.185 inches wide and 2.20 inches tall.

assembly is shown in Figure 4. Female SMA bulkhead connectors soldered to the PCB provide RF input and output, ground to shield integrity from the PCB to the enclosure through the end plate, and hold the board to the end plate of the enclosure. The three feed-through capacitors are mounted in the end plate between the two SMA connectors and connected to the PCB by short wires. Ground integrity is further enhanced by horizontal ground traces on the PCB and wide ground planes along each edge on both sides of the PCB that slide into slotted shelves in the main body of the enclosure. These features should minimize ground plane potential differences across the PCB and provide redundant ground connection to the enclosure when the PCB is slid into slots inside the main enclosure.

The enclosure provides RF shielding as well as a mechanically sturdy housing. I chose the Hammond 1457C1201 enclosure, cut in half. Other enclosures may also work, but when cut in half this one provided the most compact overall enclosure. It is basically a short length of extruded aluminum channel with two aluminum end caps or panels, and internal ribbing features to provide for attaching the end panels and sliding a PCB into the channel.

As provided by the manufacturer, several cosmetic and weatherproofing features compromise the shielding effectiveness. Hammond also sells an EMI/RFI version of this enclosure, part number 1457C1201E. It includes end plate EMI gaskets, and it appears that the end plates may not be completely powder coated. In hindsight, I should have purchased this version if only because I might have needed to remove less powder coating from the end plates. The E-version costs \$4 more.

The end panels are provided with waterproofing (and insulating) rubber gaskets, which I discarded. Both end panels and the exterior of the main extruded body were powder coated. This powder coating is an insulator. I wanted a well-shielded enclosure, so this powder coating had to be removed in those places where I needed good metal-to-metal contact. I used sand-paper wheels and a wire brush in a Dremel® tool, and a wire brush mounted in a 1/4-inch drill to remove the coating from the inside surface of the end plates and around the mating edges of the main extruded body. A viable alternative would have been to use sand or bead blasting to remove the powder coating and polish the metal, but I do not have this capability at hand. I also buffed the open ends of the extrusion on flat sheets of fine sandpaper and emery cloth to ensure it was flat and clean to give the end panels the best chance to fit snugly and without gaps.

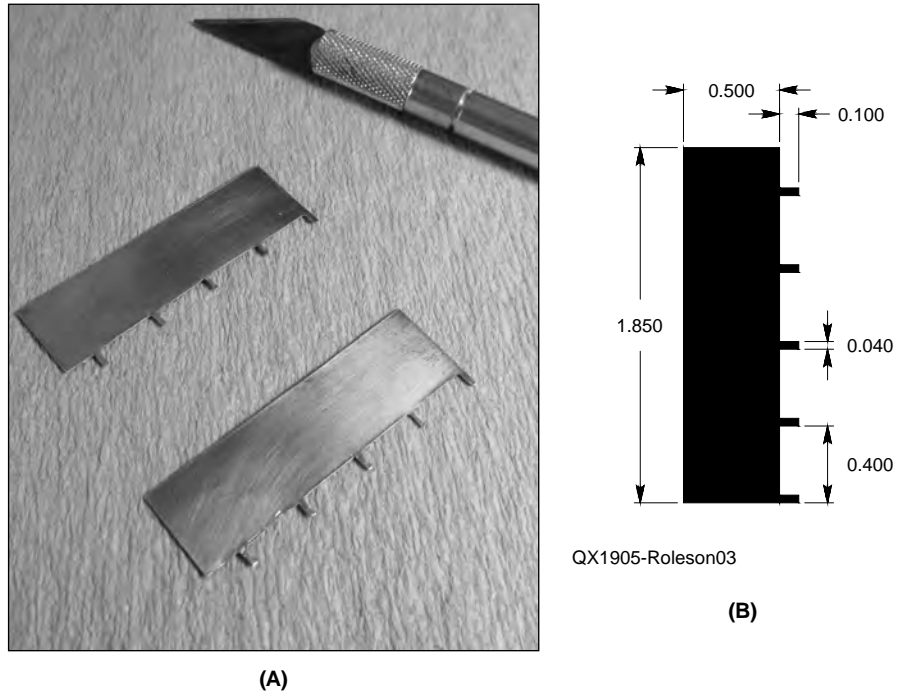


Figure 3 — Attenuator section shields (A) are cut from 0.010 inch thick brass sheet, with dimensions in (B).

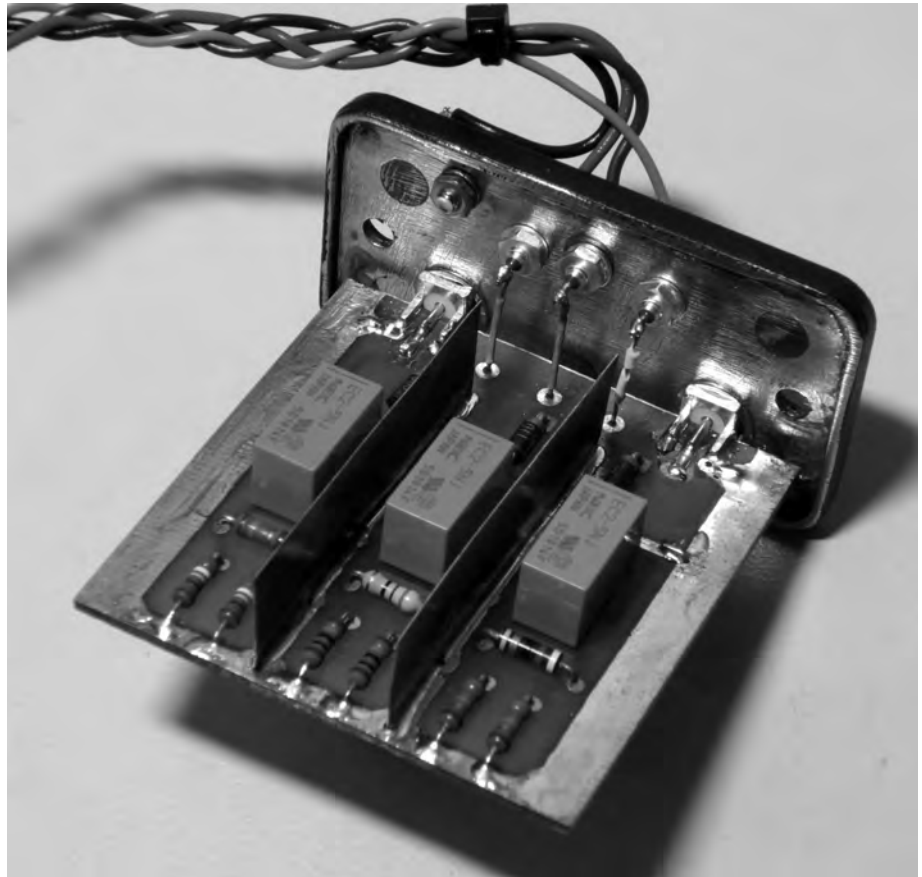


Figure 4 — Completed attenuator PC board and lid assembly.

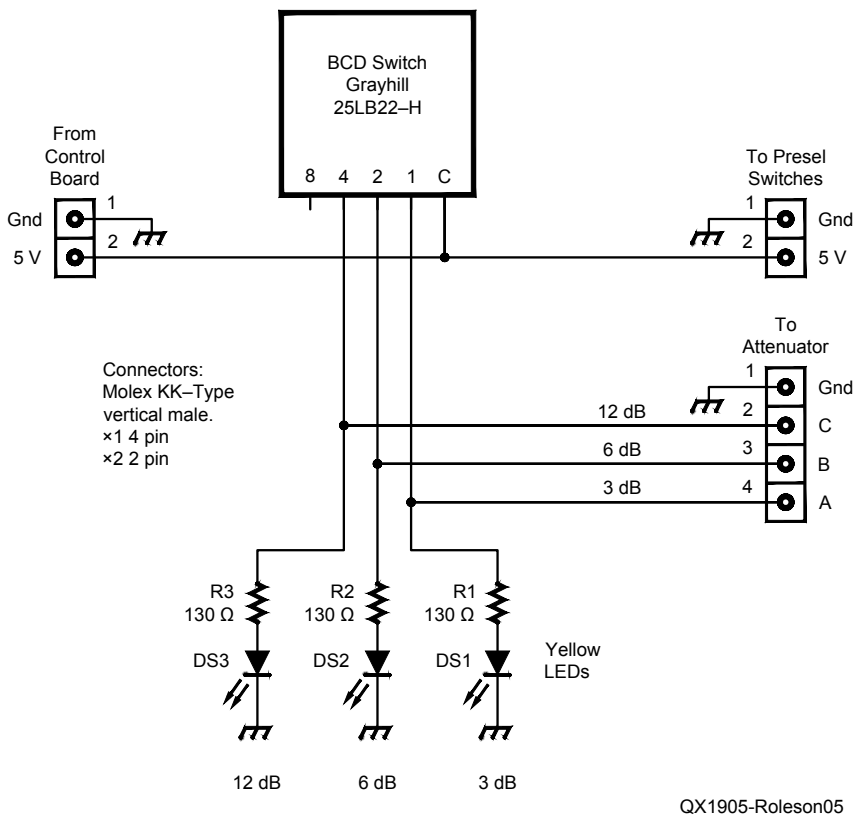


Figure 5 — BCD or hexadecimal switch assembly schematic.

The end panels are held in place on the extrusion with the provided #6 screws, two to each panel. The groove features in the main extrusion that hold the end panel screws were not tapped, and I was concerned that simply screwing into these with the provided screws might liberate small chunks of aluminum that could get into the circuitry. I was also worried that the black coating of the provided screws might be an insulator. Consequently, I tapped the grooves with a #6-32 tap and thoroughly cleaned them afterward to make sure there were no loose bits of aluminum. I also used 1/2-inch long #6 stainless steel machine screws instead of the provided screws.

Just for good measure, on final assembly I used a thin coating of electrical anti-oxidant joint compound on all interconnecting metal surfaces, including the ground plane edges of the PCB where it slides into the main extruded enclosure. Anti-oxidant joint compound is sold in electrical supply and home repair stores. A little bit goes a long way. It is basically a viscous lubricant (polybutene) infused with powdered zinc. It inhibits corrosion by sealing pressure-fit dissimilar metal joints from air. One common brand is the NOALOX® compound from Ideal Industries.<sup>8</sup>

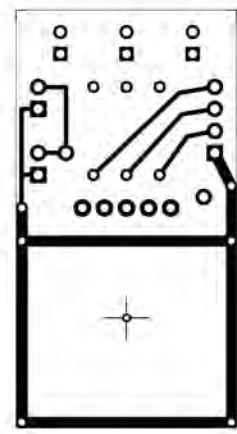
I had tinned the ground plane edges of the

PCB, but the galvanic potential difference between aluminum and tin/lead is large enough that I was concerned about oxidation.<sup>9</sup> Hopefully, the joint compound will help keep corrosion at bay. I was concerned that excessive joint compound might migrate over time, get into the circuitry, and degrade performance of the attenuators, so I used the joint compound sparingly.

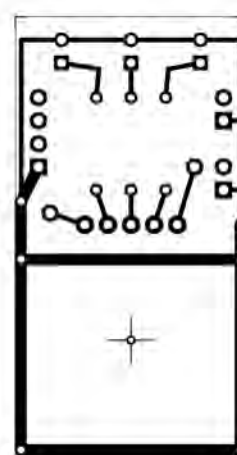
### Switching Control

I considered simply using three toggle switches to route +5 V to the three control inputs of the attenuator, but settled on a more elegant method that used a Grayhill 25LB22-H binary coded decimal (BCD) or hexadecimal (hex) mechanical encoder. This is basically a rotary switch with one input and 4 outputs. Since I had a three-section attenuator, I needed only three of the 4 BCD outputs. Rotating the switch connects the input to the outputs in a BCD or hexadecimal sequence. This allows for selecting attenuation from zero to 21 dB in 3 dB steps.

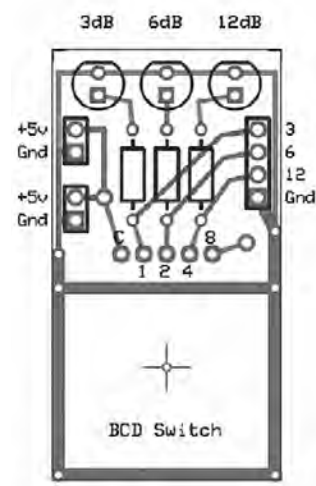
The control circuit is shown in Figure 5. A two-pin Molex KK-style connector provides for connection of 5 V dc to the “C” or common pin of the rotary encoder, and the lowest three output pins are routed to a 4-pin connector that is wired to the



(A)



(B)



(C)

Figure 6 — BCD/hexadecimal switch PCB board, (A) top layer, (B) mirrored bottom layer, (C) full layout. The board is 1.9 inches tall by 1 inch wide.

attenuator. Three yellow LEDs and current limiting resistors provide visible indication of attenuator selection. The small PC board I used is shown in Figure 6, and the final assembly is shown in Figure 7.

I also created a position or dial plate, shown in Figure 8. I created the lettering design with the same PCB software that I used to make the PC boards, transferred the image to a piece of brass sheet just as I had done when making PCBs, then coated the plate with clear spray acrylic. I carefully cut a 3/8 inch diameter hole in the center to fit over the rotary switch.

The final attenuator and control are shown in Figure 9. I soldered a short cable made from 4 wires to the feed-through capacitor attenuator control points and a ground point and connected the other end to the control assembly with a 4-pin Molex KK-series connector. While not entirely necessary, I braided the 4 wires so they would stay together in a bundle.

### Verifying the Design

Not having access to the sort of test equipment needed to properly and comprehensively test this step attenuator, and not being willing to simply incorporate the attenuator assembly into a receiver without further design verification, I was compelled to improvise.

### Input and Output Resistance Values

Firstly, while clearly insufficient, a simple dc resistance test provides a useful check of the basic assembly and design. When each relay is engaged, the Pi-network attenuator sections represent an easily calculated dc resistance to both the input and output ports. This test also checks relay function and shows mistakes like resistor selection errors or inadvertent solder bridges.

The dc resistance of a simple resistive

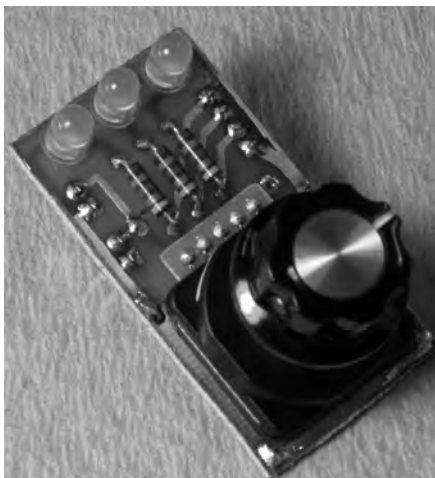


Figure 7 — Completed BCD/hexadecimal switch assembly.

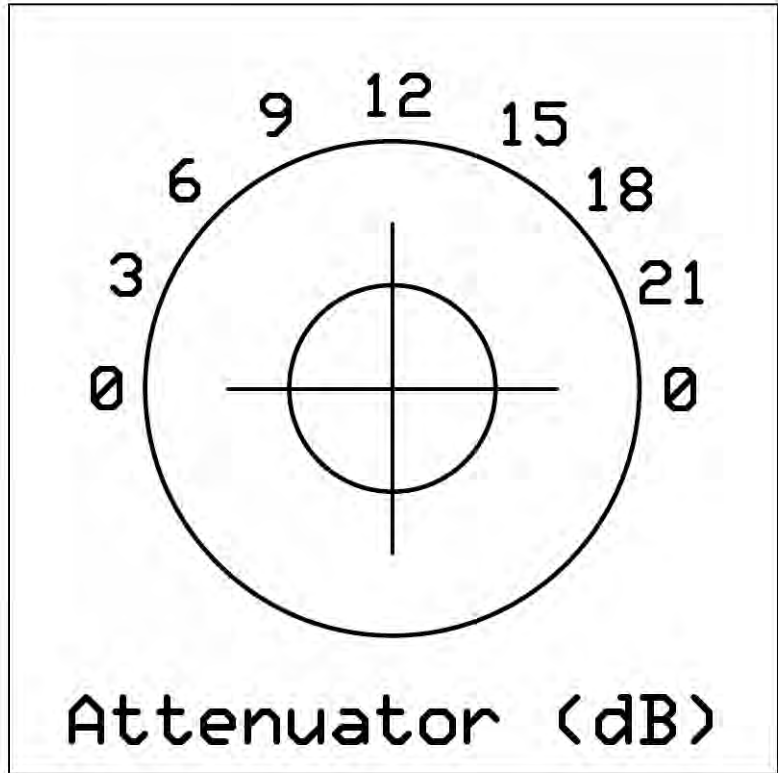


Figure 8 — BCD/hexadecimal switch position dial plate.

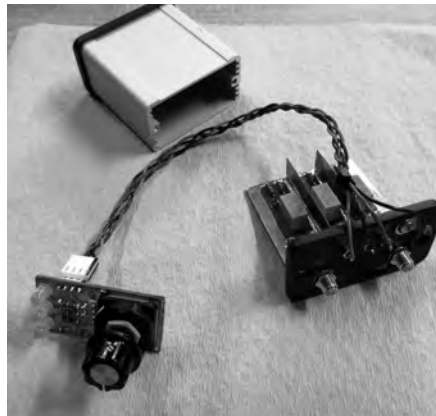
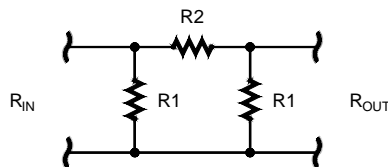


Figure 9 — Completed attenuator and BCD/hexadecimal switch.



QX1905-Roleson10

Figure 10 — Simple resistive Pi-network.

Table 2.

Attenuation for the shown resistance values.

Atten., dB	$R_1$	$R_2$	$R_{in} = R_{out}$
3	294	17.8	151.3
6	150	36	83
12	82.5	91.9	56

Pi-network(Figure 10) is,

$$R_{in} = R_{out} = \frac{(R_1 + R_2) R_1}{2R_1 + R_2}$$

Table 2 shows the resistances for each of the three attenuator sections (Figure 1). For example, for an attenuation of 3 dB in a 50  $\Omega$  Pi-network,  $R_1$  is 294  $\Omega$  and  $R_2$  is 17.8  $\Omega$  so,

$$R_{in} = R_{out} = \frac{(294 + 17.8) 294}{2 \cdot 294 + 17.8} = 151.3 \Omega$$

I used a multimeter to check the dc resistances at the input and output jacks with each of these attenuator sections engaged in turn. The measured resistances were all very close to the values in Table 2.

### Attenuation at Different Frequencies

I also wanted a way to check the attenuation at each step and in the shortwave

bands. My intention is to eventually incorporate this step attenuator in a software-defined radio, so I connected a DVB-T “dongle” with an HF up-converter to a fast desktop computer and downloaded a copy of *SDR#* software.<sup>10</sup> I connected the step attenuator between the HF converter and an outdoor HF antenna to verify that this lash-up functioned as a receiver on the HF bands. It did, so I disconnected the antenna and instead connected the input to an 80-meter VFO that I had built many years ago. I fed the VFO output through a 10- or 20-dB fixed attenuator both to reduce the signal to within the receiver’s range and to ensure the VFO was driving into a fixed 50 Ω circuit to help stabilize the VFO performance. This VFO and attenuator provided a very adequate signal at 4.0 MHz, and adequate harmonics at 12 MHz and 24 MHz.

This receiver functioned as a tunable RF voltmeter that displayed signal amplitude in relative field strength decibel values — what *SDR#* refers to as “FSDB”. The absolute FSDB didn’t matter, since I was interested in the signal strength relative to a 0 dB attenuator setting. In this way I was able to measure the VFO signals at each of the 3-dB steps up to 21 dB and calculate the actual attenuation at each step. Results are shown in Table 3.

## Closing Remarks

The attenuations at HF for the three attenuator sections (3, 6, and 12 dB) all

**Table 3.**  
Measured attenuation at 4, 12 and 24 MHz.

Atten., dB	4 MHz	12 MHz	24 MHz
3	3.1	2.7	3.1
6	6.1	5.7	5.9
9	9.0	8.5	9.0
12	12.3	11.4	12.1
15	15.5	14.2	14.8
18	17.9	17.0	17.7
21	20.4	19.8	20.6

appear very close to nominal, with the exception that the 12 MHz measurements were all slightly low. I also observed that the measured attenuations at the upper settings (18 and 21 dB) are consistently low for all three test frequencies. I will speculate that the isolation between sections may be the culprit, and that signal is leaking around the attenuators. As I noted earlier, others have reported that isolation between attenuator sections was important.

At one point I considered adding a fourth section (24 dB) to allow for higher attenuation settings, but it seems now that it might have been difficult to realize uniform higher attenuation steps without greater internal isolation. This probably would have required a much larger enclosure and larger section shields on the PC board, or possibly a design that would have better isolation between the attenuator sections. If I were to build a second unit I would try to increase the size of the internal shields to whatever the enclosure would allow to see if that would help on the higher attenuation settings. There might also be a way to use brass EMI finger stock to improve the ground connections along the edges of the PCB where it slides into the extrusion.

This step attenuator was clearly adequate for my intended use. When tuning around the HF bands, this step attenuator was a useful addition. The 3-dB steps felt about right. Smaller steps would not have been helpful. Certain very strong signals were immediately shown to be generated internally by the SDR circuit when changes in the attenuation showed no amplitude change. It was also helpful to use the attenuator in combination with the *SDR#* RF gain control to find just the right compromise of receiver sensitivity and reduction of splatter and noise from strong local signals.

*Scott Roleson, KC7CJ, was first licensed in 1964. He has been an ARRL member for over 50 years. Scott has a BSEE from Arizona State University, an MSEE from the University of Arizona, is a licensed Professional Engineer*

*in California, and is a Life Senior Member of the IEEE. From 1993 to 1995 he was a Distinguished Lecturer of the IEEE EMC Society, and was the Distinguished Lecturer program chair 1995-1997. He retired after a 32-year career in electrical engineering where he worked on spectrum analyzer design, EMC and telecom regulatory engineering. Scott now gets to pick his own projects to maximize the fun return-on-investment.*

## Notes

- <sup>1</sup>Bramwell, W7OWJ, “An RF Step Attenuator,” *QST*, Jun. 1995, pp. 33-34.
- <sup>2</sup>J. de Oñate, MØWWA and X. R. Junqué de Fortuny, “A Software Controlled Radio Preselector,” *QEX*, May/June 2008, pp. 11-18.
- <sup>3</sup>An RF step attenuator is shown on p. 25.56 in *The ARRL Handbook for Radio Communications*, 2019 Edition. Available from your ARRL dealer or the ARRL Bookstore, ARRL item no. 0888. Telephone 860-594-0355, or toll-free in the US 888-277-5289; [www.arrl.org/shop](http://www.arrl.org/shop); [pubsales@arrl.org](mailto:pubsales@arrl.org).
- <sup>4</sup>P. Ostapchuk, N9SFX, “A Rugged, Compact Attenuator,” *QST*, May 1998, pp. 41-43.
- <sup>5</sup>B. Shriner, WAØUZO and P. K. Pagel, N1FB, “A Step Attenuator You Can Build,” *QST*, Sep. 1982, pp. 11-13.
- <sup>6</sup>*Audioholics* magazine reviewed several studies of minimum detectable fluctuation in normal human hearing and found a range of values between 0.25 and 3 dB. See: Mark, “Human Hearing: Amplitude Sensitivity Part 1,” *Audioholics*, 4 Apr. 2005; online at: [www.audioholics.com/room-acoustics/human-hearing-amplitude-sensitivity-part-1](http://www.audioholics.com/room-acoustics/human-hearing-amplitude-sensitivity-part-1).
- <sup>7</sup>Resistor values for Pi- and T-networks are on p. 22.44 in *The ARRL Handbook for Radio Communications*, 2019 Edition (op. cit.), also in [www.microwaves101.com/encyclopedias/attenuator-calculator](http://www.microwaves101.com/encyclopedias/attenuator-calculator) and [chemandy.com/calculators/matching-pi-attenuator-calculator.htm](http://chemandy.com/calculators/matching-pi-attenuator-calculator.htm).
- <sup>8</sup>For more information, see: [www.idealindustries.ca/products/wire\\_installation/accessories/noalox.php](http://www.idealindustries.ca/products/wire_installation/accessories/noalox.php).
- <sup>9</sup>A good discussion of galvanic corrosion can be found at: H. W. Ott, *Noise Reduction Techniques in Electronic Systems*, Second Edition, John Wiley & Sons, 1988, pp. 23-25.
- <sup>10</sup>This simple SDR arrangement was similar to those described by R. Nickels, W9RAN, “Cheap and Easy SDR,” *QST*, Jan. 2013, pp. 30-35, and J. Forkin, WA3TFS, “All-Mode 1 kHz to 1.7 GHz SDR Receiver,” *QST*, Jan. 2016, pp. 30-33.

**Table 4**  
Bill of materials.

Item	Qty	Source
Brass sheet, 0.010 inch thick, K&S Stock #251 or equiv.	1	Available in hobby or hardware stores
Diodes, 1N4001 or equiv.	3	<a href="http://www.jameco.com">www.jameco.com</a>
EMI filters, Tusonix bushing style (0.01μF feed-thru capacitors), type 4400-035LF	3	<a href="http://www.mouser.com">www.mouser.com</a>
Enclosure, Hammond 1457C1201 or 1457C1201E	1	<a href="http://www.digikey.com">www.digikey.com</a> – HM1012-ND
Hex rotary encoder, Grayhill 25LB22-H	1	<a href="http://www.digikey.com">www.digikey.com</a> – GH3074-ND
LED, yellow	3	DigiKey, Mouser, or Jameco
Molex KK connectors (0.100 inch) 4-pin and 2-pin, male and female	5	DigiKey, Mouser, or Jameco
Relays, NEC EC2-5NJ	3	<a href="http://www.jameco.com">www.jameco.com</a>
Resistors (see Note 7), Metal film, 1/4 W, 5%	9	<a href="http://www.mouser.com">www.mouser.com</a>
Resistors, 130 Ω, 1/4 W	3	DigiKey, Mouser, or Jameco
SMA female, PCB mount bulkhead connectors	2	<a href="http://www.amazon.com">www.amazon.com</a>

# Upcoming Conferences

## 2019 Central States VHF Society, Inc. Conference

July 25 – 27, 2019

Lincoln, Nebraska

[www.2019.CSVHFS.org](http://www.2019.CSVHFS.org)

Our 2019 conference will be held July 25 – 27 at the Country Inn & Suites by Radisson, Lincoln North Hotel and Conference Center, located at 5353 North 27th Street in Lincoln, Nebraska. The conference will feature all of the activities that previous conferences have had including technical presentations, antenna range testing, preamp measurements, vendor exhibits, a VHF101 educational seminar for those who may be new to weak-signal operations, Rover Row, Dish Row, luncheons with hosted speakers, a family program for non-hams, a Saturday night banquet, and a VHF/UHF/Microwave swap fest. In addition, the conference offers a great opportunity to socialize with like-minded weak signal VHF+ operators.

Lincoln is centrally located in the USA and is within an easy day or two driving distance of most centrally located USA cities. Lincoln also features a major airport.

Please make your hotel reservations as early as possible to secure your room at the conference site, which directly supports your CSVHF Society.

See website for all the details.

## GNU Radio Conference 2019

September 16 – 20, 2019

Huntsville, Alabama

<https://www.gnuradio.org/grcon/grcon19/>

The GNU Radio Conference 2019 will be held at the "Huntsville Marriott at the Space & Rocket Center." This conference celebrates and showcases the substantial and remarkable progress of the world's best open source digital signal processing framework for software-defined radios. In addition to presenting GNU Radio's vibrant theoretical and practical presence in academia, industry, the military, and among amateurs and hobbyists, GNU Radio Conference 2019 will have a very special focus.

Summer 2019 marks the 50th anniversary of NASA's Apollo 11 mission, which landed the first humans on the Moon. GNU Radio Conference selected Huntsville, AL, USA as the site for GNU Radio Conference 2019 in order to highlight and celebrate space exploration, astronomical research, and communication.

Space communications are challenging and mission critical. Research and development from space exploration has had and continues to have far-reaching effect on our communications gear and protocols.

Registration and an online and mobile-friendly schedule will be posted at the conference website.

## ARRL and TAPR 38<sup>th</sup> Digital Communications Conference (2019)

September 20 – 22, 2019

Detroit, Michigan

[www.tapr.org/dcc.html](http://www.tapr.org/dcc.html)

Mark your calendar and start making plans to attend the premier technical conference of the year, the 38th Annual ARRL and TAPR Digital Communications Conference to be held September 20 – 22, 2019, in Detroit, MI. The conference location is the Detroit Metro Airport Marriott Hotel.

The ARRL and TAPR Digital Communications Conference is an international forum for radio amateurs to meet, publish their work, and present new ideas and techniques. Presenters and attendees will have the opportunity to exchange ideas and learn about recent hardware and software advances, theories, experimental results, and practical applications.

Topics include, but are not limited to: Software Defined Radio (SDR), digital voice, digital satellite communications, Global Position System (GPS), precision timing, Automatic Packet Reporting System™ (APRS), short messaging (a mode of APRS), Digital Signal Processing (DSP), HF digital modes, Internet interoperability with Amateur Radio networks, spread spectrum, IEEE 802.11 and other Part 15 license-exempt systems adaptable for Amateur Radio, using TCP/IP networking over Amateur Radio, mesh and peer to peer wireless networking, emergency and Homeland Defense backup digital communications, using Linux in Amateur Radio, updates on AX.25 and other wireless networking protocols.

**Call for Papers:** Technical papers are solicited for presentation at the ARRL and TAPR Digital Communications Conference and publication in the Conference Proceedings. Annual conference proceedings are published by the ARRL. Presentation at the conference is not required for publication. Submission of papers are due by July 31, 2019 and should be submitted to

Maty Weinberg, ARRL  
225 Main Street  
Newington, CT 06111

or via the Internet to [maty@arrl.org](mailto:maty@arrl.org)

## Microwave Update 2019

October 3 – 5, 2019

Dallas, Texas

[www.microwaveupdate.org](http://www.microwaveupdate.org)

The North Texas Microwave Society would like to invite you to the annual Microwave Update Conference to be held October 3 – 5, 2019 at the Hilton Garden Inn and Conference Center in Lewisville (Dallas), Texas.

Microwave Update is the premier microwave conference of the year; initially started by Don Hilliard, WØPW (SK) back in 1985. This is the ideal conference to meet fellow microwave enthusiasts and share ideas and techniques that will help you conquer your next microwave band.

We have a full slate of speakers already set up. If you are interested in speaking, please let us know.

Topics will include small-dish EME, microwave propagation, parabolic-dish feedhorn design and construction, SSPAs, circuit design, latest microwave devices, software defined radios, and digital modes, just to name a few.

We still have several surplus electronics and mechanical places in the DFW area that may be worth a visit on Thursday. A workshop on GNU Radio, led by Tom McDermott, N5EG, is planned for Thursday afternoon. GNU Radio is a development and simulation environment used to create and test software defined radio applications. This is a powerful learning tool and GNU Radio can be used to implement working radio applications. Friday morning will be dedicated to "antenna gain." An informal program for the spouses has been planned, and will include local shopping and sightseeing in the Lewisville, Grapevine and greater DFW area on both Friday and Saturday.

Our Saturday night banquet speaker will be Rex Moncur, VK7MO, who has activated over 100 grid squares on 10-GHz EME in both Australia and New Zealand. Rex will show us some of the beautiful places he has visited and talk about his adventures to some of the more remote places down under. This should be a real treat for hams and spouses.

**Call for papers:** Kent Britain, WA5VJB, will coordinate the publishing of the proceedings by the ARRL. We are always looking for additional papers for the proceedings. You don't have to be a presenter to have your paper published in the proceedings. If you have an article on your latest microwave related project that you would like published, please send your article to Kent, WA5VJB at [wa5vjb@flashnet](mailto:wa5vjb@flashnet).



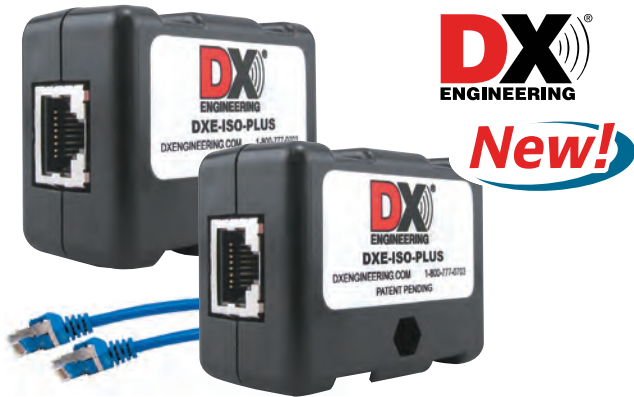
**Showroom Staffing Hours:**  
9 am to 5 pm ET, Monday-Saturday

**Ordering (via phone):**  
8:30 am to midnight ET, Monday-Friday  
9 am to 5 pm ET, Weekends

**Phone or e-mail Tech Support: 330-572-3200**  
8:30 am to 7 pm ET, Monday-Friday  
9 am to 5 pm ET, Saturday  
All Times Eastern | Country Code: +1  
DXEngineering@DXEngineering.com

**800-777-0703 | DXEngineering.com**

**Improve Performance with These Products from DX Engineering!**



**ISO-PLUS Ethernet RF Filter**

This patent-pending filter joins two RJ-45 connectors to reduce interference for frequencies from below 1 MHz to over 100 MHz without affecting Ethernet data signal levels or speed.

<b>DXE-ISO-PLUS-2</b>	2 Filters .....	<b>\$49.99</b>
<b>DXE-ISO-PLUS-10</b>	10 Filters .....	<b>\$239.99</b>



**Coaxial Cable Assemblies**

These low-loss cable assemblies are available in standard lengths with DX Engineering's revolutionary patented PL-259 connector. Use the online Custom Cable Builder at DXEngineering.com to build assemblies made to your exact specs. DX Engineering's coaxial cable is also available by the foot or in bulk spools.



**WOLF WAVE Advanced Audio Processor**

Transform your listening experience by attaching this powerful inline audio processor to your radio's headphone jack. The new Wolf-100 WOLF WAVE unit includes DSP noise reduction, fully adjustable audio band pass filtering from 50 Hz to 5 kHz, age-related hearing loss correction, real-time audio spectrum display, and much more. Enter "WOLF WAVE" at DXEngineering.com for full details.

<b>SBM-WOLF WAVE</b>	Audio Processor .....	<b>\$275.99</b>
----------------------	-----------------------	-----------------



**QRM Eliminator**

Make contacts you thought were impossible with WiMo's new adjustable phasing network for canceling out QRM. The easy-to-tune QRM Eliminator gets rid of local interference up to an S9 level. It allows you to adjust phase angle as well as amplification to cancel out unwanted signals before they reach the receiver front-end. Enter "WMO QRM" at DXEngineering.com for complete specs.

<b>WMO-26000</b>	QRM Eliminator .....	<b>\$169.99</b>
------------------	----------------------	-----------------

**YAESU** **ICOM** **KENWOOD** **ALINGO**

\*Free Standard Shipping for Orders Over \$99. If your order, before tax, is over 99 bucks, then you won't spend a dime on shipping. (Additional special handling fees may be incurred for Hazardous Materials, Truck Freight, International Orders, Next Day Air, Oversize Shipments, etc.).



**Email Support 24/7/365 at DXEngineering@DXEngineering.com**



# A PERFECT PAIR

Combine our manually tuned, ultra-portable yet high performance CrankIR Vertical with the SARK-110 pocket sized antenna analyzer!

## CrankIR

A lightweight, high performance, extremely portable vertical antenna rated at 1500 watts key-down with fully manual operation (no electrical power or controller required). An optional portable tunable elevated radial system is available and its patented folded design allows for a 40% reduction in size with only 0.3dB reduction in gain performance when compared to a full sized antenna. With available versions that cover 80m-2m and 40m-2m (and every frequency in between), the CrankIR sets up quickly and provides flexibility to change the bands quickly. This antenna is the choice of amateur radio operators and emergency communications teams world-wide, in both portable and permanent applications. Consider purchasing one of our SARK-110 battery powered pocket sized antenna analyzers for use with the CrankIR – a custom 3D printed mounting bracket is available to secure the SARK-110 to your CrankIR!

## SARK-110

The SARK-110 antenna analyzer is a pocket-sized instrument that provides fast and accurate measurement of the vector impedance, VSWR, vector reflection coefficient, return loss and R-L-C. Typical applications include checking and tuning antennas (such as the CrankIR), impedance matching, component test, cable fault location, measuring coaxial cable losses and cutting coaxial cables to precise electrical lengths. The SARK-110 has full vector measurement capability and accurately resolves the resistive, capacitive and inductive components of a load. The SARK-110 is intuitive and easy to use, and utilizes four operating modes: sweep mode, smith chart mode, single frequency mode and frequency domain reflectometer (cable test).



## SARK-110

Ask us about our new 3D printed SARK-110 bracket, designed specifically for the CrankIR! (Prototype holder shown)

**"We introduced the CrankIR to be a world-class portable antenna – little did we know that scores of amateur radio operators would make this their home station antenna as well!"**

– John Mertel, WA7IR  
CEO SteppIR Communication Systems



FOR DETAILS ON THESE PRODUCTS AND TO ORDER:

[www.steppir.com](http://www.steppir.com) 425-453-1910

CrankIR



